REDUCTION IN PRE-RETINAL NEOVASCULARIZATION BY RIBOZYMES THAT CLEAVE THE A_{2B} RECEPTOR mRNA

By

AQEELA AFZAL

A DISSERTATION PRESENTED TO THE GRADUATE SCHOOL
OF THE UNIVERSITY OF FLORIDA IN PARTIAL FULFILLMENT
OF THE REQUIREMENTS FOR THE DEGREE OF
DOCTOR OF PHILOSOPHY

UNIVERSITY OF FLORIDA

2003

To my son, Faris Wasim.

ACKNOWLEDGMENTS

It is a pleasure to thank the many people who have made this dissertation possible. Many people have been a part of my graduate education as friends, teachers and colleagues. My mentor, Maria Grant, has been all of those. It is difficult to overstate my gratitude for her. She has instilled in me the qualities of being a good scientist. Her infectious enthusiasm for clinical research has been a major driving force during my career at the University of Florida. This dissertation is a small tribute to an exceptional woman from a student who is still anxious to learn from her.

My sincerest thanks are also due to Lynn Shaw. He patiently taught me all the techniques I needed to complete my work. He also spent countless hours editing and doing the graphics for this dissertation. His insightful comments were crucial for editing the many drafts into the final dissertation. My thanks are also due to Polyxenie E. Spoerri who taught me all the tissue culture techniques I needed to complete this dissertation. Thanks also to Sergio Caballero, Rehae Miller and past and present members of the Grant lab: Tom Ruzich, Nilanjana Sengupta, Christopher Beadle, Hao Pan

I would like to thank my committee members: Dr. Don. A. Samuelson (Professor of Veterinary Medicine); Dr. Dennis. E. Brooks (Professor of Veterinary Medicine); Dr. John. B. Dame (Professor of Veterinary Medicine); Dr. Donald. A. Armstrong, Dr. Elizabeth C. Uhl (Clinical Assistant Professor of Veterinary Medicine) and Dr. Harm J.

Knot (Assistant Professor of Pharmacology and Therapeutics) for their guidance over the years.

My son, Faris Wasim, has been a great source of inspiration. Being tired of not being able to fulfill his requests when I wanted to and missing him has been the best motivation for completing this dissertation. My husband, Wasim Asghar, has also shared this exciting journey with me. He has provided constant support and encouragement throughout my graduate career.

A very special thanks to the two people to whom I owe everything I am today, my parents, Mohammed Afzal and Mussarat Afzal. Their unwavering faith and confidence in my ability and in me is what has shaped me to be the person I am today. Thank-you for everything. My thanks are also due to my sister, Aneela Afzal, and brother Yaseen Afzal, for their support and countless hours of babysitting. My family opened their hearts to me and my little one and made it possible for me to come to work knowing that he was in good hands.

In addition, I would also like to thank the Department of Pharmacology and Therapeutics at the College of Medicine at the University of Florida, and the College of Veterinary Medicine at the University of Florida for their financial support during my graduate career.

Thanks also to the men and women who donated their eyes to our research. Their gift has made it possible for us to understand several eye diseases and prevent them in the future.

TABLE OF CONTENTS

page

LIST OF FIGURES

LIST OF ABBREVIATIONS

a-LDL	Acetylated 1,1'-Dioctdycl-3,3,3',3' tetra methyl indocarbocyanin perchlorate
ABAM	Antibiotic antimycotic mix
A_1	Adenosine receptor type 1
A_{2A}	Adenosine receptor type 2A
A_{2B}	Adenosine receptor type 2B
A_{2B} Rz1	Adenosine receptor type 2 ribozyme 1
A_{2B} Rz2	Adenosine receptor type 2 ribozyme 1
A2R	Adenosine receptor type 2
A_3	Adenosine receptor type 3
ADA	Adenosise deaminase
AK	Adenosine kinase
AMP	Adenosine monophosphate
ANG-1	Angiopoeitin 1
ANG-2	Angiopoeitin 2
ARMD	Age Related Macular Degeneration
ARNT	Aryl hydrocarbon receptor nuclear translocator
ARVO	Association for Research in Vision and Ophthalmology
ATP	Adenosine triphosphate
$\alpha_v\beta_3$	Alpha $_V$ beta $_3$ integrin

$\alpha_v\beta_5$	Integrin
bFGF	Basic fibroblast growth factor
BSA	Bovine serum albumin
cAMP	3c, 5c-cyclic monophosphate
CAT	Chloramphenicol acetyltransferase
CGS21680	A2A agonist. 2-{4[(2-carboxylethyl)-phenyl]ethylamine}-5'-N-ethylcarboxamidoadenosine
CHA	Cyclohexyladenosine
CHO	Chinese hamster ovary cells
CMV	Cytomegalovirus
DMEM	Dubellco's modifeid eagle medium
DMSO	Dimethyl sulfoxide
DNA	Deoxyribonucleic acid
DPSPX	Non-seletive adenosine receptor antagonist. 1,3-dipropyl-8(p-sulfophenyl)xanthine
DTT	Dithiothreitol
ECM	Extracellular matrix
EDTA	Ethylenediamine tetraacetic acid
EGS	External guide sequence
Eph receptor	Ephrin receptor
FAK	Focal adhesion kinase
FAT	Focal adhesion targeting sequence
FBS	Fetal bovine serum
Flt	VEGF fms like tyrosine kinase
GAGs	Glycosaminoglycans

GC	Guanosine cytosine content
GCL	Ganglion cell layer
GFP	Green fluorescent protein
GPI	Glycosylphosphatidylinositol
HBSS	Hanks balanced salt solution
HDV	Hepatitis delta virus
HEK 293	Human embryonic kidney cells
HIF	Hypoxia inducible factor
HIV	Human immunodeficiency virus
HRE	Hypoxia response element
HRECs	Human retinal endothelial cells
HSPGs	Heparan sulfate proteoglycans
IACUC	Institution Animal Care and Use Committee.
IB-MECA	Selective A3 adenosine receptor agonist. N6 (3-iodobenzyl)Ado-5'N-methyl Uronamide
ICROP	International classification of Retinopathy of Prematurity
ILM	Inner limiting membrane
INL	Inner nuclear layer
IP3	Inositol triphosphate
IPL	Inner plexiform layer
KDR	VEGF kinase insert domain
LAP	Latency associated peptide
MMP	Metalloproteinases
NAD	Nicotinamide adenine dinucleotide

NBTI	Nitrobenzylthioinosine
NECA	N-ethylcarboxyamidoadenosine
NFL	Nerve fibre layer
NPDR	Non proliferative diabetic retinopathy
5'NT	5' Nucleotodase
OLM	Outer limiting membrane
ONL	Outer nuclear layer
OPL	Outer plexiform layer.
PAs	Plasminogen activators
PAI-1	Plasminogen activator inhibitor-1
PAI-2	Plasminogen activator inhibitor-2
PBS	Phosphate buffered saline
PDGF	Platelet derived growth factor
PKC	Protein kinase C
PLC	Phospholipase C
PDR	Proliferative diabetic retinopathy
rAAV	Recombinant adeno associated virus
RBCs	Red blood cells
ROP	Retinopathy of Prematurity
RNA	Ribonucleic acid
rRNA	Ribosomal RNA
RNasin	Ribonuclease inhibitor
RPE	Retinal pigment epithelium

R-PIA	Selective A1 receptor agonist. R-phenylisopropyl-adenosine
SAH	S-Adenosylhomocysteine
TBS	Tris buffered saline
TGF	Transforming growth factor
Tie 1 and 2	Angiopoeitin receptors 1 and 2
TIMPS	Tissue inhibitors of matrix metalloproteinases
TNF-α	Tumor necrosis factor alpha
tPA	Tissue type plasminogen activator
tRNA	Transfer RNA
TR	Inverted terminal repeats
uPA	Urokinase type plasminogen inhibitor
VE cadherin	Vascular endothelial cadherins
VEGF	Vascular endothelial growth factor
VEGF-R1	Vascular endothelial growth factor-receptor 1
VEGF-R2	Vascular endothelial growth-receptor 2
WBCs	White blood cells
XAC	Xanthine amine cogener
XDH	Xanthine dehydrogenase
XO	Xanthine oxidase

Abstract of Dissertation Presented to the Graduate School
of the University of Florida in Partial Fulfillment of the
Requirements for the Degree of Doctor of Philosophy

REDUCTION IN PRE-RETINAL NEOVASCULARIZATION BY RIBOZYMES THAT CLEAVE THE A_{2B} RECEPTOR MRNA

By

Aqeela Afzal

May 2003

Chair: Dr. M.B. Grant
Cochair: Dr. D. Samuelson
Major Department: Veterinary Medical Sciences

Tissue hypoxia and ischemia initiate events that lead to pre-retinal angiogenesis. Adenosine modulates a variety of cellular functions by interacting with specific cell surface G-protein coupled receptors (A_1, A_{2A}, A_{2B}, A_3) and is a potential mediator of angiogenesis. The A_{2B} receptor has been implicated in the mediation of angiogenesis. The lack of a potent, selective A_{2B} receptor inhibitor has hampered its characterization. Our goal was to design and characterize a hammerhead ribozyme that would specifically cleave the A_{2B} receptor mRNA and examine its effect on retinal angiogenesis. Active and inactive ribozymes specific for the mouse and human A_{2B} receptor mRNAs were designed and cloned in expression plasmids. HEK 293 cells were transfected with these plasmids, and A_{2B} mRNA levels were determined by quantitative RT-PCR. Human retinal endothelial cells (HREC) were also transfected, and cell migration was examined. The effects of these ribozymes on the levels of pre-retinal neovascularization were determined using a mouse model of oxygen-induced retinopathy. We produced a

ribozyme with a Vmax of 10.8 pmole min^{-1} and a kcat of 36.1 min^{1}. Transfection of HEK 293 cells with the plasmid expressing ribozyme resulted in a reduction of A_{2B} mRNA levels by 45%. Transfection of HREC reduced NECA stimulated migration of the cells by 47%. Intraocular injection of the constructs into the mouse model reduced pre-retinal neovascularization by 54%. Our results suggest that the A_{2B} receptor ribozyme will provide a tool for the selective inhibition of this receptor, and provide further support for the role of the A_{2B} receptor in retinal angiogenesis.

CHAPTER 1
BACKGROUND AND SIGNIFICANCE

The formation of blood vessels is a fundamental process that can be broken down into two basic pathways. The first is vasculogenesis, which is the formation of new blood vessels such as seen in embryogenesis. The second is angiogenesis, which is the formation of blood vessels from pre-existing blood vessels. Angiogenesis is common in both normal physiological processes (pregnancy, menstruation, wound healing) and disease states (cancer, retinopathies, psoriasis). The focus of this study is the process of angiogenesis in retinopathies, including diabetic retinopathy, the leading cause of blindness in adults, and retinopathy of prematurity (ROP).

Anatomy of the Eye

The two eyes in humans are oriented to facilitate binocular single vision, which results from the forward position of the eyes and the chiasmal crossing from axons of ganglion cells. Axons from the right visual field carry impulses to the left optic tract and vice versa. The eye contains the elements that take in light and converts them to neural signals. For protection, the eye is located within the bone and connective tissue framework of the orbit. The eyelids cover and protect the anterior surface of the eye and contain glands, which produce a lubricating film (tears).[1]

The globe has three spaces within it: the anterior chamber, posterior chamber and the vitreous chamber. [1] (Figure 1-1)

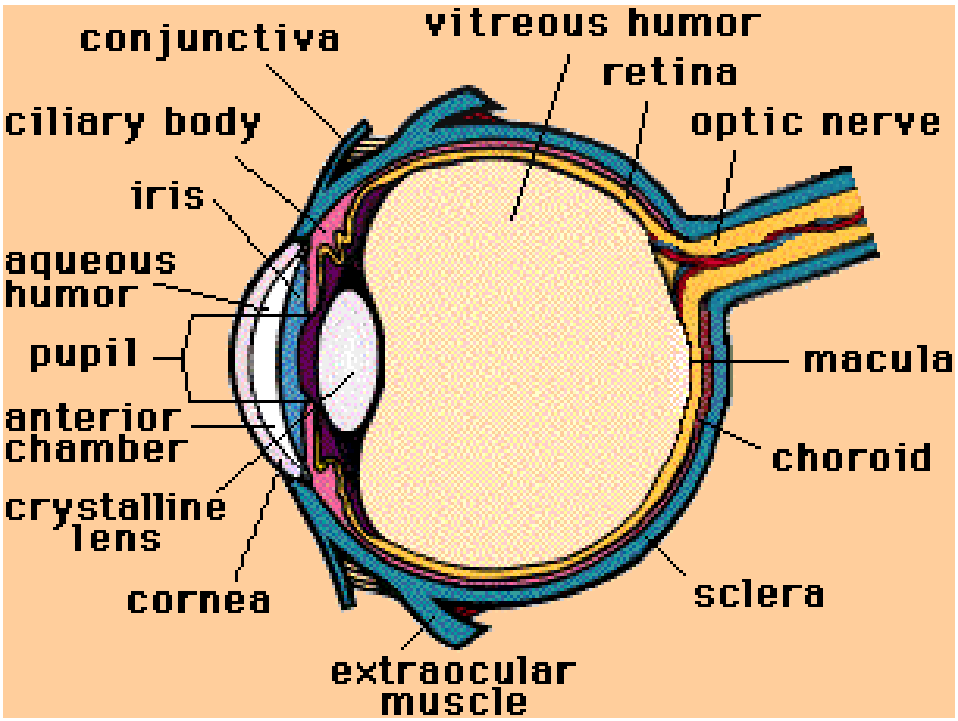

Figure 1-1. Cross sectional view of the components of the eye

The anterior and posterior chambers contain aqueous humour, which is produced by the ciliary body and provides nourishment for the surrounding structures. The vitreous chamber is the largest space in the eye and lies adjacent to the inner retinal layer and contains the gel-like vitreous humor.[1]

The eye is made up of three layers: an outer fibrous layer, a middle vascular layer and an inner neural layer (retina).[1] The outer fiber layer is a dense connective tissue that provides protection for structures within, maintains the shape of the eye, and provides resistance to the pressure of the fluids inside the eye. The sclera is the opaque white of the eye, and the cornea is transparent and allows light to enter the eye where the lens refracts it to bring light rays into focus on the retina.[1]

The middle layer of the eye is made up of three structures. The iris acts as a diaphragm to regulate the amount of light entering the pupil. The ciliary body produces components of the aqueous humor and has muscles that control the shape of the lens during accomodation. The choroid is an anastomosing network of blood vessels with a dense capillary network.[1]

The principle functions of the choroid are to nourish the outer retina and to provide a pathway for the vessels that supply the anterior eye. The choroid is an egress for catabolites from the retina, which diffuse through Bruch's membrane into the choriocapillaris. The suprachoroidal space provides a pathway for the posterior vessels and nerves that supply the anterior segment.[1,2] The choroid also plays a role in the maintenance of intraocular pressure due to the high blood flow in its vessels. The choroid has the largest sized and the greatest number of vascular channels in the eye, and the amount of blood flowing through these channels at any time has an effect on the

intraocular pressure. The choroid also provides a regular smooth internal surface for the support of the retina. The smoothness of Bruch's membrane is important in maintaining the exact relationship between the retinal pigment epithelium (RPE) and the outer segments of the adjacent photoreceptor rods and cones. [1,3]

The Retina

The retina is located between the choroid and the vitreous, and extends from the circular edge of the optic disc, where the nerve fibers exit the eye, to the ora serrata and is continuous with the epithelial layers of the ciliary body.[1,4] The retina is a thin, delicate and transparent tissue that lines the inner eye. The neural retina is attached loosely to the choroid through the pigment epithelium. Externally, the RPE contacts the collagen and elastic tissue of Bruch's membrane of the choroid. Bruchs membrane is an elastic layer that stabilizes the RPE and the photoreceptors. Internally, the retina lies next to the vitreous. Anteriorly, the RPE gives rise to the ciliary body, and posteriorly, all the retinal layers terminate at the optic disc except the nerve fiber layer. The retina is thickest at the equator and thins at the ora serrata.[1]

The retina can be divided into the central retina and the peripheral retina. The central retina is thick and includes the macula, fovea and foveola. The macula has a yellow appearance due to xanthophyl (a carotenoid), which is found in the ganglion cells. The peripheral retina includes the remainder of the retina from the macula to the temporal or nasal side. The ora serrata is the extreme periphery of the retina. It is the junction where the retina ends and gives rise to the teeth like processes that form the ciliary body. The peripheral retina ends at the ora serrata and forms the teeth like processes that form the base of the ciliary body.[1]

Under the light microscope, ten layers of the retina can be differentiated (Figure 1-2): RPE, rod and cone layer, outer limiting membrane (OLM), outer nuclear layer (ONL), outer plexiform layer (OPL), inner nuclear layer (INL), inner plexiform layer (IPL), ganglion cell layer (GCL), nerve fibre layer (NFL) and the inner limiting membrane (ILM). The visual pathway consists of three interconnecting neurons and some receptor cells. The neurons include the bipolar cells, located within the retina; the ganglion cells, located in the inner retina, the axons of which go through the optic nerve to the chiasm and end in the lateral geniculate nucleus; and the third neuron is from the geniculate body to the occipital cortex.[1]

The rods and cones are the sensory receptors. The outer segments have photopigments, which are excited by light, resulting in a visual response. The cell bodies of the rods and cones lie in the ONL and the axons synapse with dendrites of bipolar cells in the OPL. The dendrites of the bipolar cells extend to the OPL and synapse with axons of rods and cones; their axons extend to the IPL and synapse with dendrites of the ganglion cells from the NFL. The INL also has horizontal and amacrine cells. The horizontal and amacrine cells in this layer provide horizontal integration.[1] The RPE is a single layer of uniform cells. It is located in the outer circumference of the retina and extends from the edge of the optic disc to the ora serrata. The cells of this layer are hexagonal shaped and carry a brown pigment. These cells may be multinucleated, especially in the ora serrata. The RPE provides metabolites to the receptors and removes the outermost ends of external segments of the photoreceptors. If the RPE cells are damaged or diseased, these cells are not replaced; instead, adjacent cells slide laterally to fill the space of the necrotic cells. The RPE cells possess microvilli on

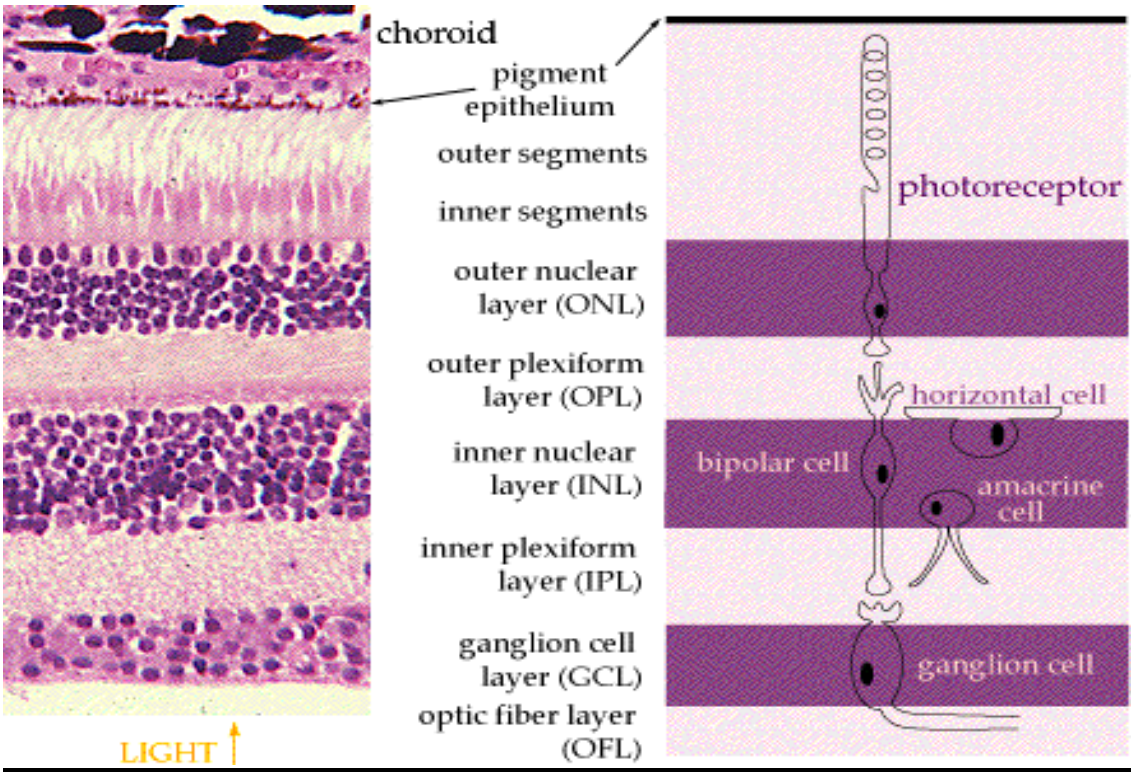

Figure 1-2. The ten layers of the retina include: retinal pigment epithelium, rod and cone layer, outer limiting membrane, outer nuclear layer, outer plexiform layer, inner nuclear layer, inner plexiform layer, ganglion cell layer, nerve fibre layer and the inner limiting membrane

the apical surface that interdigitate with the photoreceptors. The RPE is critical to vitamin A metabolism and photoreceptor maintenance.[1]

The rod and cone layer lies external to the OLM. It has a thick inner segment and thin outer segments joined by a slight constriction. The cell membrane is continuous between the constrictions. The outer segments have parallel processes, which are short in cones and long and thin in rods. [1]

The OLM under a light microscope has a thin fenestrated membrane-like appearance. However, the OLM is not a basement membrane. Electron microscopy revealed it to be a zonula adherens between the photoreceptors and the Müller cells. The zonula adherens probably serve to keep the highly elongated photoreceptors in place.[1]

The ONL has the cell bodies of the rods and the cones. The axons of the rods and cones synapse in the OPL with bipolar and horizontal cells.[1]

The OPL is a reticular structure, which is a transition zone between the receptors (neuroepithelial). The OPL is a layer of synaptic contacts between photoreceptors, bipolar cells and horizontal cells. The axons of the rods end here in spherules (oval shaped) and those of the cones end in pedicles (broad conical swellings). The spherules are invaginated and synapse with bipolar dendrites or horizontal cells, and can make 2-4 contacts. The pedicles, on the other hand, contact many dendrites of horizontal cells and bipolar cells.[1]

The INL is a band of nuclei belonging to horizontal cells, bipolar cells, and amacrine cells. The Muller cells provide support and nutrition to the retina. They surround capillary walls and extend from the ILM to the extracellular membrane.[1]

The IPL is a junction between the first order neuron (bipolar cells) and the ganglion cell layer. This layer contains the nuclei of displaced ganglion or amacrine cells and processes of the Müller cells.[1]

The GCL contains the cell bodies of ganglion cells, which are thin in the nasal area and thicker near the macula. The axons of the ganglion cells run internally and then become parallel to the inner surface of the retina to give rise to the NFL and the optic nerve fibres.[1] The NFL has the axons of the ganglion cells and is thickest around the optic nerve.[1] Branching processes of the Müller cells and a basal lamina like structure secreted by them forms the ILM. The macula is the center of the retina (area centralis) and is divided into the fovea (cone dominated), parafovea (ganglion cell dominated) and the perifoveal retina (single layer of ganglion cells).[1]

Blood Supply to the Retina

The retina has the highest rate of metabolism of any tissue in the body and thus has a dual blood supply from the retinal and choroidal capillaries. If either of these sources is interrupted, ischemia develops and leads to loss of function. The outer retina is supplied by the choriocapillaris and the central retinal artery supplies the remainder. The retinal artery is different from other arteries and does not have an internal elastic lamina but does have a prominently developed muscularis.[1,5]

The outer retinal layers receive their nutrition from the choroidal capillary bed; metabolites diffuse through Bruch's membrane and the RPE into the neural retina. The central retinal artery provides nutrients to the inner retinal layers. The artery enters the retina through the optic disc, usually slightly nasal of center, and branches into a superior and inferior retinal artery, each of which further divides into nasal and temporal branches, and these vessels continue to bifurcate. The nasal branches run a relatively straight

course toward the ora serrata, but the temporal vessels arch around the macular area en route to the periphery. Two capillary networks exist within the retina. The deepest one lies in the inner nuclear layer near the outer plexiform layer, and the superficial one is in the nerve fiber or ganglion cell layer. The OPL is avascular and thought to receive its nutrients from both retinal and choroidal vessels.[1,5]

Retinal arterial circulation is terminal; therefore there is no direct communication between the retina and other vessel systems. The junctions of endothelial cells in retinal vessels are tight or occluded. Thus, to enter or leave the retina, most substances require active transport across the endothelial cells. The outer retinal layers receive their nutrition from the choroidal capillary bed; the central retinal artery provides nutrients to the inner retinal layers. These vessels are distributed to the four quadrants of the retina.[6] The retinal artery and vein to a particular quadrant supply most of the quadrant. If arterial supply to a retinal quadrant is interrupted, infarction of that section occurs. The retinal capillaries supply the inner two thirds of the retina; the choroidal circulation supplies the remaining outer retina via regulated transport across the pigment epithelium.[1,5]

The Blood Retinal Barrier

The epithelial portion of the blood-retinal barrier is the retinal pigment epithelium. This barrier separates the choroidal tissue fluid, which is similar to plasma, from the retinal tissue fluid. Tight junctions that exist between the endothelial cells of the retinal vessels and similar tight junctions in the RPE maintain the blood retinal barrier. Thus, the retinal vessels are impermeable to the passage of molecules greater than 20-30 kDa, and small molecules such as glucose and ascorbate are transported by facilitated diffusion through the RPE.[1,5,7]

Vascular beds are situated to provide nourishment. To avoid problems with the presence of blood vessels in the outer retina, the outer layers of the retina receive their nourishment from the choriocapillaris.[1]

Retinopathies

The retina of the eye is uniquely situated to provide optimal vision. Blood supply to the retina is also strategically placed to avoid any hindrance of the visual pathway. Retinopathies (diseases affecting the retina) disrupt this balance and lead to loss of vision. Retinopathies affecting humans include: age related macular degeneration (ARMD), which primarily affects the aging population; diabetic retinopathy (DR), which primarily affects the working population; and retinopathy of prematurity (ROP) which primarily affects the newborns.

Age Related Macular Degeneration

ARMD is a disease which affects the RPE and leads to blindness in the aged populations.[8] There are two forms of ARMD: dry and wet.[9-11]

Dry ARMD is characterized by the presence of soft drusen and pigmentary abnormalities. Drusen is an amorphous acellular debris present within the basement membrane of the RPE. It is seen as 'yellow' spots within the macula. Low amounts of drusen are a consequence of age; however, a larger amount present within the retina is indicative of ARMD.[10] Drusen leads to mild vision loss and increases the risk of progression of the disease to the wet form of ARMD.[8,9]

The wet form of ARMD (also known as the exudative or the neovascular phase) is characterized by choroidal neovascularization, RPE detachment and disciform scarring. The wet form of ARMD leads to rapid vision loss. The choroidal neovascularization

(CNV) leads to the formation of immature blood vessels which result in leakage of serum and blood and loss of central vision.[9,12] (Figure 1-3)

Diabetic Retinopathy

Diabetes Mellitus affects millions of people worldwide and is the leading cause of blindness in working age adults.[13,14,15] There are two forms of diabetes mellitus: Type I, which typically affects juveniles and is known as insulin dependent diabetes mellitus, and type II, which is the adult onset form of diabetes and is known as non-insulin dependent diabetes mellitus.[15] Diabetes also leads to systemic complications such as kidney failure, hypertension and cardiovascular disease.[16,13] DR is the most frequent diabetic complication. Eye problems due to diabetes can be asymptomatic and if left untreated can lead to serious visual loss. The longer a patient has diabetes, the more likely they are to develop diabetic retinopathy.[13,16,17,15] Diabetic eye disease can be divided into two phases: background diabetic retinopathy (non-proliferative phase) and proliferative diabetic retinopathy (PDR).

Non-Proliferative Diabetic Retinopathy (NPDR)

In NPDR small retinal blood vessels are damaged. NPDR is the result of two major processes which affect retinal blood vessels, vessel closure and abnormal vessel permeability.[13] The vessels leak fluid (edema) and later blood (hemorrhage) into the retina. Macular edema is the most common cause of reduced vision in patients with non-proliferative diabetic retinopathy and is seen as milkiness of the retina surrounded with exudates (yellow clumps). [16],[15] These exudates are the result of fat or protein leaking out of the vessels. Water is quickly reabsorbed into the vessels

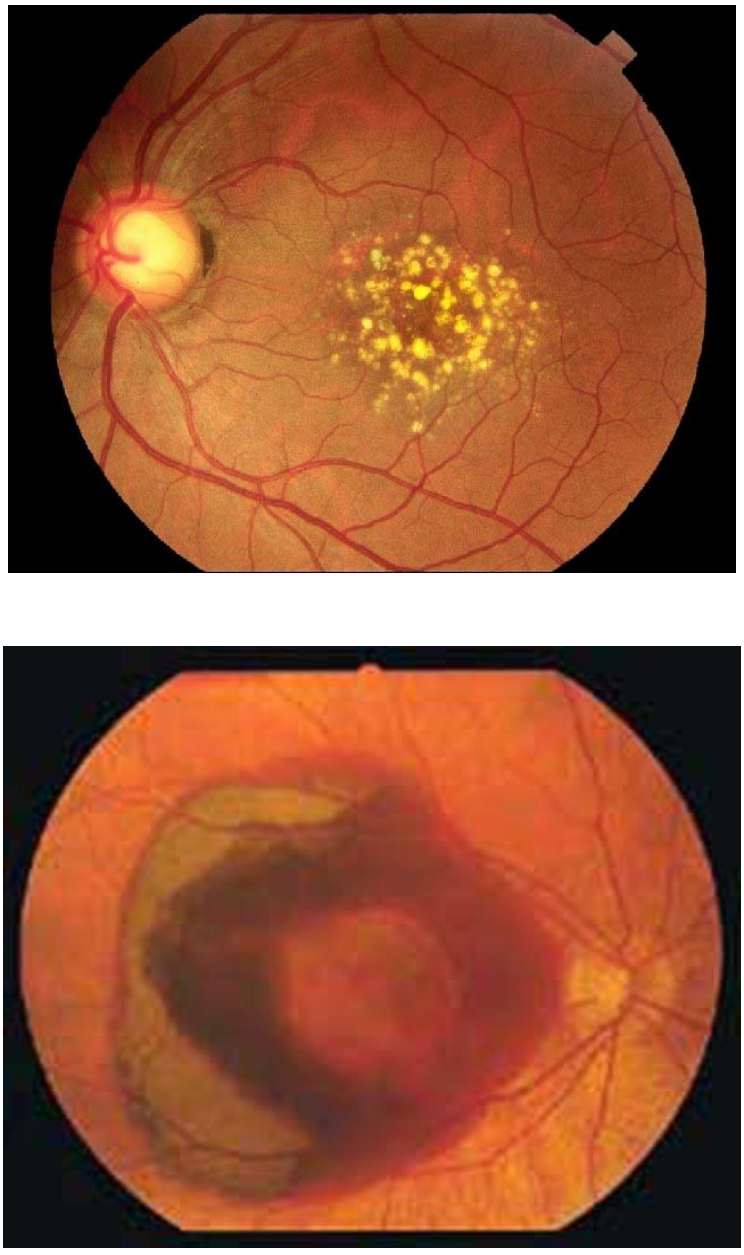

Figure 1-3. A. A fundus shot showing drusen (yellow). B. Wet form of ARMD showing blood leakage. (National Eye Institute)

or tissue under the retina. However, the fatty material is absorbed very slowly and thus left behind surrounding the leakage site.[16,18] (Figure 1-4)

Vessel closure may be due to blood cell clumping, damaged endothelium, swelling of an abnormally permeable vessel wall or compression of the capillary by surrounding retinal swelling. Diabetic patients have closure/non-perfusion of capillaries, which leads to a decreased oxygen supply. In areas surrounding the area of non-perfusion capillaries dilate to compensate for the decreased oxygen supply. Small focal dilations (microaneurysms) of retinal capillaries also develop due to weakened capillary walls, thus allowing for bulging. [13] When multiple areas of the retina have lost their blood supply, angiogenic factors are released which stimulate proliferation of new blood vessels. These new blood vessels are small and fragile, therefore, cause bleeding and the formation of scar tissue within the retina. Small arterial closures follow capillary closure, and deprive larger regions of the retina of blood supply. This is seen as 'cotton wool spots' on the retina in fluorescein angiography.[16]

Blood vessels in the body are usually fenestrated allowing fluid to pass through vessel walls. These openings are small enough to allow water and ions to pass through, while preventing the passage of blood cells and larger proteins. In contrast, retinal blood vessels have tight junctions between the endothelial cells of blood vessel. Therefore, all fluids and molecules exiting the vessels have to pass through the cell. This lack of fenestration helps to keep the retina thin and dehydrated for proper function. These tight junctions form the blood retinal barrier, which partitions the neural retina from the circulation and protects the retina from circulating inflammatory cells.[16] The tight junctions are formed by a number of proteins such as: occludin and claudin. These

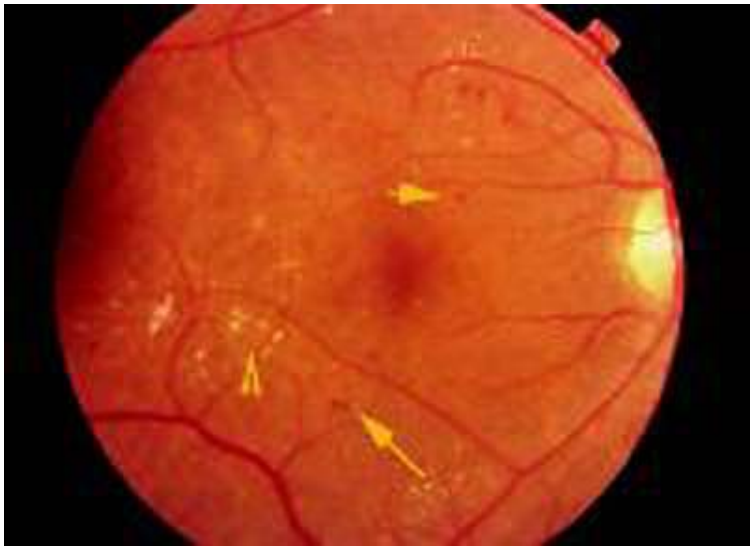

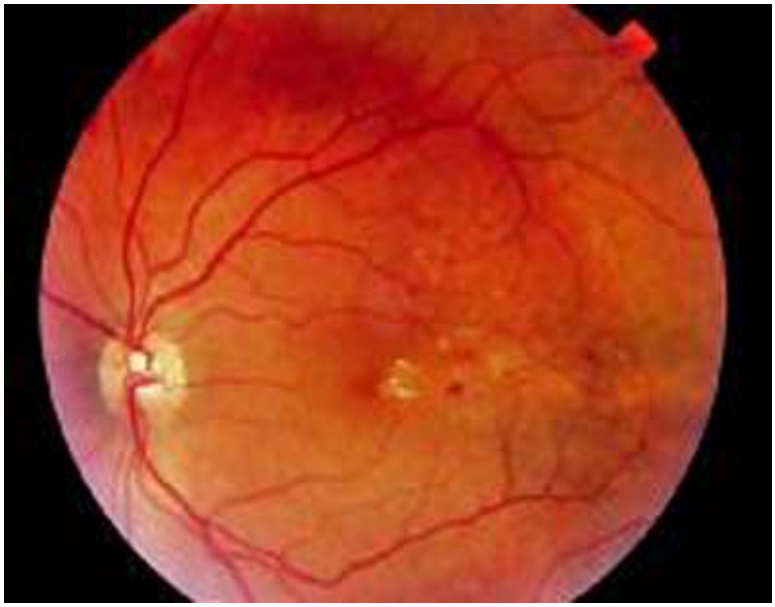

Figure 1-4. A. Non-proliferative retinopathy. Hemorrhage (arrowhead) short arrow microaneurysm, larger arrow exudates. B. Macular edema. (National Eye Institute)

proteins limit the flow of fluid between endothelial cells. Diabetic patients have a lower amount of occludin at the tight junctions in the retinal endothelial cells and can leak fluid.[16]

Proliferative Diabetic Retinopathy (PDR).

Proliferative diabetic retinopathy is the stage of diabetes characterized by angiogenesis on the surface of the retina. [13] Patients can have NPDR for years before progressing to PDR. PDR is diagnosed by the presence of proliferating blood vessels within the retina or optic disc. These vessels grow on the retinal surface or into the vitreous cavity and take on a frond-like configuration as they grow.[19] (Figure 1-5) The new blood vessels form due to the closure of retinal capillaries, which leads to ischemia. As patches of the retina are deprived of oxygen and nutrients, vasoproliferative factors are released which diffuse into the vitreous cavity. These factors stimulate growth of new vessels throughout the retina.[15]

The new blood vessels are not located in the same location as the ischemically damaged retina and are very fragile and bleed into the vitreous. A small amount of blood may be removed in a few weeks and larger blood hemorrhages may take a few months. If dense blood from multiple recurrent hemorrhages occurs, then vision may not be restored since the residual inflammatory debris and dead cells cannot be removed. Another complication of PDR is traction retinal detachment. New vessels grow and regress and lay down fibrous scar tissue, which contracts and shrinks as it matures. If the neovascularization is on the surface of the retina then contraction of the fibrous scar distorts the retina. However, if the vessels grow into the vitreous and contract, retinal detachment occurs which leads to blindness. [13,15]

Figure 1-5. New blood vessel growth around optic nerve in PDR (Top). Hemorrhage from new blood vessel growth (Bottom). (National Eye Institute)

Retinopathy of Prematurity

Retinopathy of prematurity (ROP), also known as retrolental fibroplasia, is a potentially blinding condition affecting the retina of newborns. In the 1950s, it was associated with the use of high oxygen levels in neonatal units.[20] Modern neonatal care has curbed the incidence of ROP, but because the survival rate of low-birth-weight infants is increasing, the exposure of surviving babies to high oxygen levels is also increasing and ROP is still a relevant clinical problem.[21,22]

ROP causes more blindness among children in the world than all other causes combined. It begins after removal from high oxygen conditions and may progress rapidly to blindness over a period of weeks.[23] Active growth of the fetal eye occurs between the last 12 weeks of full term delivery (28-40 weeks of gestation). At 16 weeks of gestation, blood vessels gradually grow over the surface of the retina. Vessels reach the anterior edge of the retina and stop progressing at about 40 weeks of gestation.[20,21,24,25]

The international classification of ROP (ICROP) defines retinopathy by several distinct criteria: location, extent, stage, and plus disease.[26] Location refers to the location of the damage to the retina relative to the optic nerve. Normally retinal vessels begin growth at the optic nerve and gradually move toward the edge of the retina. Vessels further from the optic nerve are more mature. To standardize the location of ROP, the retina is divided into three zones: Zone I is centered on the optic disc and extends from the optic disc to twice the distance between the disc and macula; Zone II is a concentric ring around zone I and extends to the nasal ora serrata (the edge of the retina on the side toward the nose); and zone III is the remaining crescent of retina on the temporal side (side towards the temple) (Figure 1-6). The extent of ROP is described by the clock hours

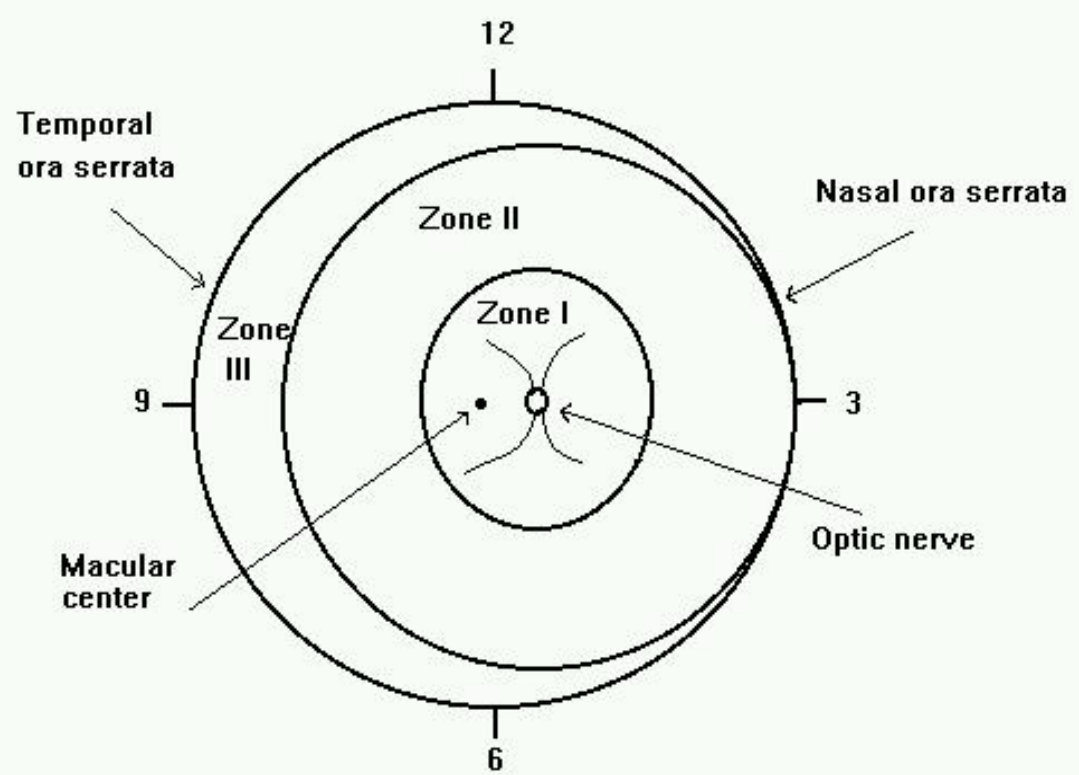

Figure 1-6. ICROP definition of retinopathy. The retina is divided into three zones: Zone I, Zone II and Zone III .

of the retina involved in the ROP. For example, if the ROP extends from 1:00 to 5:00, the extent of ROP is 4 clock hours.[24,27]

ROP is a progressive disease that begins with some mild changes in vessels and may progress on to more severe changes. The five stages of ROP describe the progression of the disease (Figure 1-7). Stage 1 is characterized by a demarcation line between the normal retina (near the optic nerve) and vascularized retina. In stage 2, a ridge of scar tissue rises up from the retina due to growth of abnormal vessels. This ridge forms in place of the demarcation line. In stage 3, the vascular ridge grows due to spread of abnormal vessels and extends into the vitreous. Stages 4 and 5 refer to retinal detachment; stage 4 refers to a partial retinal detachment caused by contraction of the ridge, thus pulling the retina away from the wall of the eye; and stage 5 refers to complete retinal detachment. Plus disease is a very severe form of ROP which is characterized by the abnormal growth of blood vessels near the optic nerve.[24,28]

Treatment of Retinopathies.

Spot laser photocoagulation is used for the treatment of ROP.[29] This uses an argon/diode laser to burn spots on the peripheral and middle portions of the retina. When laser light hits blood or pigment, it is absorbed as heat energy and produces a small burn. The laser treatment leads to a decrease in the level of vasoproliferative factors produced by the ischemic retina. The avascular retina is treated using a small laser spot (Figure 1-8). The laser spot directly treats the retina and the underlying tissue, thus reducing inflammation and results in less damage to other ocular structures. Destruction of small patches of the ischemic retina reduces the oxygen demand and decreases the vasoproliferative factor production. Laser treatment also thins the pigmented tissue under

Stage 1 ROP is characterized by a demarcation line. The orange vascular retina is on the left and the gray peripheral retina is on the right separtated by the white line.

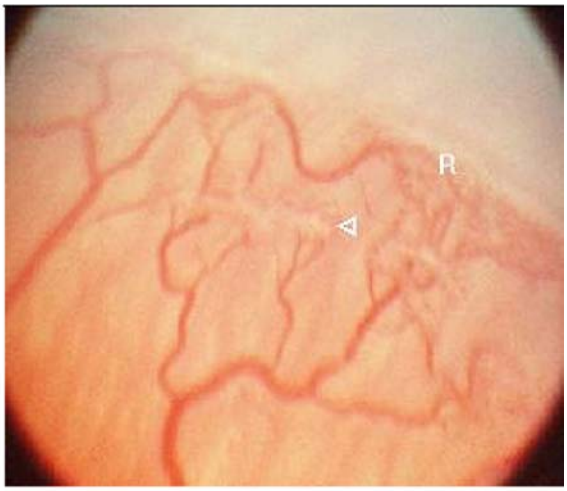

Stage 2 ROP; the white line is replaced by a ridge of scar tissue R. The arrow shows a tuft of new vessels.

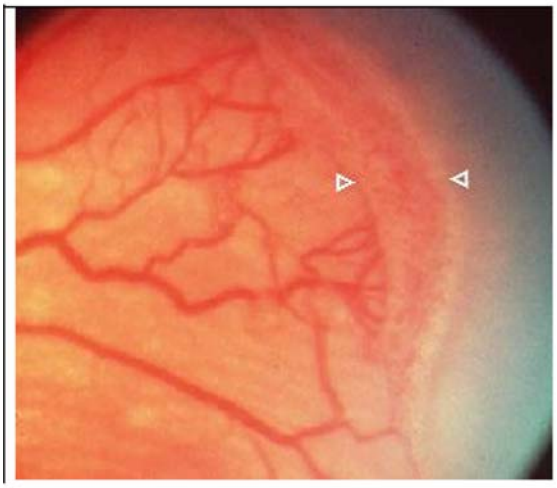

Stage 3 ROP. The size of the ridge has increased (between arrows) and the growth of the ridge extends into the vitreous.

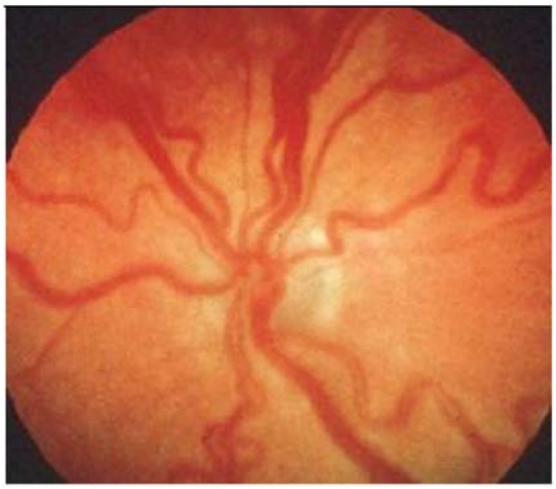

Plus disease shows dilation and tortuosity of blood vessels near the optic nerve.

Figure 1-7. The five stages of ROP (National Eye Institute)

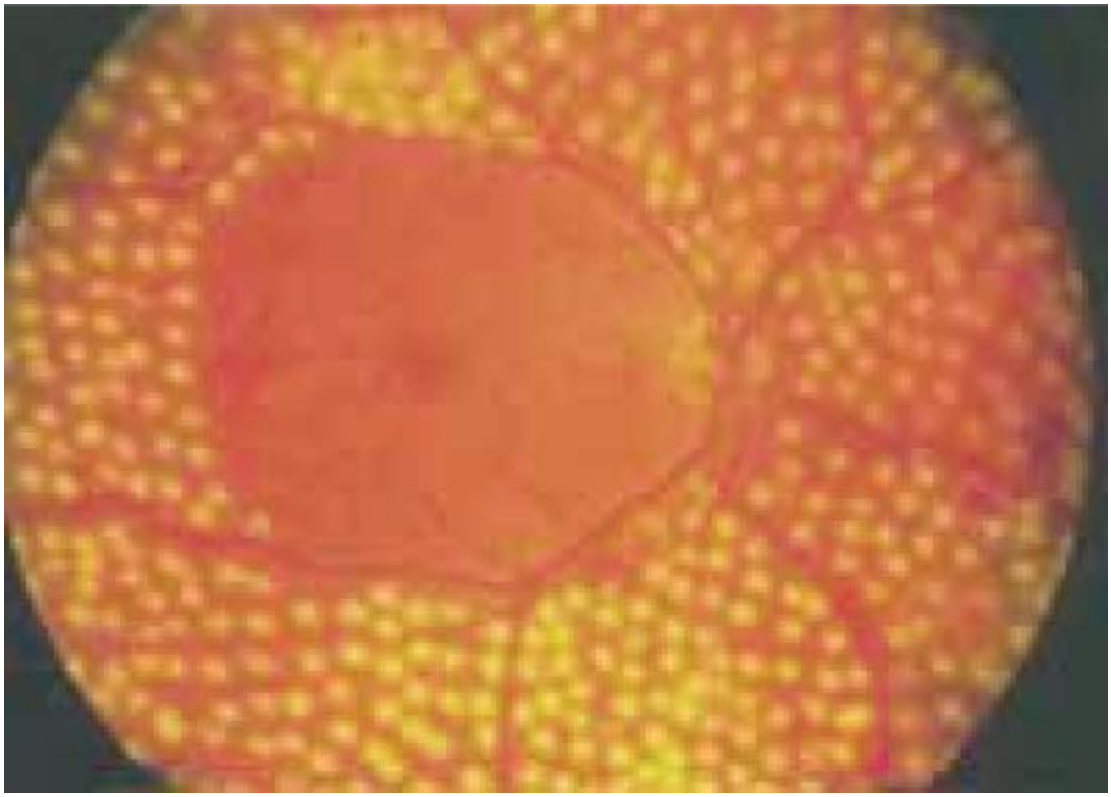

Figure 1-8 Laser treatment of the eye. The laser spot directly treats the retina and the underlying tissue. Laser treatment thins the pigmented tissue under the retina and allows more oxygen to diffuse in from the vessels under the retina

the retina thus allowing better oxygen diffusion in the retina. Laser treatment increases oxygen supply, lowers the demand for oxygen and lowers the incidents for new vessels growth.[30,28] Laser photocoagulation also causes less pain than other therapies. Currently laser treatment is the best option for the treatment of retinopathies.[14,31,29,32]

Cryotherapy is also one of the treatments available for the treatment of retinopathies.[33,34] This technique involves placing a cold probe on the sclera until an ice ball forms on the retinal surface. Multiple applications are done to cover the entire vascular area (Figure 1-9). This thins the tissue under the retina (by destroying it) and allows easier oxygen diffusion through the retina.[31] Due to the pain involved in cryotherapy, anesthesia has to be administered which is a risk factor for premature infants. If no anesthesia is administered, cardiac arrest follows. Another complication is hemorrhage due to excessive bleeding.[31,33,35,36]

If laser photocoagulation or cryotherapy is unsuccessful, a scleral buckle may be used.[37] This involves surgery and is used if there is shallow retinal detachment due to the

contraction of the ridge. A silicone band is tightly placed around the equator of the eye thus producing a slight indentation on the inside of the eye.[38] This indentation relieves traction of the vitreous gel and allows the retina to flatten back onto the wall of the eye. The silicone band is then removed a few months later to allow the eye to grow.[14,31,39] If the scleral buckle is not sufficient, vitrectomy may be performed. Small incisions are made into the eye, the vitreous removed and replaced by saline. This technique also has had limited success. Current available therapies for the different types of retinopathies have had limited success. The underlying cause of retinopathies is angiogenesis

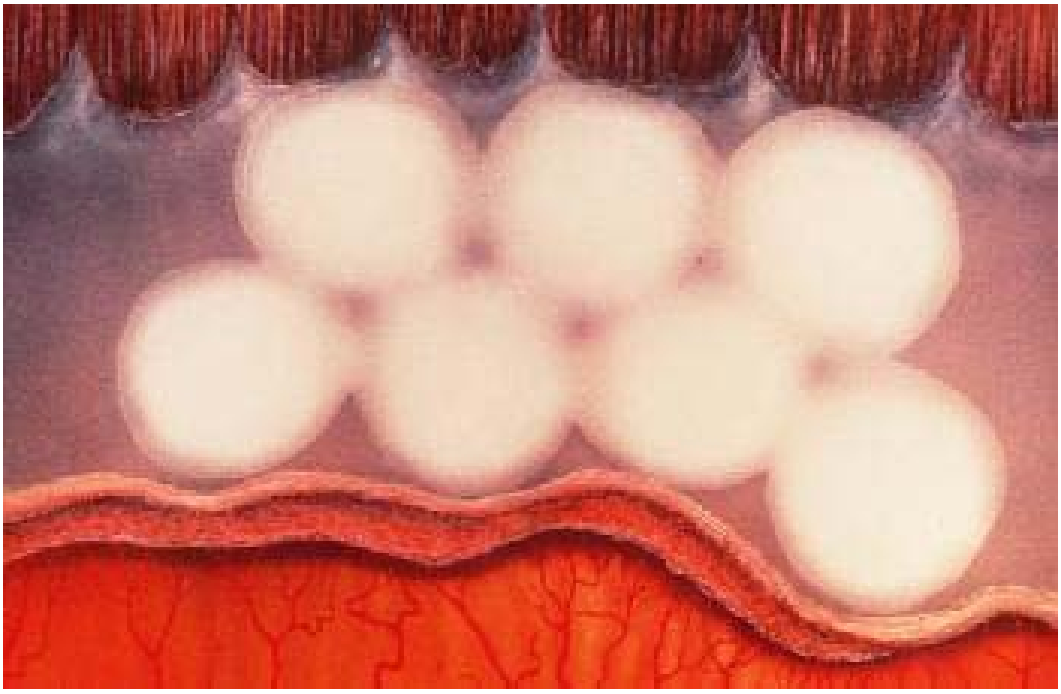

Figure 1-9. Cartoon showing cryotherapy application to the anterior avascular retina. A cold probe is placed on the sclera till an ice ball forms on the retinal surface. Multiple applications are done to cover the entire vascular area. This treatment thins the tissue under the retina and allows easier oxygen diffusion through the retina

(abnormal blood vessel formation). Development of other effective therapies for the diseases requires an understanding of the process of angiogenesis.[28,33,40-42]

Angiogenesis

Vasulogenesis is the formation of new blood vessels. Precursor cells (angioblasts) differentiate into endothelial cells which later link to form blood vessels. Angiogenesis on the other hand is the sprouting of blood vessels from pre-existing blood vessels.[43] The vasculature of the retina undergoes both vasculogenesis and angiogenesis. The superficial retinal vessels, which originate at the optic disc, are formed by the process of vasculogenesis and the process of angiogenesis later forms the capillary beds.

The process of angiogenesis involves endothelial branching, sprouting, migration, proliferation and anastomosing with endothelial cells in existing vessels.[43-45] (Figure 1-10) Vascular endothelial cells form a monolayer throughout the entire vasculature. They are polarized cells with an apical surface and a basal surface, which is surrounded by a basal lamina.[46-49] Mural cells wrap around this structure and are contractile cells, which regulate vessel diameter and consequently blood flow.[47,50] On large vessels they are multi layered and referred to as smooth muscle cells. On capillaries mural cells are sparse and usually referred to as pericytes.[48,50] The extracellular matrix, bound factors and the soluble growth factors all play an important role in the process of angiogenesis.

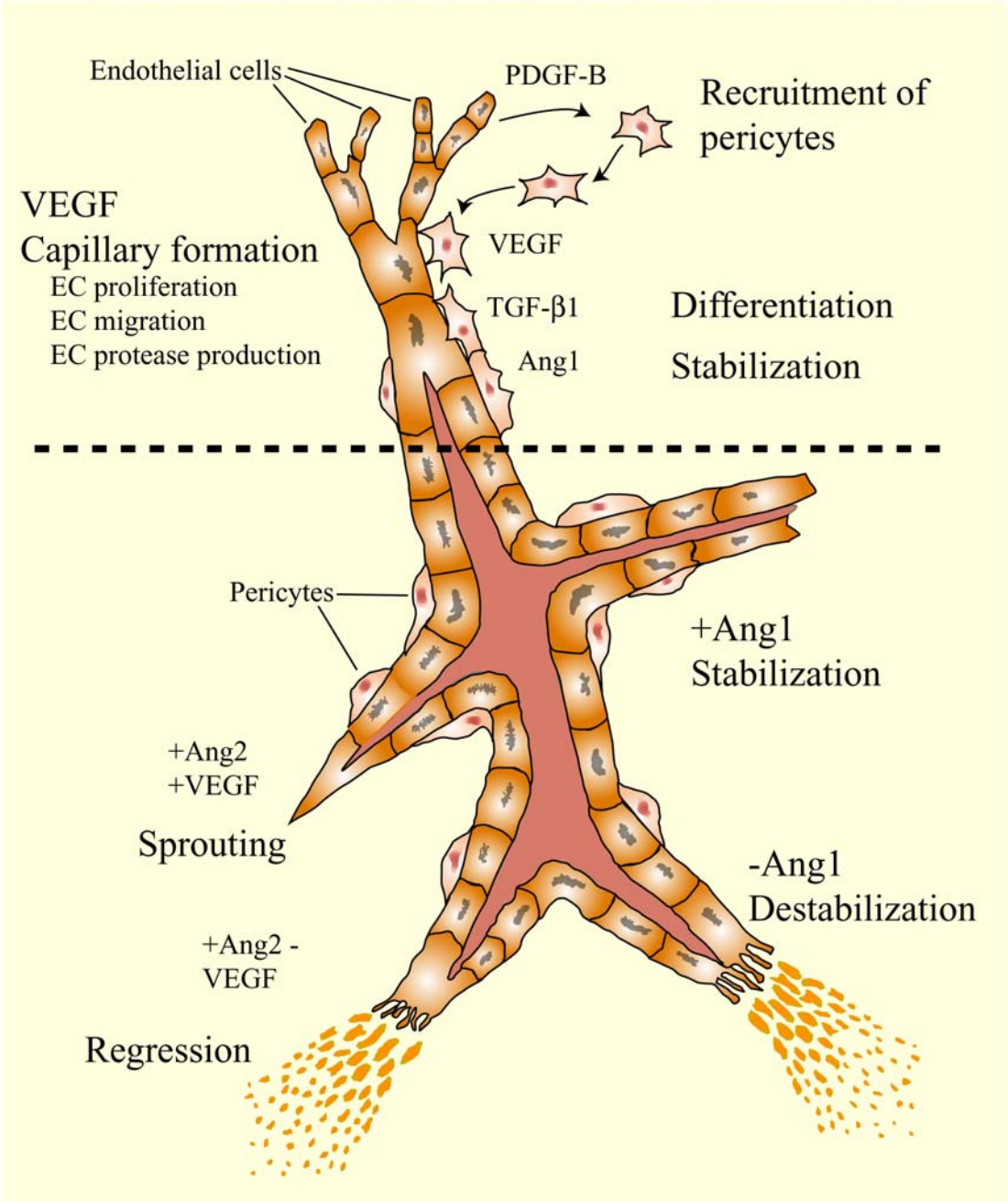

Figure 1-10. The process of angiogenesis. The process of angiogenesis involves endothelial branching, sprouting, migration and proliferation. Vascular endothelial cells form a monolayer throughout the entire vasculature. Pericytes wrap around these cells.

Extracellular matrix (ECM).

The ECM surrounds and provides mechanical support for blood vessels. The activated endothelial cells cerate gaps in the basement membrane, which allows them to sprout into the ECM. The ECM is composed of two compartments: the interstitial matrix and the vascular basement membrane.[51,52]

The interstitial matrix consists of fibrillar collagen and glycoproteins (e.g. fibronectin, laminin). Fibronectin attaches cells to a variety of ECM components, and laminin anchors cell surfaces to the basal lamina. Collagen provides structural support, is synthesized by fibroblasts and is the most abundant protein comprising the ECM. There are 12 types of collagen and types I, II and III are the most abundant types of collagen in the ECM.[51,52] The vascular basement membrane lies between the endothelial cells and pericytes. It is composed of type IV collagen, which forms the basal lamina upon which the endothelium rests, and heparan sulfate proteoglycans.[51]

Proteoglycans are glycosaminoglycans (GAGs) linked to proteins. Cell surface heparan sulfate proteoglycans (HSPGs) function as endothelial cell receptors that recognize the ECM. They are present in the basement membranes and cell surfaces. These proteoglycans modulate the response of endothelial cells to basic fibroblast growth factor (bFGF), vascular endothelial growth factor (VEGF) and other heparan binding angiogenic factors by sequestering these molecules in the ECM. Heparatinases trigger the release of these growth factors from the ECM and make them available for angiogenic stimuli.[51,53]

ECM degradation

Endothelial cells degrade the surrounding ECM by the release of plasminogen activators (PAs) and matrix metalloproteases (MMPs).[54] The PAs hydrolyze plasminogen

to plasmin, which is a general protease that can digest most proteins. (Figure 1-11) It also converts latent collagenase into active collagensase which can then degrade collagen type I, II and III. [54] There are two types of PAs: tissue type PA (tPA) and urokinase-type PA (uPA).[55] Both PAs utilize the same substrate, plasminogen, and both have two specific inhibitors, plasminogen activator inhibitor-1 (PAI-1) and plasminogen activator inhibitor-2 (PAI-2). PAI-1 is produced by endothelial cells to inhibit PA activity to ensure a balanced degradation of the ECM. uPA and PAI-1 are also upregulated by angiogenic factors such as basic fibroblast growth factor (bFGF) and vascular endothelial growth factor (VEGF)[54-56]

Matrix metalloproteases (MMPs) are zinc dependent endopeptidases which are secreted as zymogens and proteolytically activated by other MMPs or plasmin.[51] MMP expression may also be regulated by growth factors such as VEGF, bFGF and TGF-β.[51,56] MMPs degrade components of the ECM and are subdivided into: collagenases, stromelysins (cleave laminin and fibronectin), matrilysins, gelatinases (cleave collagen type IV), membrane type (MT) MMP and other MMPs. Endothelial cells, smooth muscle cells and fibroblasts produce collagenase 1 (MMP-1), stromelysin (MMP3), gelatinase A (MMP-2), gelatinase B (MMP-9), matrilysin (MMP-7), and MT1-MMP (MMP-14, which has fibrinolytic activity).[54,55]

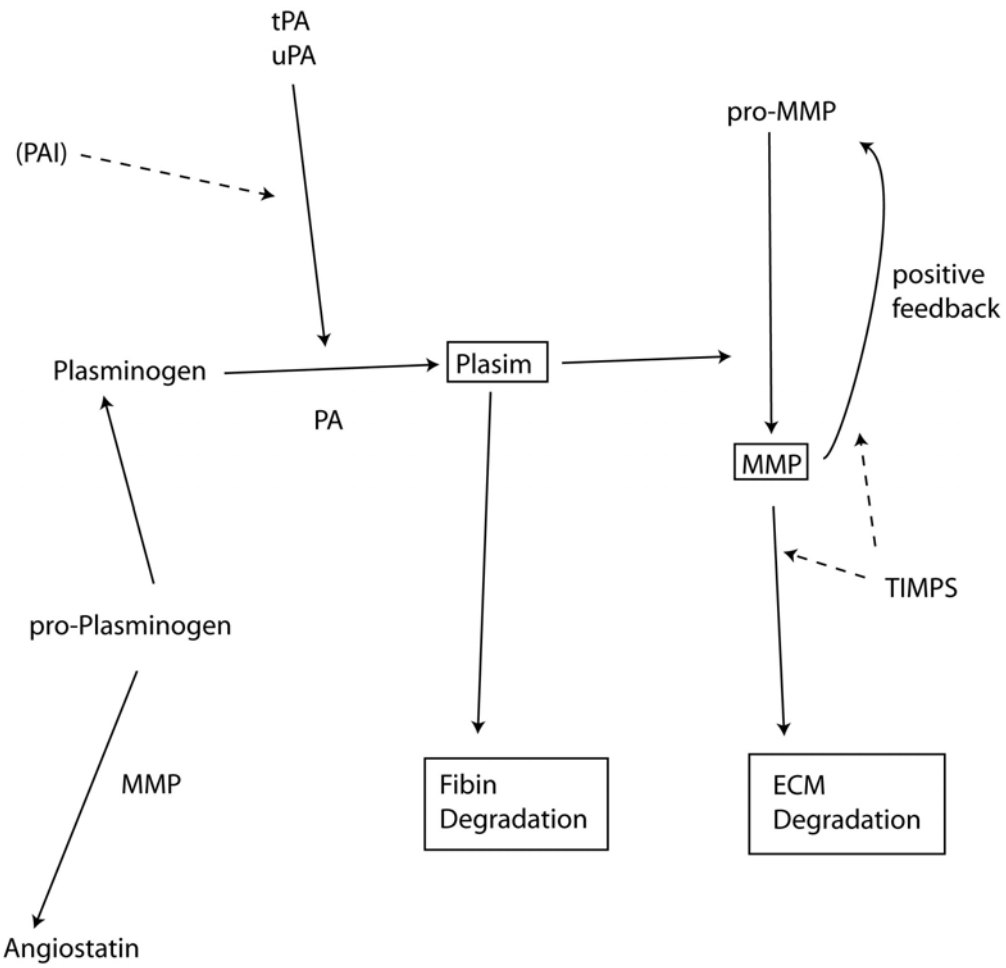

Figure 1-11. PAs hydrolyze plasminogen to plasmin. Plasmin subsequently activates matrix metalloproteases, which degrade the extra cellular matrix. PA=plasminogen activator; uPA=urokinase type PA; tPA=tissue type PA; PAI=plasminogen activator inhibitor; MMP=matrix metalloproteases; TIMPs=tissue inhibitors of MMPs

Endothelial cells also produce tissue inhibitors of MMPs (TIMPs) that are specific inhibitors of MMPs and modulate the degradation of the ECM. TIMPs are secreted proteins, which inhibit MMPs in a 1:1 stoichiometry. They reversibly interact with the catalytic domain of the MMPs to inhibit their activity. TIMPs differ in their ability to interact with various MMPs. For example, TIMP2 inhibits MT-MMP and TIMP3 inhibits MMP9. TIMPs also bind to the heparan sulfate proteoglycans in the ECM and concentrate them to the specific regions within the tissue. [56]

Angiostatin and endostatin are naturally occurring anti-angiogenic molecules, however, they are also produced by proteolytic cleavage by MMPs from the pro-forms of plasminogen and collagen XVIII, respectively.[57] The production of MMPs, however, is cell and tissue specific. For example, bFGF and VEGF upregulate interstitial collagenase (MMP-1) and also increase the formation of plasmin. Plasmin converts the inactive form of MMP-1 to the active form. Gelatinase A (MMP-2) is upregulated by calcium influx. It is responsible for the angiogenic switch and for the differentiation of the endothelial cells into tubes. MMPs promote capillary tube formation, however, at high concentrations, they have an opposite effect.

ECM degradation produces fragments, which have the opposite effect of the intact molecule. For example, hyaluronan, a GAG found in the ECM, has anti-angiogenic properties. However, when cleaved, it enhances the action of angiogenic factors. Conversely, proteolytic degradation of fibronectin, plasminogen and collagen produces fragments, which have both anti-angiogenic and angiogenic activity. MMP2 undergoes proteolysis to produce PEX, which is the C-terminal non-catalytic domain of MMP2. PEX is anti-angiogenic and inhibits the gelatinolytic activity of MMP2.

Bound Factors.

Activated endothelial cells are anchorage dependent for survival. In addition to degradation of the ECM, the endothelial cells require bound factors to help in migration towards the ischemic stimulus. These bound factors include integrins, Eph receptor Eph/Ephrins complexes, and VE cadherins

Integrins.

Integrins provide the scaffolding for the cells to migrate upon and are used by the endothelial cells to recognize the ECM.[58] Integrins play a role in regulating cell growth, differentiation and survival.[59-63]

Integrins are cellular receptors for ECM proteins and are expressed by all adhesive cells.[64] Integrins are composed of α and β chain heterocomplexes, which are integral membrane glycoproteins. They have long extracellular domains, which are the ligand binding regions. Eighteen different α subunits, and 8 β subnits have been identified. These subunits can associate in 24 known combinations. A short transmembrane region follows the short intracellular domains of both the α and the β subunits and the cytoplasmic tail of the beta subunit links the integrins to cytoskeletal actin of the endothelial cell.[62,63,65]

Integrins are linked intracellulary to actin filaments by specific actin binding proteins, such as Talin, alpha actinin, vinicluin and paxillin.[66] Focal adhesion kinase (FAK) is a protein with tyrosine kinase activity and is composed of a large kinase domain flanked by an amino and carboxyl terminus. A region of the c-terminus, known as focal adhesion targeting sequence (FAT) recruits FAK to paxillin. Integrin mediated cell adhesion occurs when FAK is tyrosine phosphorylated.[58]

$\alpha_v\beta_3$ has a well-characterized role in angiogenesis. It mediates adhesion of cells to vitronection, fibronectin, von Willebrand factor, osteopontin, tenascin and thrombospondin. Although the $\alpha_v\beta_3$ integrin is minimally expressed on normal resting blood vessels, it is significantly upregulated in newly formed blood vessels within tumors, in healing wounds and in response to certain growth factors. $\alpha_v\beta_3$ expression is

upregulated in endothelial cells exposed to angiogenic factors and those exposed to hypoxia. Integrins also help to target the activity of the MMPs, for example, $\alpha_v\beta_3$ interacts with MMP-2 and also regulates signaling via the vascular endothelial growth factor receptor –2 (VEGF-R2). Natural components of the ECM, such as, endostatin, angiostatin, thrombospondin and tumastatin are all anti-angiogenic and exert their effect by binding to the $\alpha_v\beta_3$ intergrin and disrupting the endothelial cell-ECM interaction. If this integrin is disrupted using an antibody (LM609) or a peptide antagonist (cyclic peptide 203, RGDfv), it results in the disruption of angiogenesis progression. VEGF and bFGF are capable of inducing the expression of $\alpha_v\beta_3$ integrin of endothelial cells.[67,68]

EpH receptors.

To discriminate cell partners from fibroblasts or inflammatory cells, the Eph receptor is utilized. The Eph receptor is the largest receptor of the receptor tyrosine kinase family (RTK) family.[69,70] The receptors are divided based on ligand affinity into class A and class B. The extracellular domain of the Eph receptor consists of the ligand binding globular domain, cysteine rich region and 3 fibronectin type II repeats. The cytoplasmic portion of the receptor consists of a juxtamembrane domain, and a carboxyl terminus. The ligands for these receptors are ephrins, which are also divided into subclass A and subclass B. Ephrins subclass A are anchored to the plasma membrane by

glycosylphosphatidylinositol (GPI) anchor and ligands A1-A5 have been identified. Ephrins subclass B have a short transmembrane domain and a short cytoplasmic tail. Only three subclass B ephrins have been identified (B1-B3). Both the receptor and the ligands are membrane bound and therefore a signal is transduced in the receptor expressing cells and the ligand expressing cells.[70,71]

Prior to cell-cell contact, the Eph receptor and ehprins ligand are loosely clustered at the cell surface. Following cell-cell contact, the receptor and ligand heterodimerize and tetramerize. These receptors are capable of bi-directional signaling (forward and reverse signaling). Eph A receptor enhances the adhesion of cells and the number of focal adhesion points and is known to be involved in forward signaling. Eph receptor B is phosphorylated in the intracellular domain and is known to be capable of both forward and reverse signaling.[72]

Vascular endothelial (VE) cadherins

Endothelial cells express at least three cadherins: N-, P and VE cadherin. N-cadherin is diffusely spread across the cell, P cadherin is present in trace amounts and VE cadherin is specifically localized to inter endothelial cell junctions. Beta catenine and plakoglobulin are anchored to the cadherin through actin and α catinine. VE cadherin mediates contact inhibition of endothelial cells by decreasing the amount of proliferation and allows endothelial cell monolayers formation in the vessel wall. VEGF increases endothelial cell permeability by phosphorylation of a tyrosine residue of VE cadherin. This phosphorylation leads to dissociation of the VE cadherin and translocation of the beta catenine/plakoglobulin complex to the nucleus to regulate gene transcritption.[73-75]

Growth Factors.

The process of angiogenesis requires co-ordination of several growth factors, which play distinct roles in the process, examples include: angiopoeitins, vascular endothelial growth factor (VEGF), fibroblast growth factor (FGF), platelet derived growth factor (PDGF) and transforming growth factor (TGF).

Angiopoeitins

Angiopoeitins are secreted ligands for the two Tie receptors: Tie 1 and Tie2 (Tek). Both receptors are endothelium specific,[73] and have an extracellular domain composed of two immunoglobulin like folds and three fibronectin repeats. The cytoplasmic region has a tyrosine kinase domain interrupted by a short kinase insert.

Angiopoeitin-1 and angipoeitin-2 are ligands for the Tie receptors. Both ligands can bind the receptors, however, only ANG1 can phosphorylate the receptor.[76] ANG-2 inhibits Tie2, detaches pericytes and loosens the matrix surrounding the vessel. ANG-1 does not initiate endothelial network organization it stabilizes networks initiated by VEGF by enhancing the interaction between endothelial cells and pericytes. Binding of ANG1 to the Tie 2 receptor initiates cell survival through the PI3 kinase, Akt pathway. Akt leads to the upregulation of survivin, which is an apoptosis inhibitor. Phosphorylation of Tie2 leads to the phosphorylation of Dok. Dok then activates the Ras, Nck, and Crk pathway, which are involved in cell migration, proliferation and organization of the cytoskeleton. Molecules interacting with the Tie2 SH2 domains are Grb2, SHP2 which modulate cell growth, differentiation, migration and survival.[76] (Figure 1-12)

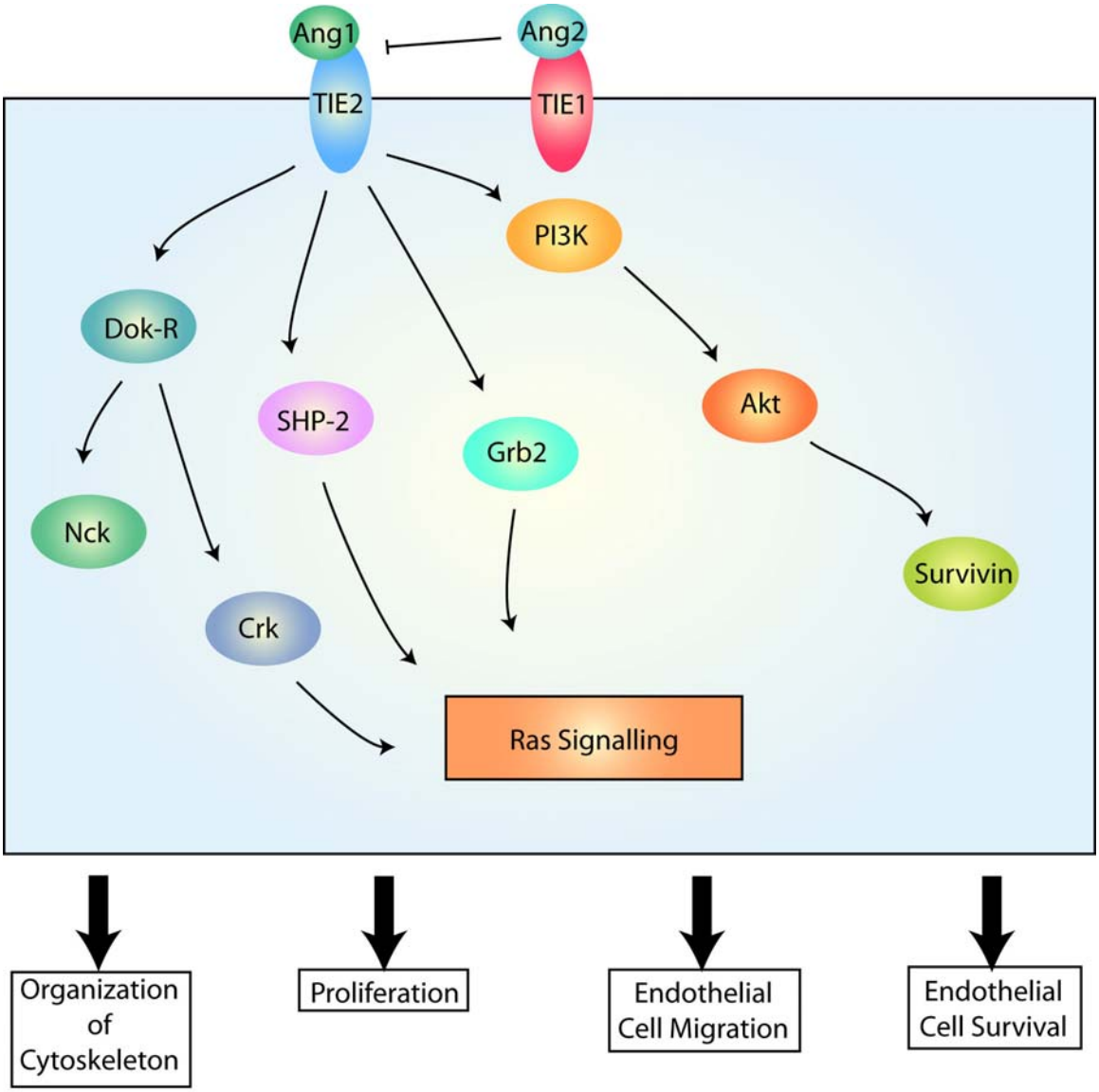

Figure 1-12. Angiopoeitins are ligand for the Tie 1 and Tie 2 receptors. Binding of angiopoeitin 1 to the Tie 2 receptor leads to endothelial cells proliferation, migration and cell survival. Angiopoeitin 2 inhibits Tie 2. ANG-1=angiopoeitin 1; ANG-2=angiopoetin 2.

Vascular Endothelial Growth Factor

VEGF is a heparan binding potent endothelial cell mitogen. It promotes endothelial cell survival via activation of the phosphatidylinositol 3-kinase (PI3K/Akt) pathway and inhibits apoptosis.[77] VEGF undergoes alternative splicing to produce 5 known isoforms: VEGF 121, VEGF 145, VEGF 165, VEGF 189 and VEGF 206.[73] The isoforms differ in storage in the ECM and their extracellular pathways.[78] VEGF 121 and VEGF 165 are secreted extracellularly, whereas VEGF 189, VEGF 206 and possibly VEGF 165 are either cell or matrix associated due to their affinity for heparan sulfate. VEGF is a mitogen for endothelial cells and each isoform has varying effects during angiogenesis:[73] VEGF 189 decreases lumen diameter, 121 and 165 increase lumen diameter and increases vessel length. VEGF 165 binds to the ECM and releases bFGF stored in the ECM, thus, bFGF and VEGF have a synergistic angiogenic effect. [78]

There are three tyrosine kinase receptors for VEGF: VEGF R1 (Flt1), VEGF R2 (KDR/Flk-1) and VEGF R3 (Flt3).[73] The receptors all have seven immunoglobulin like extracellular domains, a transmembrane domain and an intracellular tyrosine kinase domain, which is interrupted by a kinase insert.[78] VEGFR1 and VEGR2 transduce different signals to endothelial cells. VEGFR1 promotes cell migration and VEGFR2 is mitogenic for the endothelial cells and also promotes migration. [73] Hypoxia upregulates VEGFR1 and induces the expression of VEGF by endothelial cells. The increased production of VEGF activates the VEGFR2 receptor phosphorylation and cell proliferation. [78] Ligand binding to VEGFR1 leads to the activation of the small adaptor proteins: Fyn, Yes and GAP. Ligand binding to VEGFR2, however, leads to phosphorylation of the SHP-1 and SHP-2 adaptor proteins and PLC-gamma. PLC gamma hydrolyzes phosphatidyl inositol 4,5-bisphosphate (PIP2) to form inositol

triphosphate (IP3) and diacylglycerol (DAG). The DAG remains associated with the plasma membrane and activates protein kinase C (PKC). PKC is a soluble cytosolic protein, which is activated by the increase in calcium concentration. Activation of PKC leads to cell proliferation and permeability. VEGFR2 also leads to the activation of the PI3 kinase/Akt pathway, which enhances cell survival. VEGFR2 plays a role in cell migration by recruiting FAK. The MAPK pathway is also activated through Grb2, which is an SH2 adaptor protein. It has two SH3 domains, which bind the guanine nucleotide exchange factor SOS. SOS then leads to the activation of RAS. Activated RAS binds to the N-terminal of RAF which phosphorylates MEK and phosphorylates MAP kinase.[78] The activated MAPK pathway then leads to the activation of the intranuclear proteins such as cyclin D which is important in the progression of the cell cycle from the G1 phase to the S phase.[79] (Figure 1-13) VEGF also increases vascular permeability and allows leakage of plasma proteins, formation of the ECM and upregulates the production of uPA and tPA and PAI-1 by endothelial cells. VEGF production is regulated by local oxygen concentrations. Hypoxia upregulates production of VEGF by binding to the hypoxia inducible factor (HIF).[73]

During retinal development astrocytes and neuronal precursors migrate away from existing blood pre-existing blood vessels. As the distance between the astrocytes and the pre-existing blood vessel increases, the astrocytes sense a state of hypoxia. Astrocytes are more sensitive to hypoxia than neuronal cells and thus the astrocytes upregulate the production of VEGF, which leads to angiogenesis. This upregulation of VEGF by the astrocytes creates a concentration gradient of VEGF. This stimulates blood

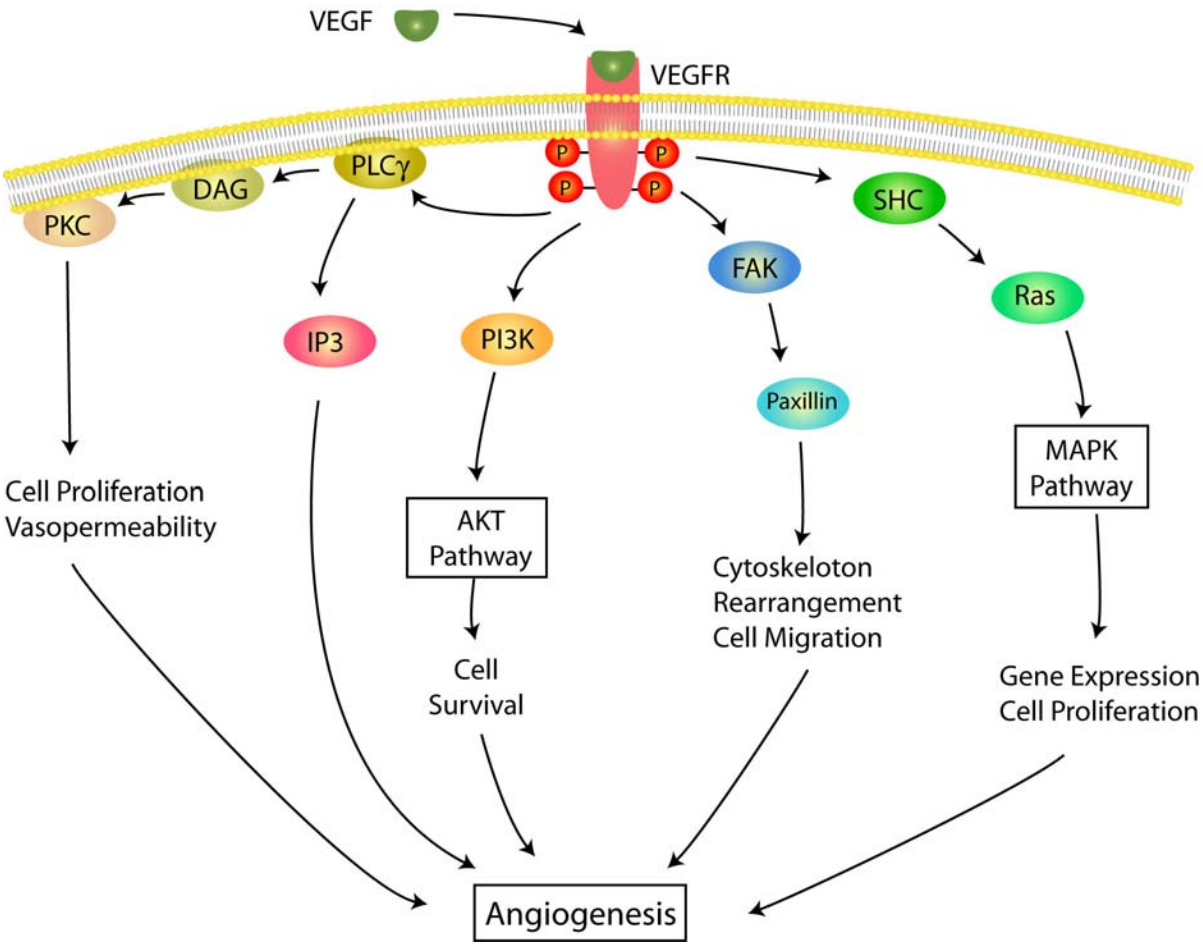

Figure 1-13. The vascular endothelial cell growth factor (VEGF R2) signaling pathway. VEGFR2 activates several pathways all of which lead to angiogenesis.

vessel formation towards the astrocytes, which produce VEGF. In ROP babies are placed in a high oxygen incubator because their lungs are not fully developed. The hyperoxia inhibits the VEGF production by the astrocytes thus causing newly formed blood vessels to regress. Once the babies are taken out of the incubator all the cells of the retina sense hypoxia and upregulate the production of VEGF. This leads to abnormal angiogenesis and unregulated blood vessel growth.[78]

Fibroblast Growth Factor

Fibroblast growth factor (FGF) is ubiquitously expressed as either basic FGF or acidic FGF. FGF is either in the cytoplasm or bound to the ECM due to its intrinsic affinity for heparan.[73] FGF binds to four related receptors, which are expressed on many cells. Ligand binding induces receptor dimerization. Endogenous heparan sulfate in cells is required for the activation of FGF. The receptor for FGF has three immunoglobulin like folds; two intracellular tyrosine kinase domains, a short transmembrane region and a juxtamembrane domain, which is longer than any other receptor.[80] The intracellular domain has two phosphorylation sites.[81] Ligand binding to the FGF receptor induces tyrosine phosphorylation of an adaptor molecule, FRS2. The phosphorylated FRS2 then allows binding of a small adaptor molecule GRB2. GRB2 is involved in the activation of the GTP binding protein Ras. Since FRS2 does not have an SH2 domain, another adaptor molecule, SHP-2 associates with FRS2 alpha in the active FGF receptor.[81] The importance of the association of this molecule with the FRS2 is not well defined. GRB2 exists with SOS, which catalyses the exchange of GDP for GTP on Ras for activation. Therefore, SOS, facilitates the coupling of GRB2 to Ras.[81] The activated MAPK then leads to the activation of the intranuclear proteins such as cyclin D which progresses the cell from the G1 phase to the S-phase.[79] (Figure 1-14) This growth factor induces

processes in endothelial cells and stimulates proliferation and migration of endothelial cells and pericytes, and production of PA by the endothelial cells. bFGF plays a role in blood vessel remodeling by stimulating endothelial cells to form tube like structures.[73,82]

Platelet Derived Growth Factor

Platelet derived growth factor (PDGF) is a mitogen for smooth muscle cells[73] and potent chemoattractant factor for smooth muscle cells, monocytes and fibroblasts. PDGF is a dimer consisting of two polypeptide chains: A and B. These chains combine to form 3 PDGF isoforms of PDGF AA or BB or heterodimers of PDGF AB.[73,83] The PDGF receptor consists of a single transmembrane domain which has intrinsic kinase activity.[83] The receptor is also a dimeric mixture of the alpha and beta subunits.[73] Ligand binding induces receptor dimerization and transphosphorylates tyrosine residues in the cytoplasmic domain of the receptor.[83] Endothelial cells express the beta receptor and are stimulated by PDGF-BB.[73,83] PDGF-BB acts through the MAPK/ERK pathway to stimulate c-jun/c-fos related genes in the nucleus to stimulate proliferation.[83] PDGF also acts through the PI3kinase pathway to activate PKB, which stimulates cell survival and proliferation. PDGF also plays a role in angiogenic chords formation and stimulates sprout formation. PDGF also mediates proliferation and migration of pericytes along angiogenic sprouts.[73] (Figure 1-15)

Transforming Growth Factor-β

Transforming growth factor beta (TGF-β) is produced by almost all cells and thus its activation represents an important control mechanism.[84] TGF-β is hydrolyzed

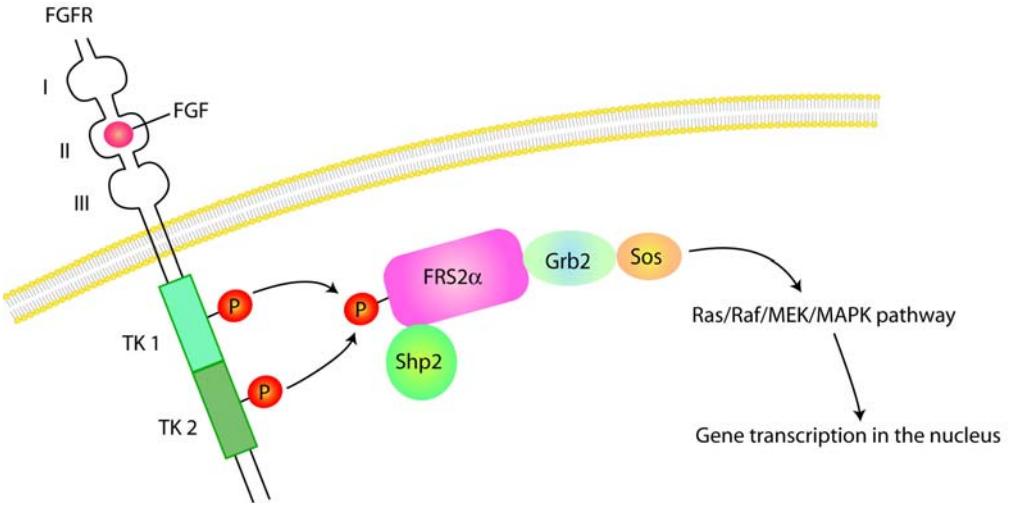

Figure 1-14. The FGF receptor and signaling pathway. Ligand binding to the FGF receptor leads to tyrosine phosphorylation of adaptor molecules and activation of the MAPK pathway. The MAPK pathway leads to endothelial cell proliferation, and migration.

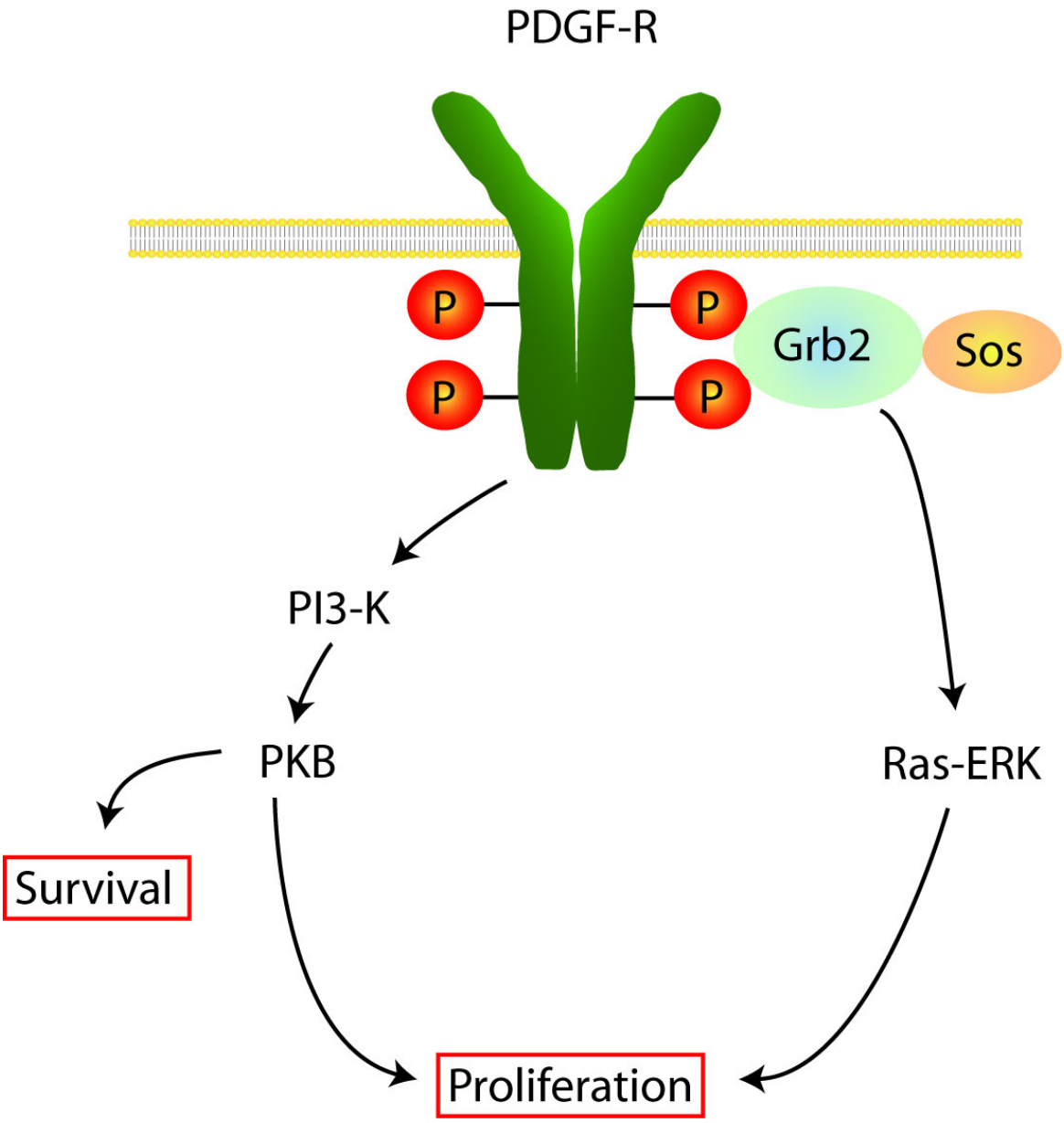

Figure 1-15. The PDGF receptor and signaling pathway. The PDGF receptor acts through the MAPK pathway to stimulate proliferation and also stimulates endothelial cell survival through the PI3-kinase/PKB pathway.

intracellularly by a furin peptidase to produce the carboxyl terminal peptide.[73] This peptide associates with the amino terminal to form the latency associated peptide (LAP). The LAP dimerizes to form the mature TGF-β which is then secreted in the inactive form.[73] Plasmin activates the latent complex. TGF-β also produces PaI-1 which inhibits plasminogen. Thus, showing that the action of TGF-β is self limiting.[85]

There are three different types of TGF-β receptors designated, I, II and III. TGF-β binds directly to the TGF-βII receptor. Binding of the II receptor is followed by the recruitment of the TGF-β I receptor. Both the receptors then form a stable complex and receptor II then phosphorylates receptor I which induces the signal cascade of the receptor.[85] Once the TGF-βR2 is bound to the TGF-β1 receptor, the kinase activity of receptor 1 is activated. This leads to the recruitment and the accumulation of the Smad proteins, which are then phosphorylated by the receptor. The name SMAD is derived from the genes encoding them. The genes were first identified in drosophila and C. elegans. The drosophila gene was named MAD (mother against decapentapleigic) and the gene from C. elegans was named SMA (small body size).[86,87] (Figure 1-16)

TGF-β is a bifunctional regulator. At low levels, TGF-β stimulates angiogenesis, and at high levels it inhibits angiogenesis.[85] TGF-β is found in the ECM, on endothelial cells and on pericytes. It supports the anchorage independent growth of fibroblasts.[73] TGF-β also controls cell adhesion by regulating the production of ECM and integrins. Endothelial cell migration and formation of tube like structures are regulated by TGF-β. TGF-β also upregulates the production of TIMPS, thus has anti-proteolytic activity. [73] TGF-β inhibits endothelial cell proliferation[73] by blocking the effect of other mitogenic growth factors and enhances pericyte differentiation. It helps to form the vessel

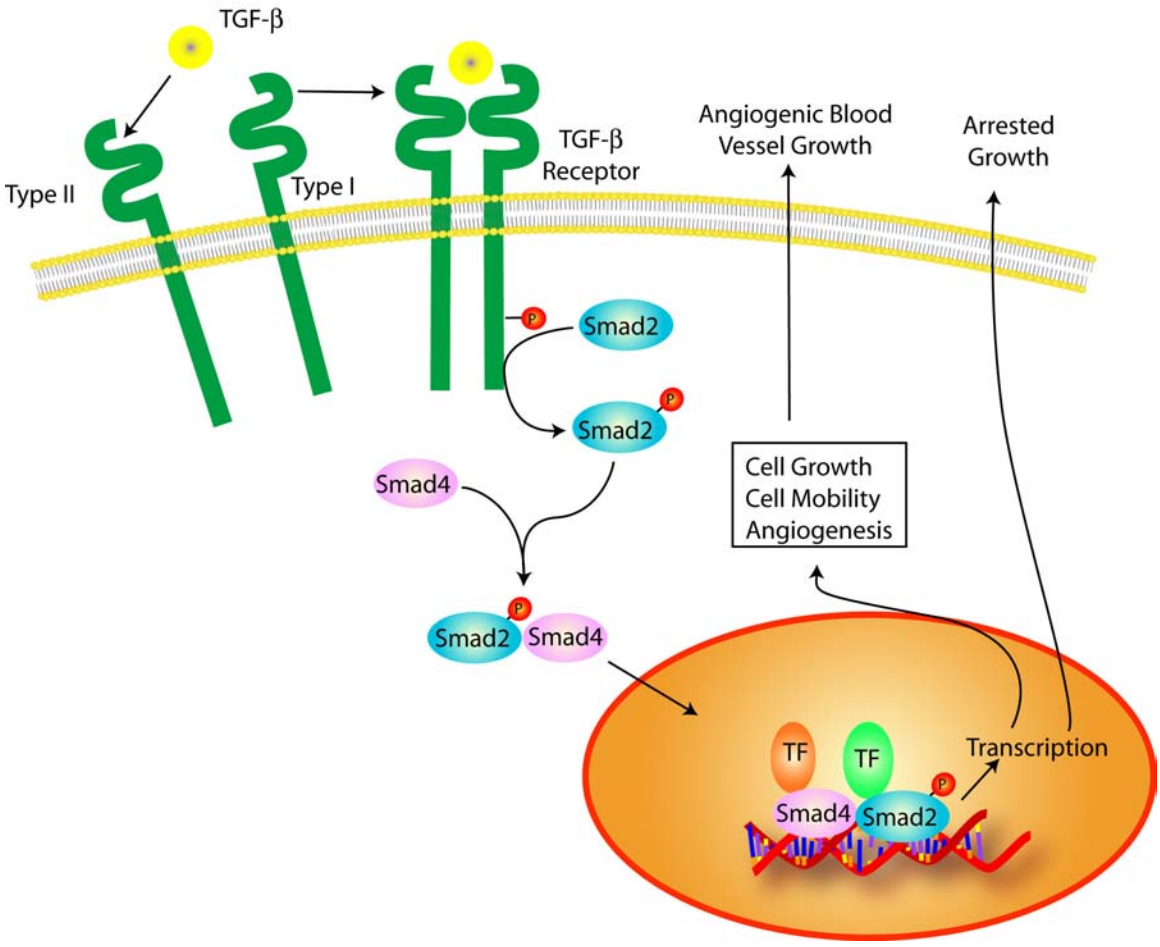

Figure 1-16. The TGF-β receptor signaling pathway. Ligand binding to the TGF- β receptor II leads to the recruitment of TGF- β receptor I. The activated receptor recruits the Smad proteins and stimulates angiogenesis at low levels and inhibits angiogenesis at high levels of TGF-β .

wall by stimulating the production of the extracellular matrix, strengthens the vessel wall and has matrix modulating effects and also stimulates tube assembly.[73,87]

Angiogenesis is a complex process, which involves the extracellular matrix, bound factors and soluble factors. Of the soluble factors, VEGF plays an important role in the early phases of angiogenesis. VEGF is an important mediator of compensatory angiogenesis and is a potent mitogen induced by hypoxia and nucleosides such as adenosine. [53,88,89] However, even though the angiogenesis process may solve the nourishment aspect of the outer retinal layers if the choriocapillaris was impaired, it would still cause vision impairment.[90,90-94]

Tissue hypoxia and ischemia initiate a series of events which lead to the development of collateral blood vessels, followed by compensatory angiogenesis, which is detrimental and results in aberrant blood vessels that are friable and prone to bleeding.[92,95] Mediators of compensatory angiogenesis include VEGF, which is a potent mitogen induced by hypoxia and nucleosides such as adenosine.[95-97] Depending on the character of the ischemic stimulus, adenosine plays two roles: as an intracellular signaling factor which promotes neovascularization following chronic hypoxia or ischemia, and as an endogenous protective factor which is capable of protecting the retina from acute ischemia. Adenosine also upregulates VEGF in retinal endothelial cells. Therefore, adenosine may be a critical signal in the control of gene expression after retinal ischemia.[91,98,99]

Adenosine

Adenosine is an endogenous nucleoside, which modulates many physiological processes such as cardiac myocyte contractility, modulation of neurosecretion and neurotransmission, cell growth and gene expression, regulation of intestinal tone and

control of vascular tone.[100] Adenosine serves as a signal to increase energy supply and demand by affecting cellular metabolic rates and tissue perfusion. Metabolites of adenosine may also have significant physiological and pathological effects. The level of adenosine available for these effects is determined by a number of factors including the rate of production, transport and metabolism.[100]

Stimuli that mediate the local production of adenosine include hypoxia, ischemia and inflammation. The endothelium is a barrier to adenosine, thus the adenosine formed within the lumen of the blood vessels may be derived from nucleotides released from platelets or endothelial cells. Ischemic parenchymal cells or nucleotides derived from nerves or intestinal mast cells give rise to interstitial adenosine. This adenosine may produce vasodilation via the A_{2A} receptor on vascular smooth muscle cells, which are especially accessible to the interstitial nucleoside. Adenosine may also be derived from adenine nucleotides from many cell types by mechanisms which are not well understood.[100,101]

Since AMP is derived from the breakdown of ATP, adenosine formation is closely linked to the cellular energy state. Adenosine may be formed intra or extracellularly. (Figure 1-17) The enzyme 5' nucleotidase (5'N) cataylzes the metabolism of ATP to adenosine. S-adenosylhomocysteine hydrolase also catalyses the break down of S-adenosylhomocysteine (SAH) into adenosine. SAH contributes significantly to adenosine formation in the heart and ischemic conditions in the brain. Once formed, intracellular adenosine is transported out of the cell to exert effects on specific cell surface receptors. The transport of adenosine is bidirectional.

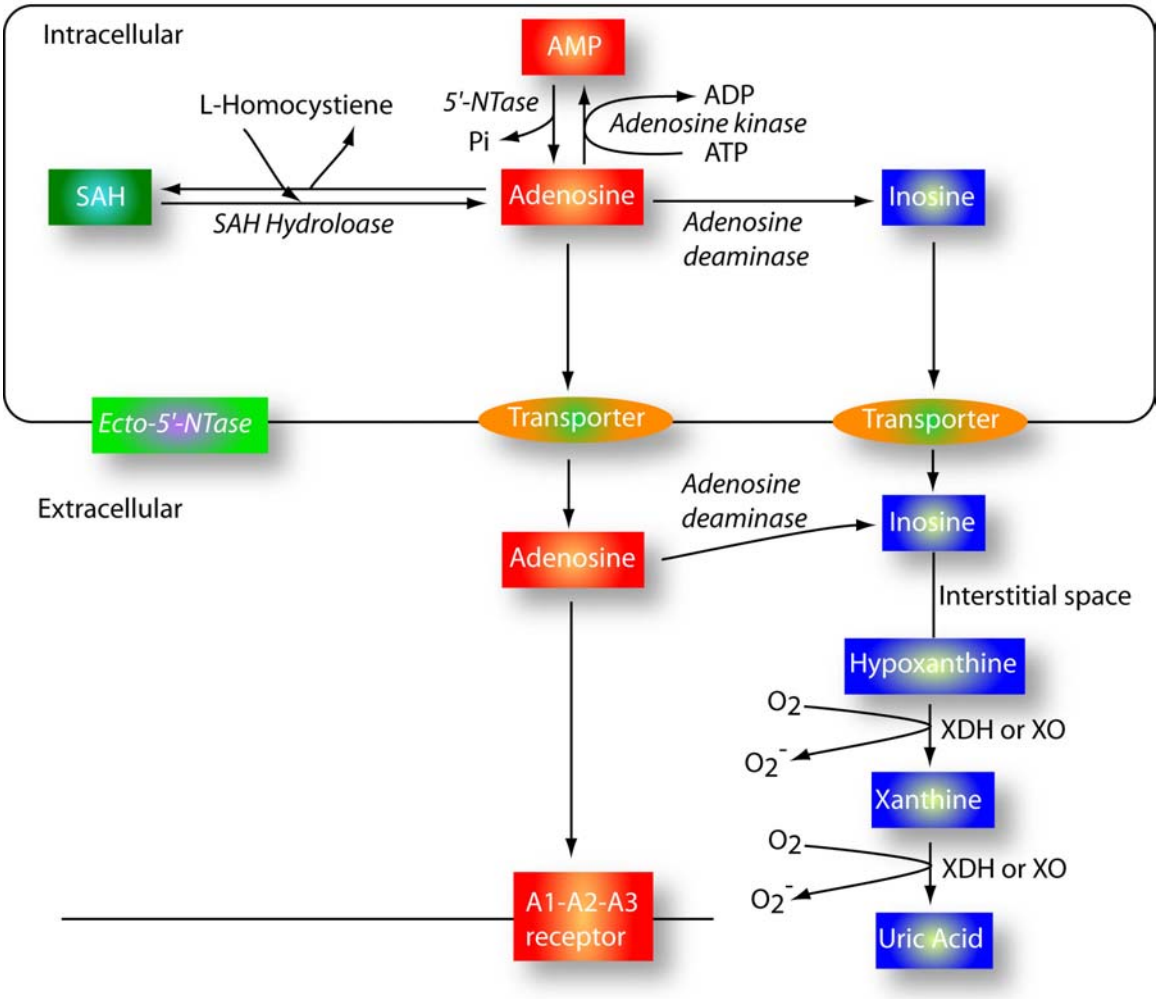

Figure 1-17. Intracellular and extracellular production of adenosine. SAH hydrolase: S-adenosyl homocysteine hydrolase. 5'NT:5'nucleotidase. XDH:xanthine dehydrogenase. XO:xanthine oxidase

Ecto 5'N catalyses the breakdown of 5'AMP to adenosine, thus giving rise to extracellular adenosine. The intracellular and the extracellular adenosine can be differentiated from each other using specific inhibitors of ecto 5'N.[100,101]

Adenosine deaminase (ADA) and adenosine kinase (AK) catalyze the breakdown of adenosine in the cytoplasm. Both ADA and AKA are found in the cytoplasm. ADA is a 36 kDa protein which catalyzes the formation of inosine. ADA is heterogeneously distributed in tissues and highest activity is during development. AK is a 38-56 kDa monomeric protein. It is also widely distributed throughout the body. AK catalyses the phosphorylation of adenosine to 5'AMP. If the intracellular adenosine is high, then AK is inhibited.[100,101]

Five types of adenosine transporters have been classified according to sensitivity to nitrobenzylthioinosone (NBTI), which is an adenosine transport inhibitor. Most of these transporters are sodium dependent and are bidirectional. Following degradation of adenosine, inosine leaves the intracellular environment and forms hypoxanthine. Xanthine dehydrogenase catalyses the oxidation of hypoxanthine to xanthine and subsequently to uric acid. Conversion of xanthine to uric acid also reduces NAD to NADH. Xanthine oxidase genetrates superoxide and hydrogen peroxide, both of which are damaging to cells. Endothelial cells stimulated by ischemia and reperfusion are key sources of xanthine oxidase formation and activity.[100]

Adenosine and the Retina

Adenosine is heterogeneously distributed throughout the retina of various species, such as rat, guinea pig, monkey, human and mouse.[100] Adenosine immunoreactivity is found in the ganglion cell layer, the inner plexiform layer and the inner nuclear layer.[91,102] Under resting conditions, endogenous purines in the retina are in the form of ATP

(70%) and adenosine (2%). During development, the retinal Müller cells provide glycosaminoglycan to the extracellular spaces for angioblasts which provides a scaffold for angioblast migration and organization. In developing and adult mammalian retina Müller cells express 5' nucleotidase (5'N) ectoenzyme, a glycoprotein. This enzyme catalyzes the hydrolysis of purine nucleotide monophosphates, to the corresponding nucleoside. The 5'NT can metabolize all purine monophosphates, however, the major product is adenosine. Adenosine is an intercellular communication molecule and is a modulator of synaptic transmission in the brain and the retina, and is a local regulator of blood flow in several organs. In the retina, adenosine is released in response to ischemia, thereby modulating the blood flow in the adult and neonates. Adenosine is also chemotactic and a mitogen for endothelial cells, and enhances endothelial cell migration and tube formation.[102] An increase in the 5'NT activity in cerebral ischemia was shown by Braun et al.[103] The pattern of 5'NT changes as the retina develops. In the early stages of development, the greatest activity of 5'NT is found in the inner Müller cell processes. When the inner retinal vasculature reaches completion (about 22 days of age), the inner retina activity of the enzyme decreases and the activity in the outer retina increases (in both plexiform layers).[102]

Lutty et al showed that at days 1-5, an increased adenosine immunorectivity is found in the inner retina and the edge of the formed vasculature in the neonatal dog. An increase in the adenosine product shifted toward the ora serrata as the vascular development progressed radially. On day 8 the 5'NT is increased in the inner retina, and on day 15 there is an increase in the adenosine immunorecativity in the nerve fibre layer and the inner nuclear layer. When the radial progression of the inner retinal vasculature

is complete on day 22, the 5'NT and adenosine are decreased throughout the nerve fibre layer and increased in the ganglion cell layer, the inner nuclear layer and the photoreceptor inner segments.[102] An increase in adenosine levels at most ages was found to be proportional to an increase in the 5'NT activity. In summary, the 5'NT activity shifts from the nerve fibre layer to the inner plexiform layer during development and the adenosine location is also shifted. Thus the Müller cells provide a glycosaminoglycan rich extracellular milieu for angioblast differentiation and also provide adenosine which is a stimulus for blood vessel formation.[100,102]

Adenosine Receptors

Adenosine receptors have been implicated in mast cell activation, asthma, regulation of cell growth, intestinal function, neurosecretion modulation and vasodilation. Adenosine receptors modulate cAMP (adenosine 3c, 5c-cyclic monophosphate) intracellulary. Based on their ability to inhibit or stimulate adenylyl cyclase, the adenosine receptors were initially divided into A_1 and A_2 subtypes. [100,104,105] The A_2 receptor was further divided into 2 subtypes based on the finding of a high affinity A_2 receptor in the rat striatum and a low affinity A_2R in the brain [106] Both of these receptors activate adenylyl cyclase. The high affinity receptor was designated as A_{2A} and the low affinity receptor was designated A_{2B}.[100,107]

Adenosine activates four different cell receptors: A_1, A_{2A}, A_{2B} and A_3. In most cell types, adenosine activates the A_1 receptor to lower oxygen demand, and activates the A_2 receptors to increase the oxygen supply. Thus the A_1 and A_2 receptors act to rectify imbalances between oxygen supply and demand.[100,108](Figure 1-18)

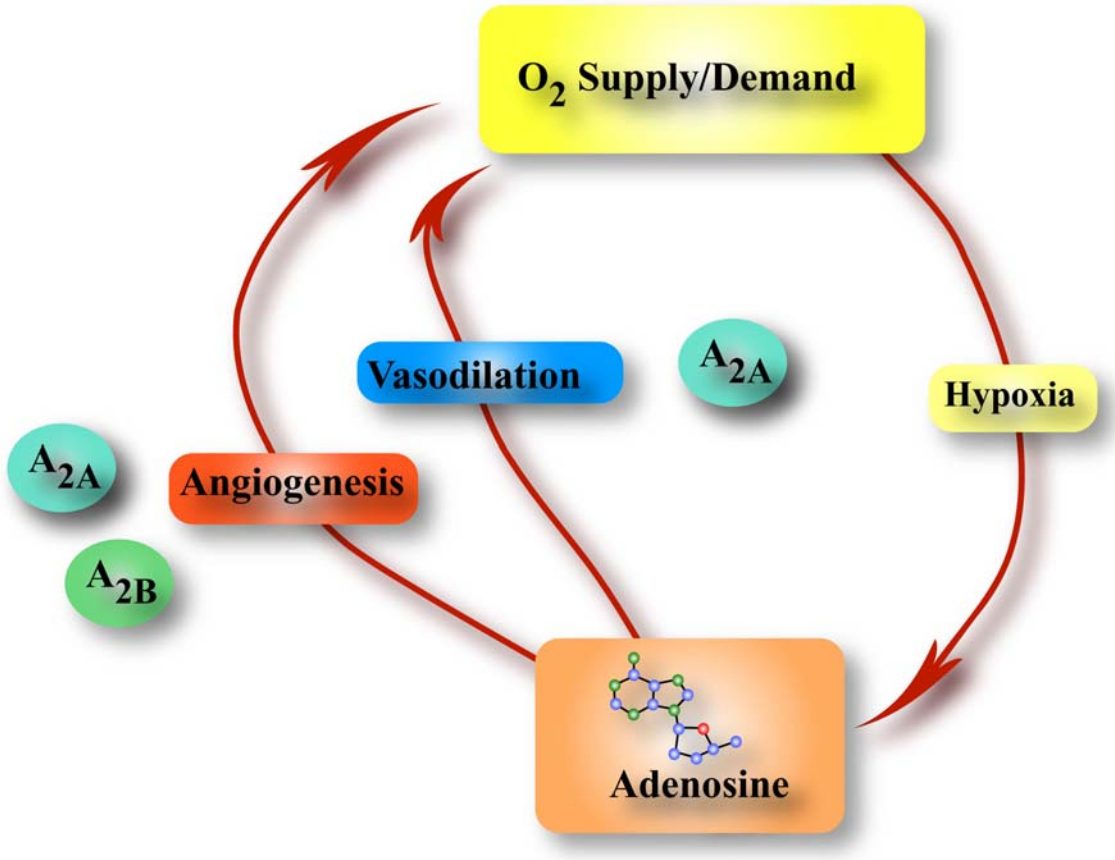

Figure 1-18. Role of the high and low affinity adenosine receptors. The A_2 receptors increase oxygen supply. The A_{2A} receptor leads to vasodilation and the A_{2B} receptors lead to angiogenesis

A_1, A_{2B} and A_3 adenosine receptors are N-linked glycoproteins, which have sites for palmitoylation near the carboxyl terminus. Glycosylation has no effect on the affinity of ligands for these receptors, thus these sites may be involved in targeting newly formed receptors to the cell surface. All receptors can be readily deglycosylated upon incubation with glycosidase.[101] The molecular pharmacological and physiological relevance of the A_1, A_{2A} and A_3 receptors is well known. However, the A_{2B} receptor is not as well characterized due to a lack of selective pharmacological probes and because this receptor has a low affinity for adenosine.[100]

The A_1 receptor was initially cloned from rat, human, bovine and rabbit. The A_1 receptor has seven transmembrane domains and is 326 amino acids in length and is about 36-37 kDa. Mutations in the H 274 and H 251 region result in loss of agonist and antagonist binding. Chimeric receptor constructs reveal transmembrane domains 5, 6 and 7 to be important for binding. In the brain, the A_1 receptors couple to G_i and G_s and inhibit the actions of adenosine.

The A_1 receptor decreases membrane potential (by increasing K^+ and Cl^- conductivity), lowers neurotransmitter release (e.g. glutamate and dopamine) and decreases calcium influx by stimulating calcium mobilization via the pertusis toxin sensitive pathway through the activation of PLC beta with G protein β/γ subunit.[101] All of these effects of the A_1 receptor lead to a decrease in neuronal excitability and metabolism. Thus, the A_1 receptor has a neuroprotective role in ischemic tissue.[100]

The A_{2A} receptor was initially cloned from canine, rat and human and produced responses which are anti-inflammatory.[101] It has seven transmembrane domains consisting of 410-412 amino acids and is about 45 kDa (comparable to A_1). Mutations in

H 274 and H 251 also lead to loss of agonist and antagonist binding. Adenosine relaxes vascular smooth muscle via the A_2 receptor mediated mechanism and thus increases tissue perfusion.

In the retina, the vasodilatory effects of adenosine are mediated by A_2 linked to potassium ATP channels.[100,101] Adenosine increases glyconeogenesis via the A_2 receptor and thus promotes an increase in the supply and demand ratio for metabolic substrates in the retina. A_{2A} decreases the superoxide release from activated neutrophils and inhibits platelet aggregation. These are all anti-inflammatory actions, the importance of which in retinal response to ischemia has not been established. Ideally, a drug that is an A_{2A} agonist and an A_{2B} antagonist is needed to further understand the two receptors.[100]

The A_{2B} receptor was initially cloned from rat hypothalamus[109], human hippocampus[110] and mouse mast cells [100] The receptor was found in these tissues by PCR with degenerate DNA oligonucleotides that recognized conserved regions of the G protein coupled receptors. The human, rat and mouse A_{2B} receptors share 86-87% amino acid homology.[109] The human A_1 and the human A_{2A}, and A_{2B} receptors share 45% amino acid homology.[100] Closely related species such as rat and mouse share 96% homology. The A_1 receptors have 87% amino acid homology in various species (Figure 1-19) [111,112,] the A_{2A} receptors have 90% homology (Figure1-20). [113] while the A_3 receptors differ significantly between species.[111,112] Figure 1-21 shows the homology between the human and the mouse A_{2B} receptor.[100]

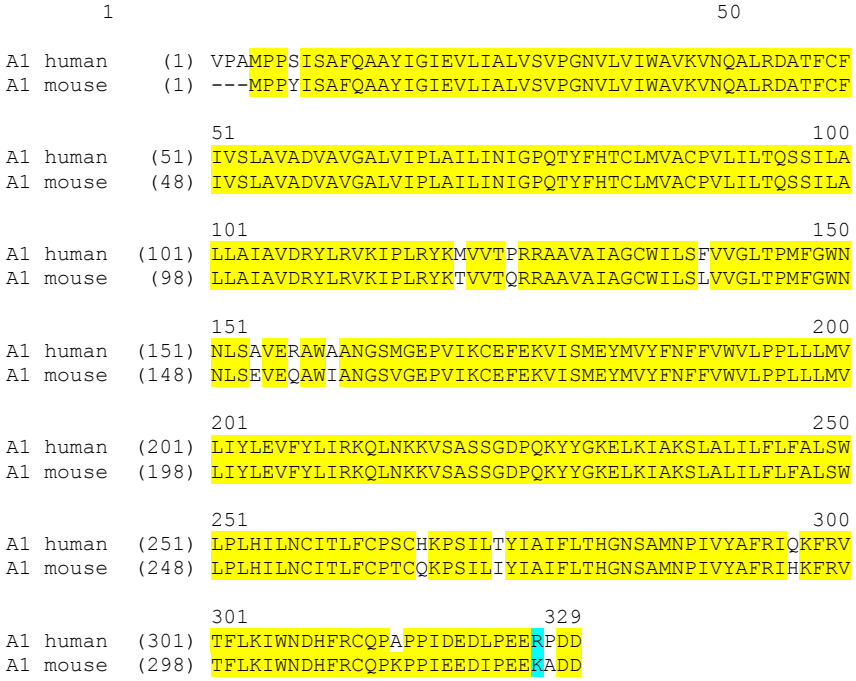

Figure 1-19. Homology of the A_1 receptor for human and mouse. The yellow sequences indicate homology between the human and mouse A1 receptor sequences. The white sequences indicate non-homologous regions and the blue sequences indicate conserved sequences.

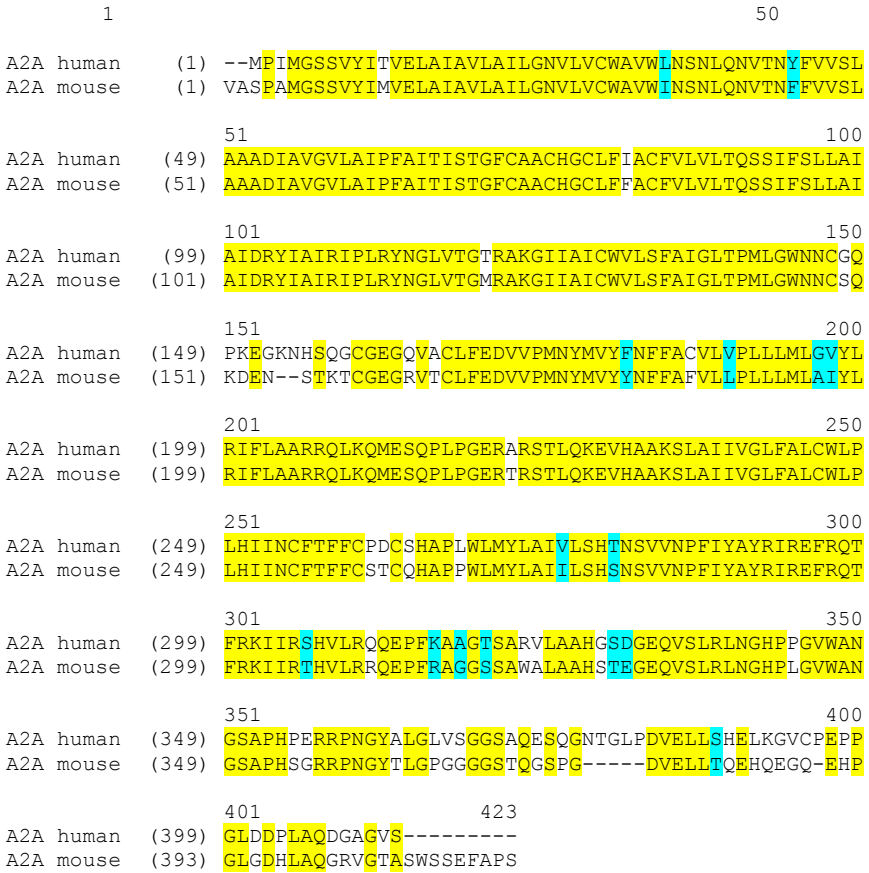

Figure 1-20. Homology of the A_{2A} receptor between human and mouse. The yellow sequences indicate homology between the human and mouse A_{2A} receptor sequences. The white sequences indicate non-homologous regions and the blue sequences indicate conserved sequences.

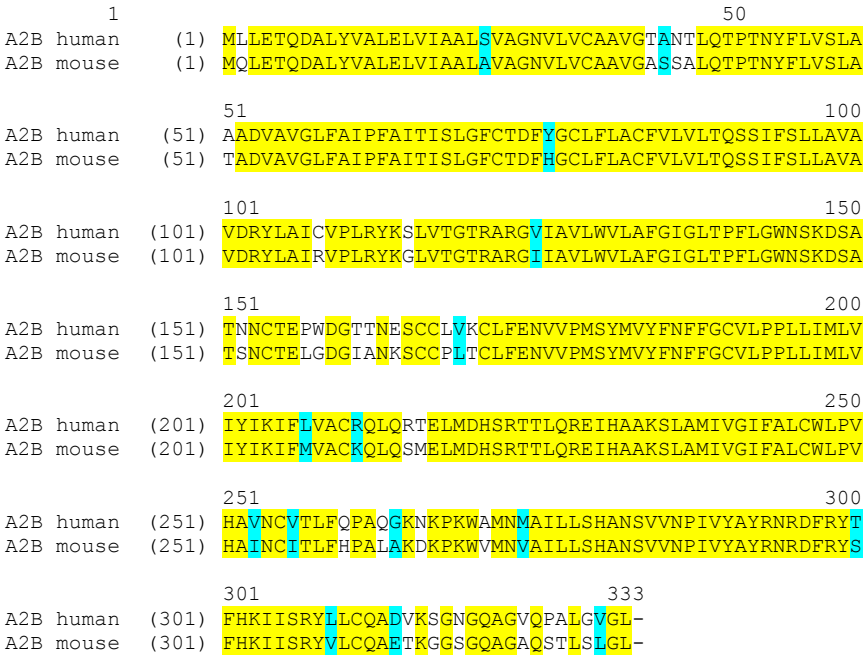

Figure 1-21. Homology of the A_{2B} receptor between the human and the mouse. The yellow sequences indicate homology between the human and mouse A_{2B} receptor sequences. The white sequences indicate non-homologous regions and the blue sequences indicate conserved sequences.

The membrane structure of the A_{2B} receptors is that of a typical G protein coupled receptor consisting of a 7 transmembrane domains connected via 3 extracellular and 3 intracellular loops. (Figure 1-22)[100,110,114]

Trans membrane domains have a high degree of amino acid homology in different species. The human, mouse and rat A_{2B} receptors have 2 potential N-glycosylation sites in the second extracellular loop.[109] The human N-linked glycosylation sites are Asp 153 and 163 which are in the second extracellular loop. Both of these sites are conserved in all of the A_{2B} sequences of all species that have been cloned.[100,115]

The A_{2A} intracellular and the third intracellular loop are involved in coupling A_{2A} receptor to G proteins. [100,111] The third intracellular loop is a 15 peptide portion of the A_{2A} receptor which has 57% amino acid homology with the A_{2B} receptor and also determines the selective coupling with GS.[100,116] Both A_{2A} and A_{2B} are coupled to G_s. The A_{2A} and A_1 receptors have 27% amino acid homology and the A_1 is not coupled to G_s. Amino acids in the second intracellular loop may modulate the A_{2A} receptor coupling since lysine and glutamic acid are necessary for efficient A_{2A} adenosine receptor Gs coupling.[100,116] Analogous lysine and glutamic acid residues are also present in the A_{2B} receptor. The major difference between the A_{2A} and the A_{2B} receptor is the long intracellular C-terminal tail of the A_{2A}. (Figure 1-23) This long tail is not involved in G_s coupling to the receptor. Removal of the c-terminal tail of the A_{2A} receptor does not inhibit stimulation of adenylyl cyclase when truncated receptor is expressed in CHO cell.[100,111,116]

Mutational studies of the A_{2A} receptors have shown that the Thr 298 residue of the C-terminal tail of the A_{2A} receptor is located close to the seventh membrane

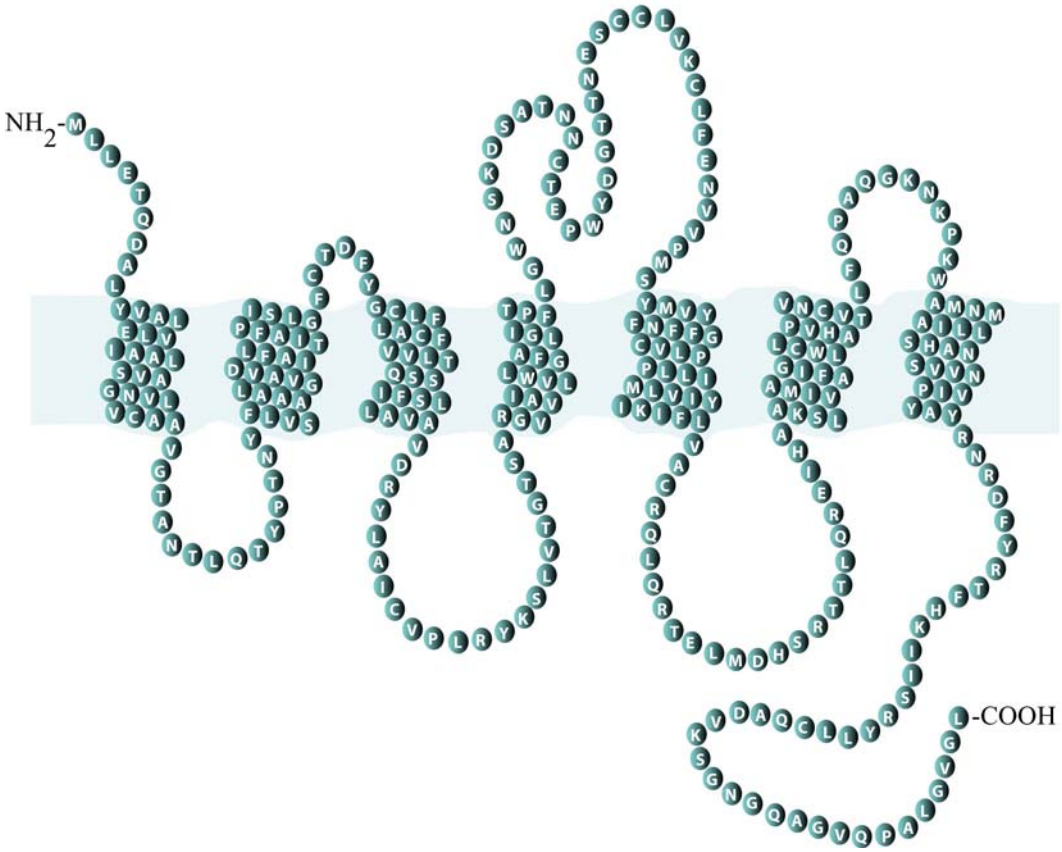

Figure 1-22. The A_{2B} receptor is a G protein coupled receptor consisting of a seven transmembrane domain connected via 3 extracellular and 3 intracellular loops flanked by an extracellular N- terminal and an intracellular C-terminal.

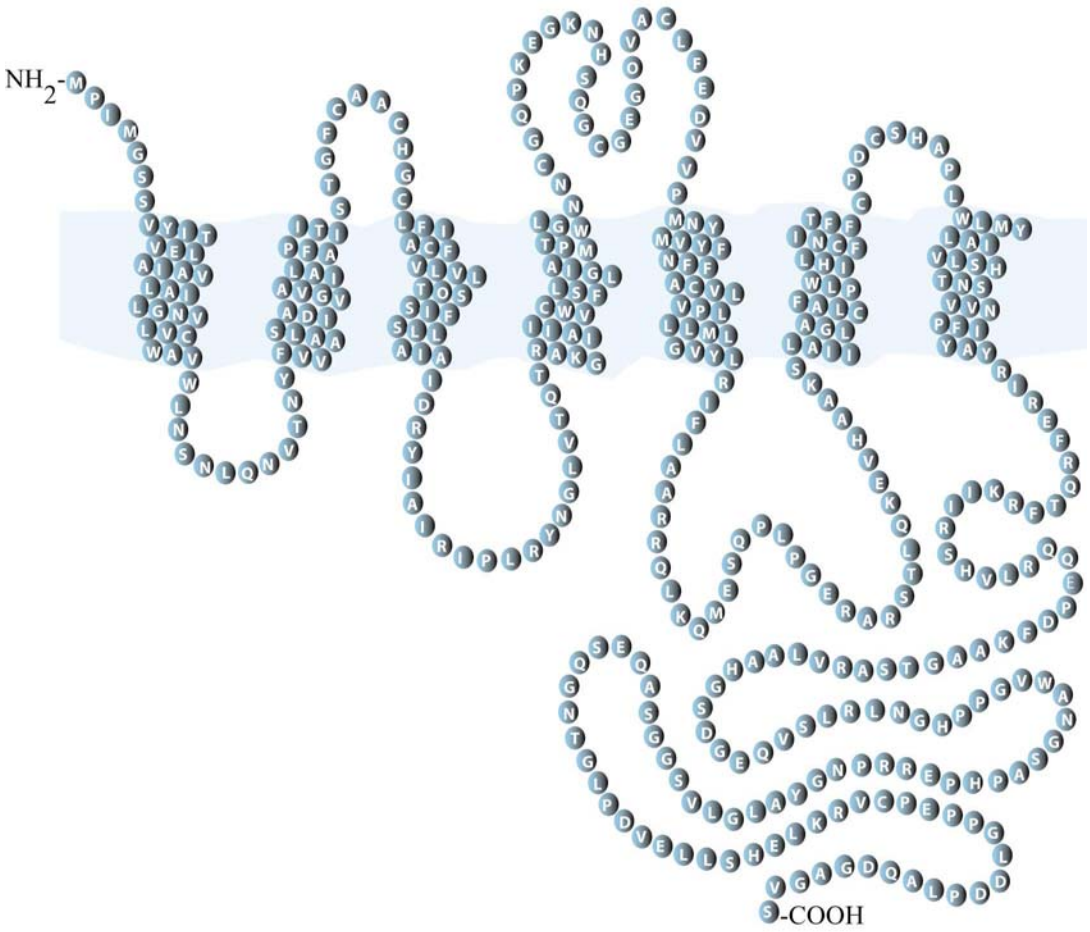

Figure 1-23. The A_{2A} receptor structure consists of 7 transmembrane domains connected via 3 extracellular and 3 intracellular loops flanked by an extracellular N-terminal and a long intracellular C-terminal.

span and is essential for the development of rapid agonist mediated desensitization.[100,111,117] The threonine residue is also present in the human A_{2B} (Thr 300), however, its role in receptor desensitization has not been explored. A_{2B} receptors can be coupled to other intracellular signaling pathways in addition to G_s and adenylyl cyclase.[100]

The A_3 receptor was cloned from the human, rat and sheep. It is composed of 320 amino acids and has about 40-50% homology to the A_1 and A_2 receptors. It has low affinity for alkylxanthine antagonists such as theophylline and caffeine (which is a classic antagonist for A_1 and A_2). The non specific A_3 antagonist IB-MECA inhibits adenyly l cylcase and increase PLC, calcium mobilization and decrease TNF-alpha. Higher concentrations of adenosine are required to activate the A_3 receptors than are required to activate the A_1 or the A_2 receptors.[100]

Pharmacology of the A_{2B} receptors

Highly selective and potent agonists designed for A_1, A_{2A}, and A_3 receptors are available and are important tools for the characterization of adenosine receptors. The lack of a potent selective A_{2B} antagonist hampers the characterization of its cellular functions. [95,100] The most potent agonist for A_{2B} is NECA.[100,118-120] At a concentration of 2μM, NECA produces half the maximal effect (EC50) for stimulation of adenylyl cyclase.[120] NECA is non-selective and thus activates other adenosine receptors with greater affinity. The EC50 for the A_1 and A_{2A} receptors is in the low nanomolar range and that of the A_3 receptors is in the high nanomolar range. Therefore, the characterization of the A_{2B} receptor depends on the use of compounds, which are potent

selective agonists of other receptor subtypes. Therefore the A_{2B} receptor is usually characterized by exclusion.[100]

CGS 21680[121] is an A_{2A} selective agonist that can differentiate A_{2A} and A_{2B} receptors.[100,122-125] The A_{2A} and the A_{2B} receptors are both positively coupled to adenylyl cyclase and are activated by the non selective agonist NECA. CGS 21680, on the other hand, is ineffective on A_{2B} receptors and as potent as NECA when activating A_{2A} receptors.[100,120-122,126-128] R-PIA is an A_1 selective agonist and the A_{2B} receptor has low affinity for it.[100,119,120]

The pharmacological characterization of the adenosine receptors is based on apparent agonist potencies. This is not ideal as it depends on agonist binding to the receptor and multiple processes of signal transduction. Therefore, for receptor subtype identification, selective antagonists are preferable [100,129] Highly selective A_{2B} antagonists are not available. However, it is known that A_{2B} has a low affinity for agonists, but a high affinity for antagonists. Enprofylline (3-n-propylxanthine) is an anti-asthmatic drug, and is the most selective, but not potent, A_{2B} antagonist known. Other potent but non-selective A_{2B} receptor antagonists include 1,3-dipropyl-8 (p-sulfophenyl)xanthine (DPSPX), 1,3-dipropyl-8-cyclopentylxanthine (DPCPX), xanthine amine cogener (XAC) and IPDX [95,119,120]

Distribution of the Adenosine Receptors

Initially the A_{2B} receptor mRNA was found in the rat. The highest levels of the receptor was found in the cecum, bowel, bladder, followed by the spinal cord, lung, epidydimus, vas deferens and the pituitary.[100,130] Subsequently more sensitive RT-PCR showed that the A_{2B} receptors were present in all tissues of the rat, with the highest level in the proximal colon and the lowest level in the liver.[131] Primary tissue cultures have

different adenosine receptors present in the cells. This may be because there are different populations of cells and each cell expresses a different type of adenosine receptor.[100,132-134] Studies on established cell lines also showed multiple adenosine receptor subtypes on a single target.[100,122,124,125] Also, studies on single cells show the presence of one or more adenosine receptor subtype.[135-137] Clonal cell lines also have co-expression of the A_{2A} and the A_{2B} receptors.[100,124] However, subsequent studies showed minute amounts of other receptors too! Therefore it is possible that adenosine selective antagonists are needed to better characterize the distribution of these receptors in cells. It is however, unclear why there is simultaneous expression of multiple adenosine receptors in a single cell. Both A_1 and A_{2A} receptors have a high affinity for adenosine and need to be blocked before the effects of the A_{2B} receptor can be seen [100,135,136,138] However, this is not always the case and may be a reason for discrepancies published in the literature. Elfman et al showed that glial cells of rat astrocytes have A_1 and A_{2B} adenosine receptors which stimulate cAMP.[133,139-141] However, when the cells were stimulated by the non-selective agonist, NECA, cAMP accumulation was seen even though there are A_1 receptors present. Therefore it may be that the importance of the A_{2B} receptors is maximal where adenosine receptor levels are high, such as, in tissues with a high metabolic demand or conditions when oxygen is decreased. Both the A_1 and the A_2 receptors may modulate the response to lower the concentrations of adenosine.[100]

The widespread unique localization of adenosine suggests that it is well positioned to serve as mediator of important physiological and pathophysiological processes in the retina. [91,100,142] In the retina, adenosine receptors are localized to the same retinal layers as endogenous adenosine. In the mouse a tritiated A_1 agonist, cyclohexyladenosine (CHA)

was used to localize the A_1 to the inner retina (over the inner plexiform layer) and the A_2 receptor was localized to the RPE (outer retina) and the outer and inner segments of photoreceptors by using tritiated NECA.[100,142] No A_3 receptor has been found in the retina. The location of adenosine receptor mRNA transcripts generally correlated with the autoradiographic localization of the A1 receptors, but not the A_2 receptors.[100]

Intracellular Pathways Regulated by A_{2B} Receptors

Adenosine receptors activate a diverse cascade of intracellular signaling. The A_1 and A_3 receptors inhibit adenylyl cyclase and stimulate PLCβ by activation of pertussis toxin sensitive G proteins G_i and G_o.[143] Adenosine binding to the A_{2A} and the A_{2B} receptors couples them to G_s and adenylyl cyclase positively, however, the A_{2B} receptor is also active in other signaling pathways. The A_{2B} receptor coupled to G_s can also increase calcium transport into the cells by the cholera toxin sensitive pathway. This pathway is cAMP independent even though it is coupled to G_s. [144,100] The A_{2B} receptor is also coupled to $G_{\alpha q}$ and leads to the activation of two distinct pathways. One of those pathways lead to the activation of the MAPK pathway and the other pathway activates the PI3 kinase/PkB pathway. (Figure 1-24)

Angiogenesis is a complex process and is the underlying cause of several retinopathies. Currently available treatments for retinopathies are painful and have had limited success. Since adenosine exerts its angiogenic effects upstream of VEGF, it is an attractive target for inhibiting the process of angiogenesis. However a lack of selective and potent A_{2B} antagonists requires the use of molecular techniques to target the A_{2B} receptor. One such approach is the use of ribozymes to target receptors at the molecular level.

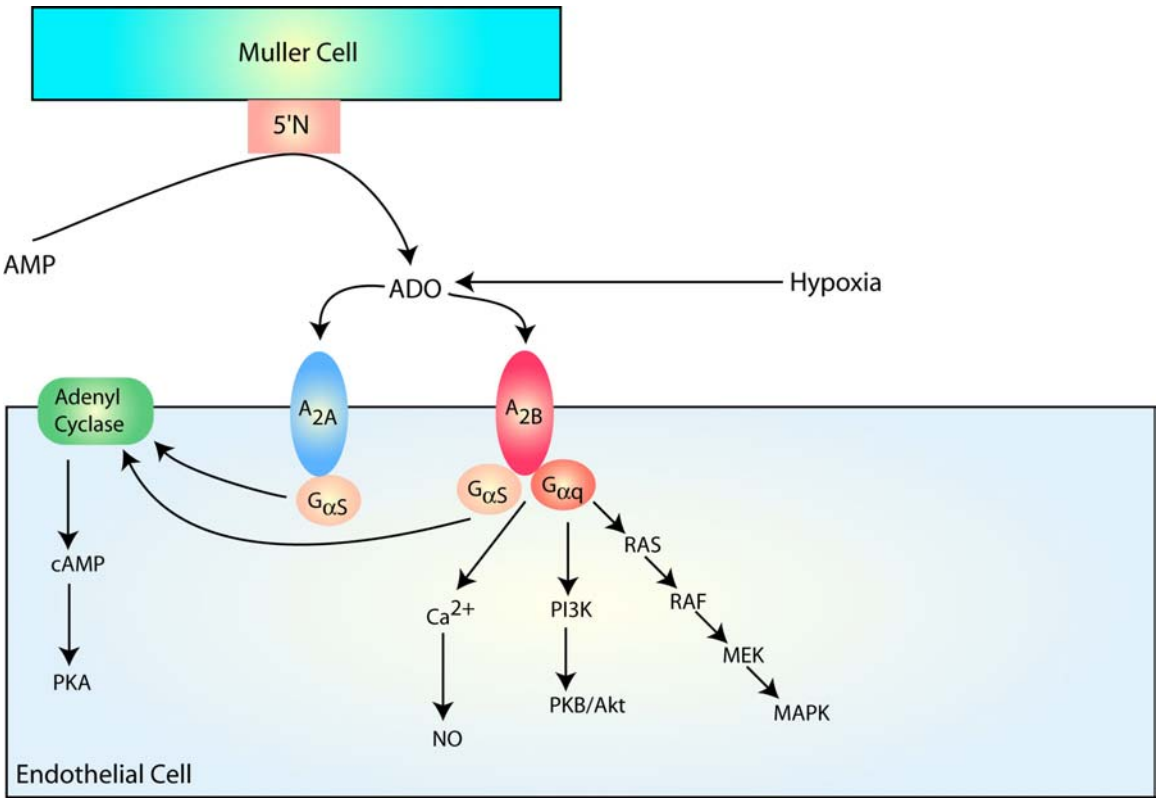

Figure 1-24. The A_{2B} signaling pathway. The A_{2B} receptor couples to G_s and $G_{\alpha q}$ and leads to an increase in calcium transport and also leads to the activation of the MAPK pathway

Ribozymes

Ribozymes are catalytic RNA molecules that cleave other RNA molecules. Ribozyme is short for ribonucleotide enzyme, which, catalyze the hydrolysis and phosphopryl exchange at the phosphodiester linkages between RNA bases resulting in cleavage of the substrate. [145,146] [146,147]

Ribozymes can be classified into 3 main groups based on function and size: self splicing introns, RNase P, small self cleaving ribozymes.

Self Splicing Introns

Group I Introns

Self splicing introns can be divided into 2 classes: Group I intron and Group II introns, based on the conserved secondary structure and splicing mechanisms (Figure 1-25). Group I introns are found in a wide number of species, such as, eubacteria, bacteriphages, fungal mitochondria, plant chloroplasts and rRNA of lower eukaryotes.[148,149,150] The splicing action consists of two consecutive transphotoesterification reactions. In a transphotoesterification reaction, the number of phosphodiester bonds remain constant, however, the position of the bonds changes. (Figure 1-26)[150,151] Only the *Tetrahymena* large rRNA group I intron has been shown to function without a protein in vivo. All other known group I introns require a single protein co-factor to provide a scaffold that helps position the introns in a catalytic conformation.[152]

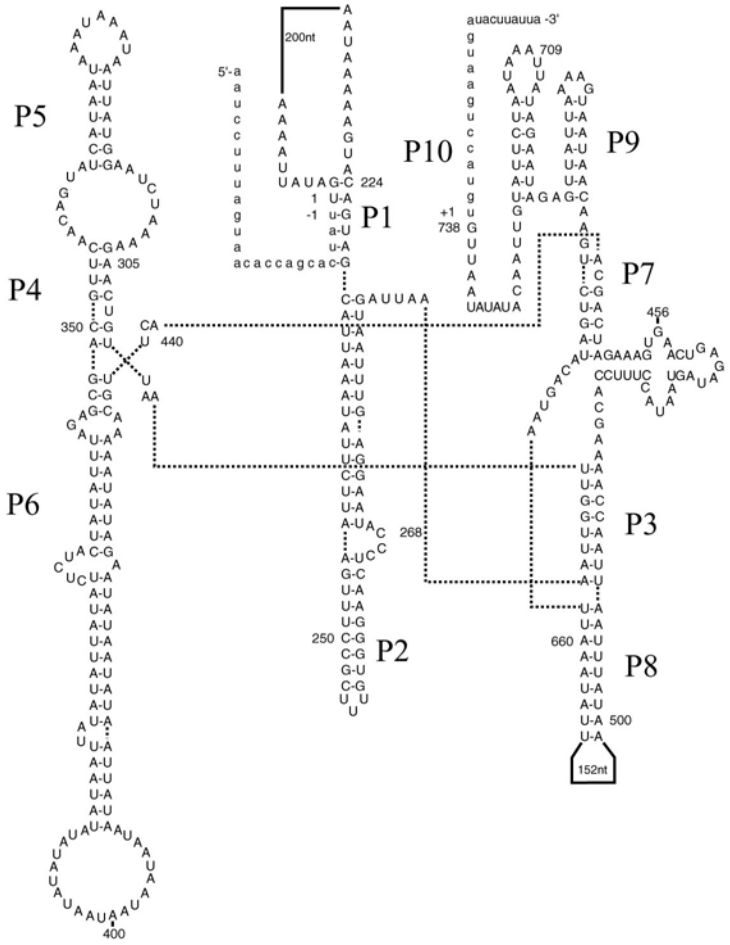

Figure 1-25. The secondary structure group I introns.

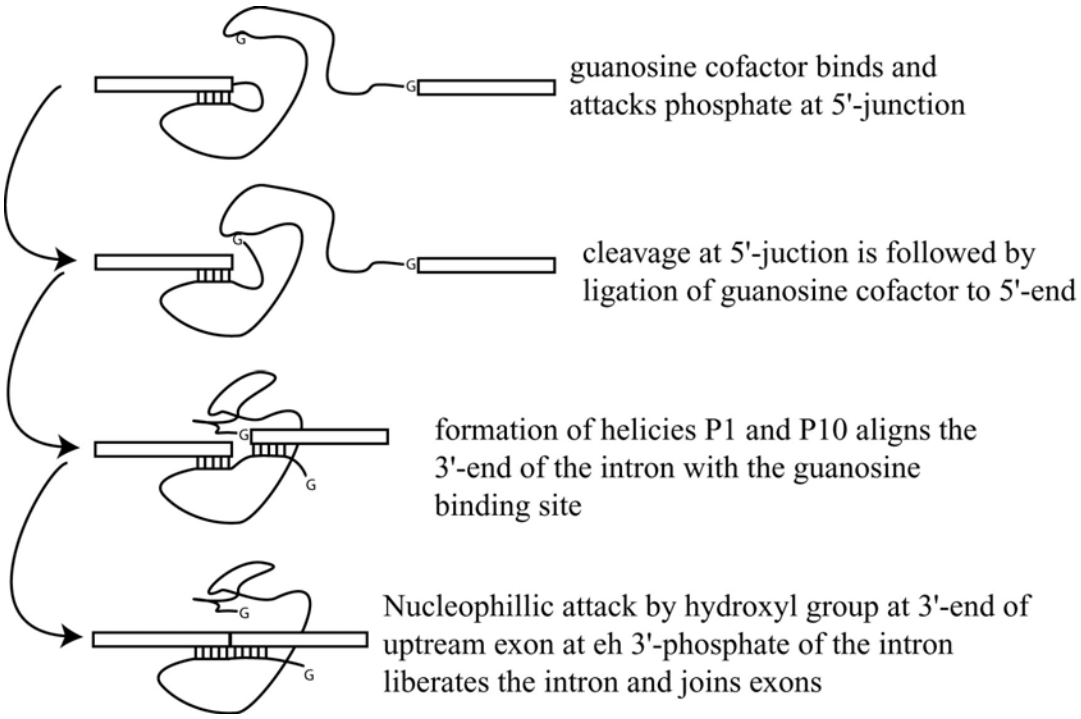

Figure 1-26. Splicing mechanism of the group I introns

Group II Introns

Group II introns are self splicing introns found within nuclear pre-mRNA and in the pre-mRNA of organelles from fungi and plants.[153] (Figure 1-27) High concentrations of magnesium and potassium ions are essential for their proper folding.[153] Group II introns also require a complex of proteins and small nuclear RNAs (SnRNA) for cleavage. These components form the spliceocome. Group II splicing occurs via two consecutive trans photoesterification reactions similar to group I introns. The main difference in the splicing mechanism between the two introns is the nature of the hydroxyl group, which initiates the initial phototransesterification reaction. In group I introns, the reaction is initiated by the 3' hydroxyl group of the exogenous guanosine and in the group II introns, the reaction is initiated by the 2' hydroxyl group of the internal adenosine.[154] (Figure 1-28)

RNase P RNA

RNase P is an endoribonuclease which removes the 5' leader sequence from precursor tRNAs. RNase P has an RNA and a protein unit, both of which are essential to its function. The RNA component is the catalytic component of the complex. The protein subunit enhances the turnover rate of the reaction by acting as a scaffold for the RNA that forces the RNA into a catalytic conformation.[155,156] RNase P can recognize and cleave 60 different tRNA substrates.[157] RNase P recognizes the structure of the tRNA and only a minimal tRNA structure is required for the creation of the RNase P cleavage site (**Figure 1-29**). [158,157]

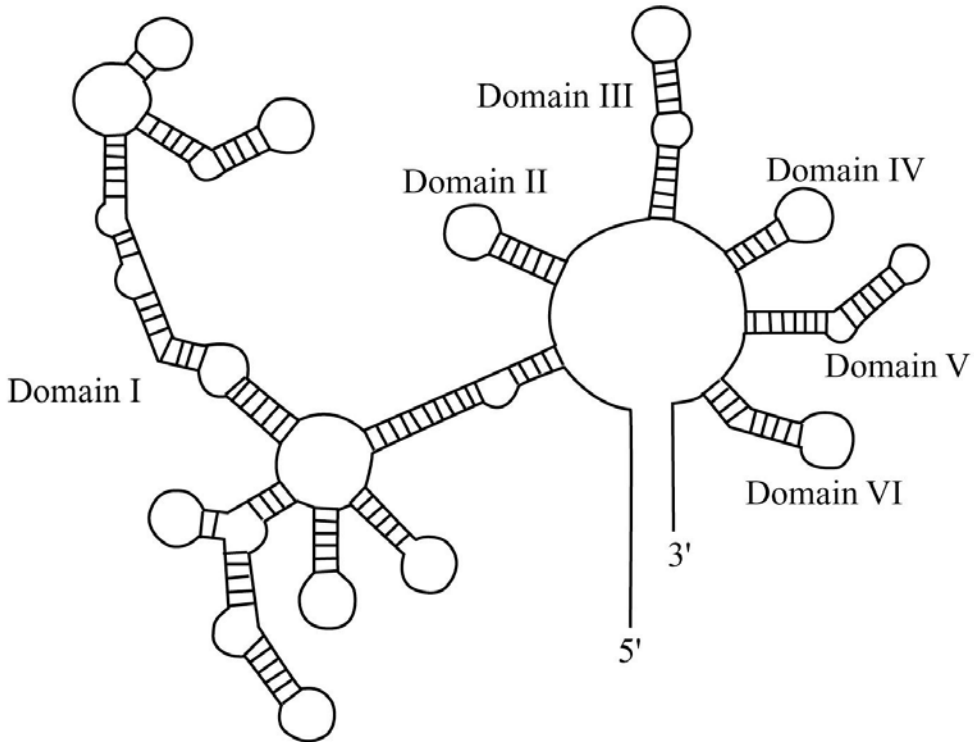

Figure 1-27. Secondary structure of Group II introns.

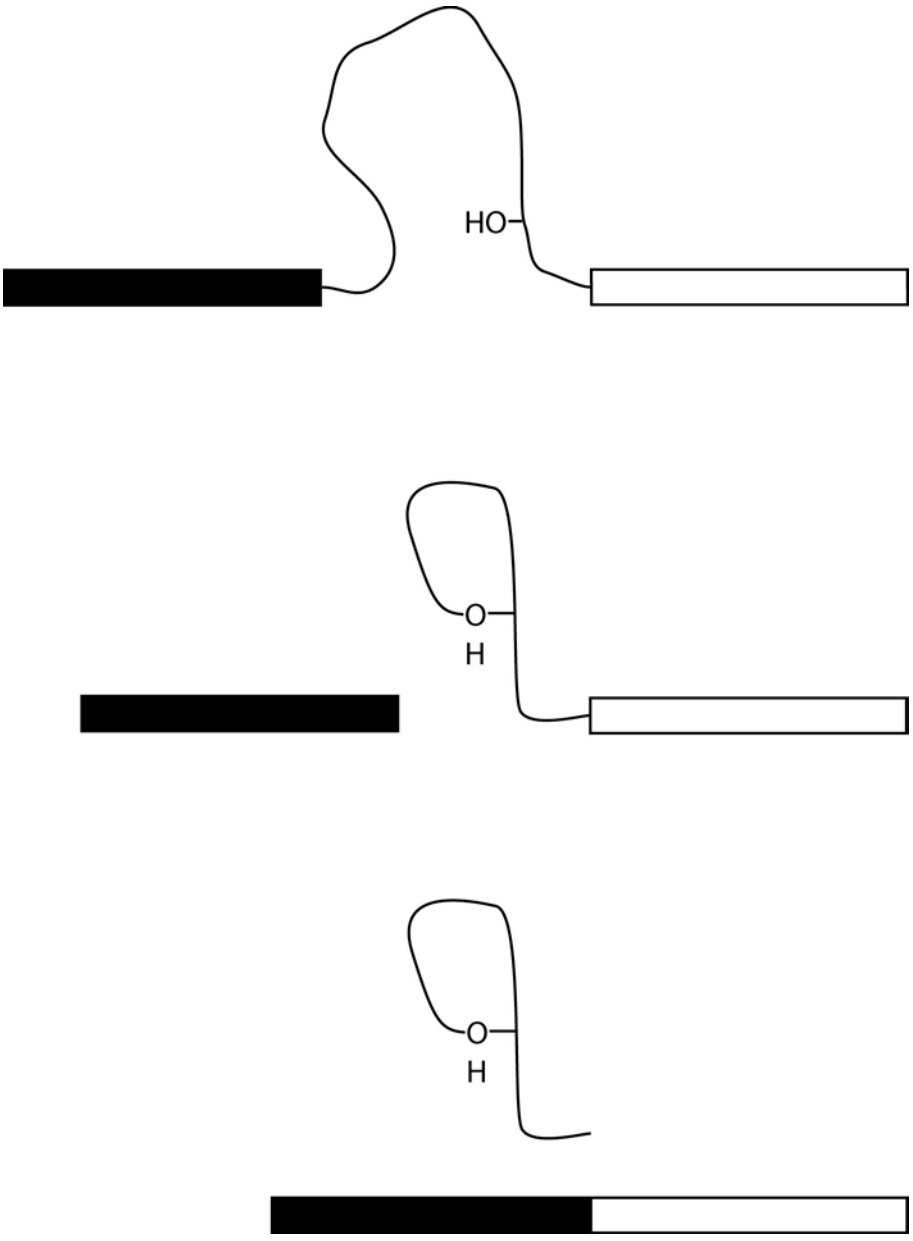

Figure 1-28. The splicing mechanism of the Group II introns.

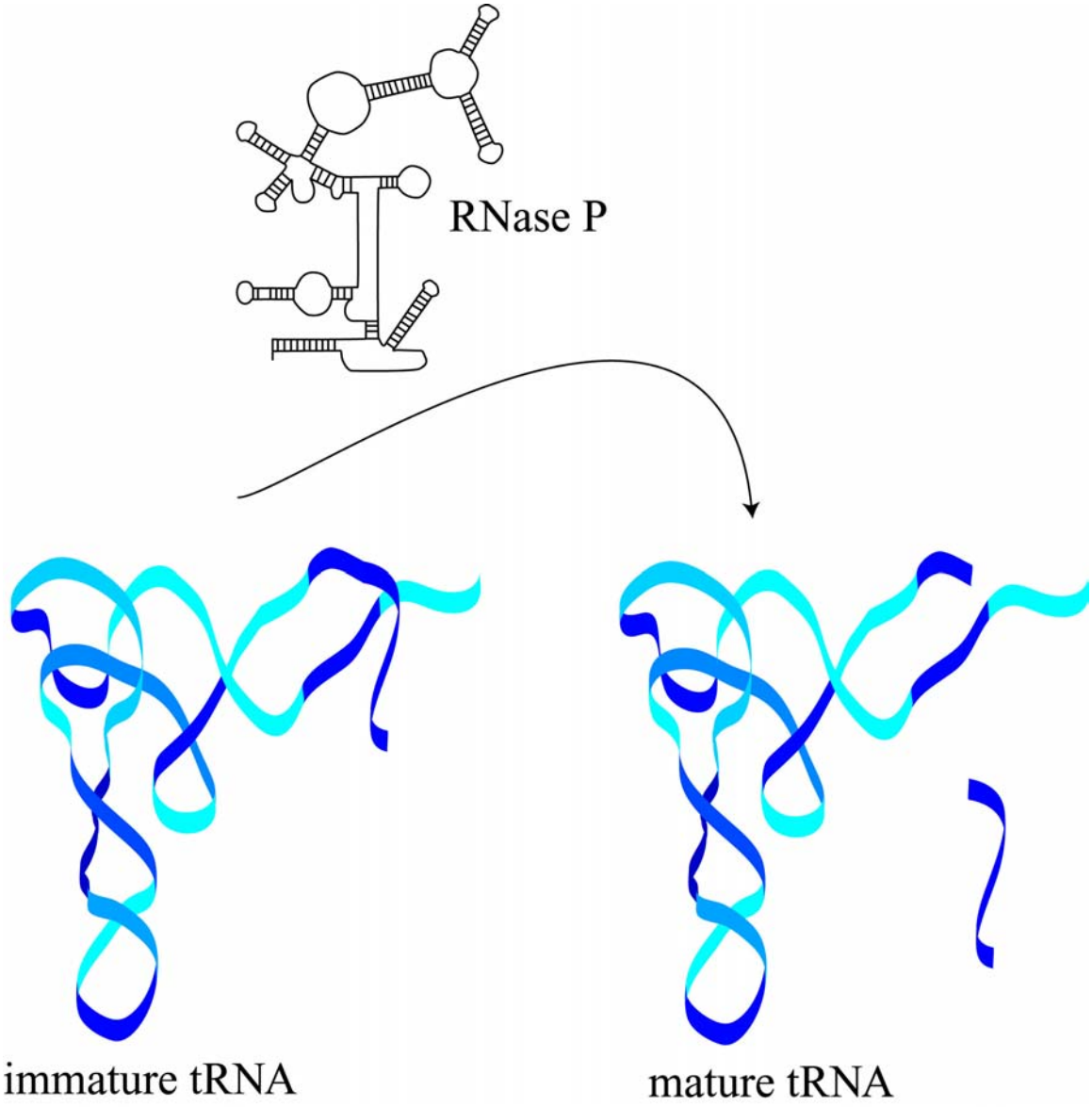

Figure 1-29. Cleavage of the tRNA 5' leader sequence by Rnase P.

Small Self Cleaving Ribozymes

Small Self cleaving ribozymes are nucleolytic RNA's and are found naturally. They are associated with viruses and satellite RNA and can catalyze RNA cleavage reactions in the absence of protein. [159] There are several types of small ribozymes, the most extensively studied ones include: hepatitis delta virus (HDV), hammerhead and hairpin ribozymes. The hammer head and hairpin ribozymes are derived from tobacco ring spot virus satellite RNA.

Hepatitis Delta Virus

Hepatitis delta virus (HDV) is a short single stranded RNA found in patients infected with human hepatitis B. It has a circular RNA genome, which encodes a ribozyme in both orientations. HDV replicates through a rolling circle mechanism like other self cleaving ribozymes (Figure 1-30), and the ribozyme is required for the cleavage of the HDV genome into discrete units prior to packaging. [160,161]

Hairpin Ribozymes

The hairpin ribozyme was originally found in the tobacco ring spot virus satellite RNA. The hairpin ribozyme binds the substrate and forms a structure with 4 helices and 2 loops (Figure 1-31). The arms of the hairpin ribozyme hybridize to the substrate molecule to from helix 1 (6 base pair) and helix 4 (4 base pair). Loop A has a BNGUC target sequence required for cleavage, where B is G, C or U, and N is any nucleotide.[162] There are no conserved nucleotides in any of the helices. [163,164]

Hammerhead Ribozymes

The catalytic domain of the hammerhead ribozyme was discovered by comparing self cleaving RNA sequences of a number of different viroid infectious RNA molecules.

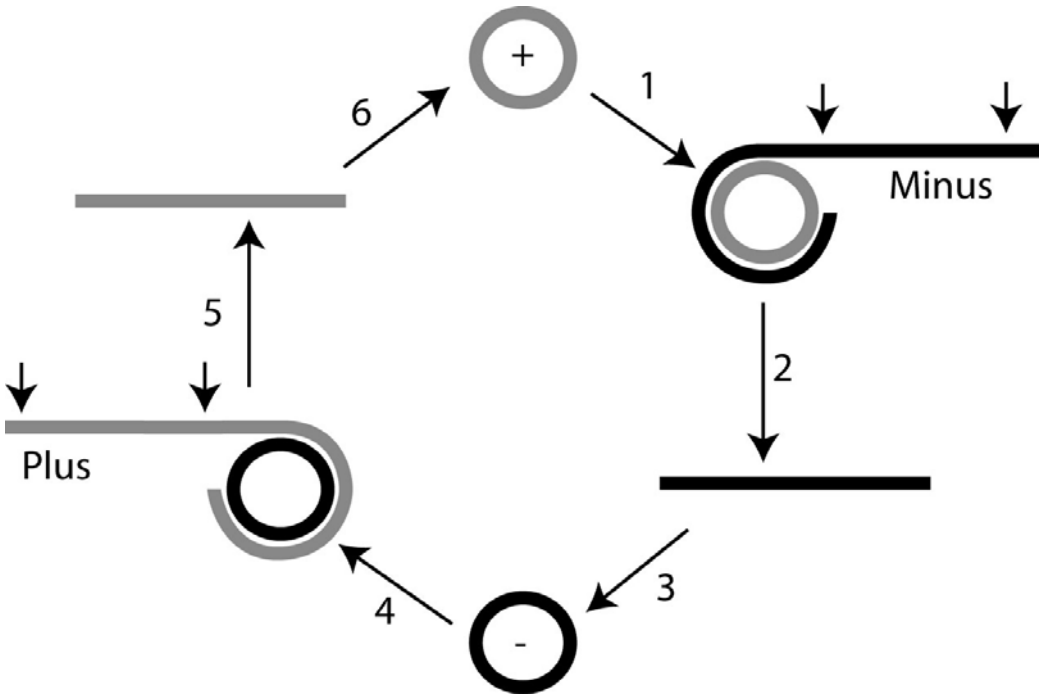

Figure 1-30. Self-cleaving ribozymes resolve concatemers formed by rolling-circle replication into individual genomic molecules

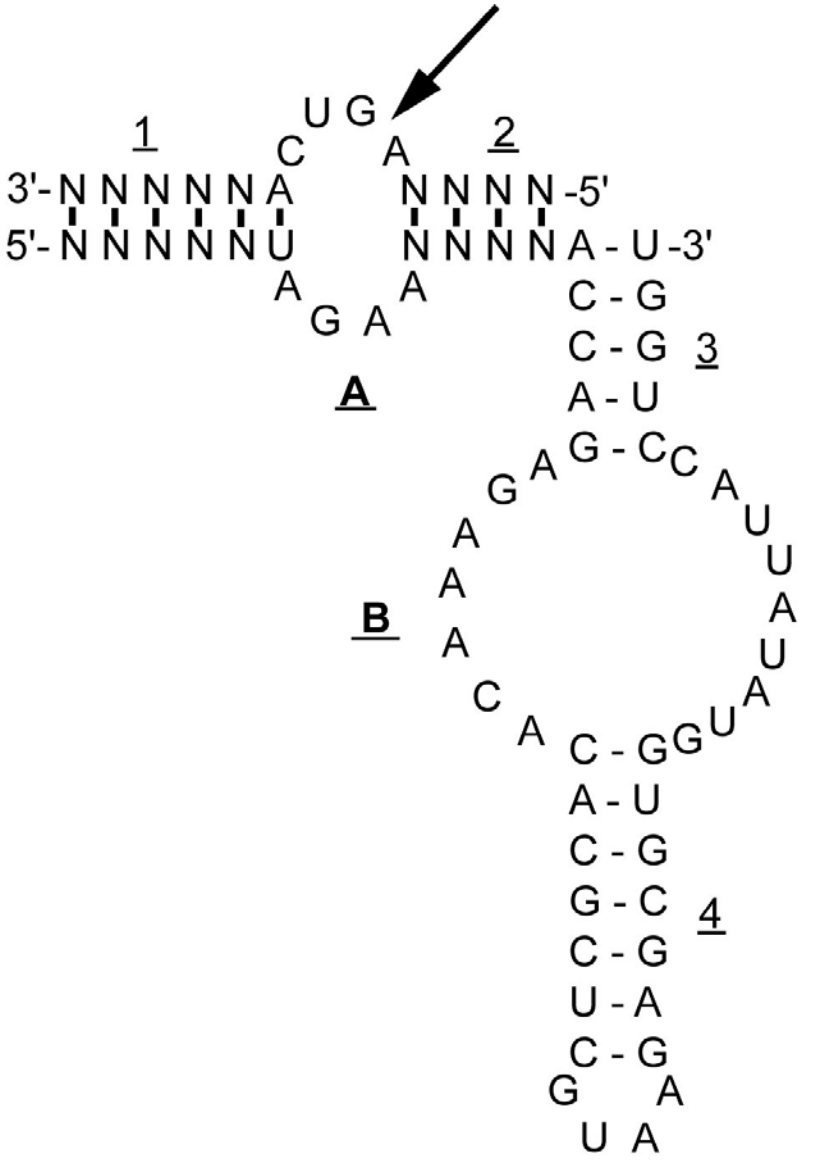

Figure 1-31. Structure of the hairpin ribozyme. The arrow indicates the site of cleavage. The hairpin ribozyme binds the substrate and forms a structure with 4 helices (1-4) and 2 loops (A and B).

Hammerhead ribozymes are small, approximately 34 base RNA molecules and cleave RNA target in trans. The hammerhead ribozymes bind substrate to form a structure, which consists of a stem and three loops and a catalytic core with a conserved nine nucleotide sequence (Figure 1-32). A mutation in any of the conserved nucleotides prevents RNA cleavage.[165]

The catalytic core of the hammerhead ribozyme has two functions: it destabilizes the substrate strand by twisting it into a cleavable conformation and binds the metal cofactor needed for catalysis.[166] The hammerhead ribozyme cleaves the substrate by a tranesterification reaction (Figure 1-33). The reaction requires the presence of magnesium and water. The hydrated magnesium ion has two functions, both mediated by water molecules. First, one molecule of water binds to one of the oxygen atoms of the phosphate group, holding it in the proper orientation for the enzymatic mechanism. Secondly, the environment of the active site lowers the pKa of another water molecule so that it can donate a proton to the aqueous environment. In the transition state, five oxygen atoms are arranged in a triangular bipyramid around the phosphorus atom. A bond is formed between the 2' oxygen of cytosine 17 and the phosphorus atom. Simultaneously a bond is broken between the phosphorous atom and the hydroxyl oxygen of the next nucleotide, adenine 1.1. This leaves the cytosine with a 2'-3' cyclic phosphate group. The 5'nucleotide recovers a proton from the aqueous environment, completing a hydroxyl group. The reaction products diffuse away from the active site leaving the ribozyme free to bind a second substrate molecule and complete another reaction cycle**.** The hammerhead ribozyme recognizes substrate sequences on either side of a NUX cleavage site, where N is any nucleotide and X is any nucleotide except G.

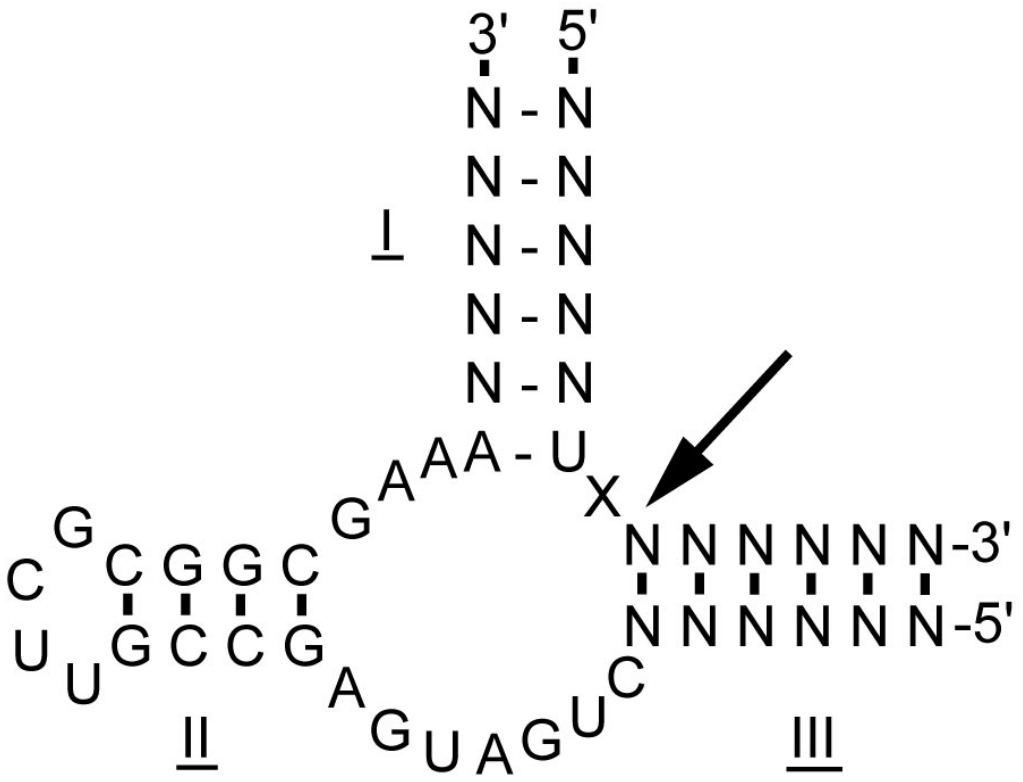

Figure 1-32. Structure of the hammerhead ribozyme. The hammerhead ribozyme binds substrate to form a structure, which consists of a stem and three loops and a catalytic core with a conserved nine nucleotide sequence. Arrow indicates site of cleavage.

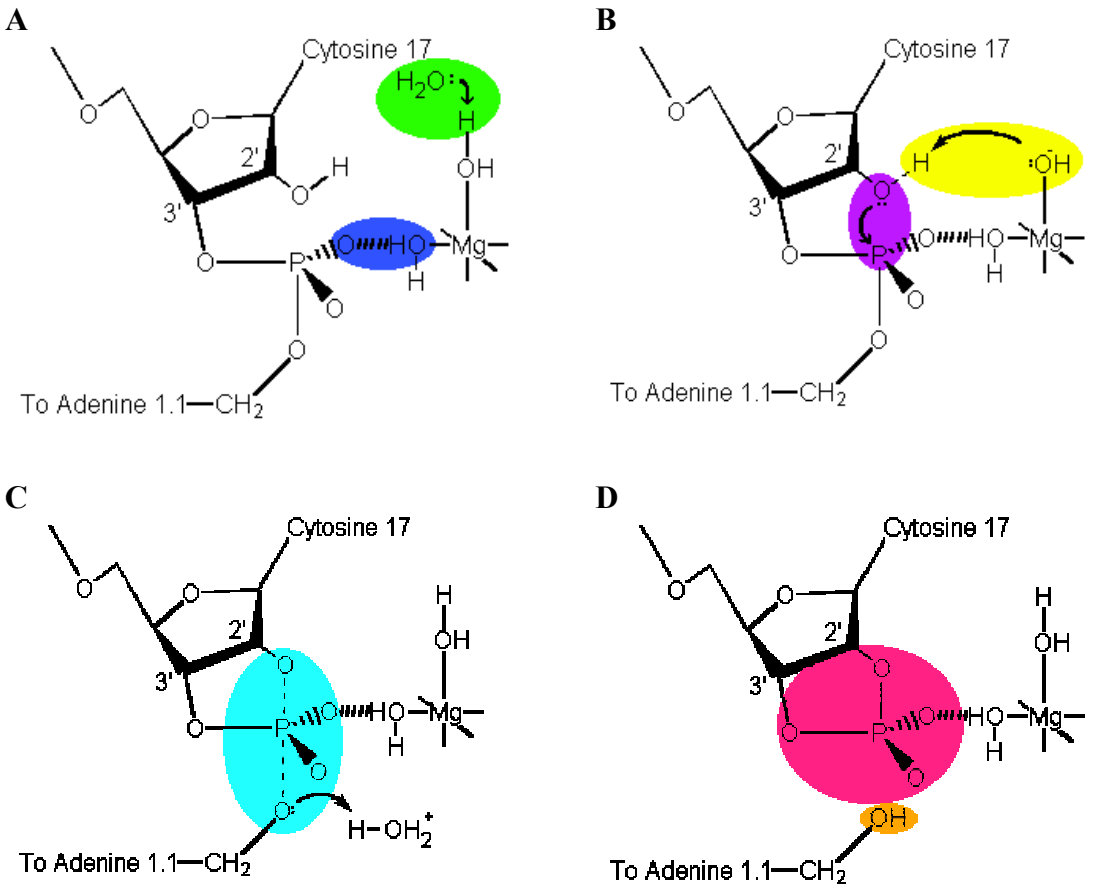

Figure 1-33. The hammerhead ribozyme cleaves its substrate by a transesterification reaction. **A**. A molecule of water binds to an oxygen of the phosphate group. **B.** Another water molecule donates a proton. A bond is formed between the 2' oxygen of cytosine 17 and the phosphorous atom. **C.** A bond is broken between the phosphorous atom and the hydroxyl oxygen of adenine 1.1. **D**. Cytosine remains with a 2'3' cyclic phosphate group. The 5' nucleotide recovers a proton to complete a hydroxyl group. The reaction products then diffuse away from the active site leaving the ribozyme free to bind a second substrate molecule and complete another reaction.

The ribozyme anneals to the substrate mRNA by means of two flanking arms which hybridize to form helices III and I. Cleavage occurs at the 3' end of the cleavage site. Not all cleavage sites demonstrate the same efficiency. Generally, GUC is the most efficient cleavage site, then CUC, UUC and AUC. The remainder of the cleavage sites are cleaved at least 10 times less efficiently than the GUC site. The hammerhead and hairpin ribozymes are being examined as gene therapies for a number of different diseases because they are small and can be easily cloned and packaged into many of the existing viral vectors for delivery to target cells. The advantage of the hammerhead ribozyme is that it can recognize a greater number of cleavage sites than HDV or hairpin ribozymes.[167,168]

Experimental Aim

Currently, the only available treatment for ROP is laser treatment of the retina, which has limited success. The aim of this project is to design a hammerhead ribozyme that will specifically target and cleave the A_{2B} receptor mRNA resulting in a reduction in expression of the A_{2B} receptor protein and a reduction of cellular and physiological functions affected by this receptor. We are using a hammerhead ribozyme primarily as a tool to study the pathways that involve A_{2B}. But this ribozyme can also be used as 'proof of concept' for conventional drugs targeting the A_{2B} receptor and, finally there is a possibility that the hammerhead ribozyme itself could be used as a therapeutic agent.

The goal of this project was to examine the effectiveness of ribozymes in the treatment of ROP. Previously we have shown that proliferative blood vessels have an enhanced expression of the A_{2B} receptor, therefore, there is justification to target this protein in controlling the disease. Ribozymes were designed to specifically cleave the mRNA of the A_{2B} receptor to decrease the expression of the receptor protein. The

underlying hypothesis was that the cleavage of the mRNA of the A_{2B} receptor at the mRNA level would prevent translation of the protein and subsequently progression of angiogenesis in ROP by preventing the growth of abnormal blood vessels. (Figure 1-34) The selected target site was a short region of the mRNA for the A_{2B} receptor. The first step of the project was to design a ribozyme to cleave the sequence of the A_{2B} receptor in the mouse and the human. (Figure 1-35) Two hammerhead ribozymes were developed, each of which had an inactive version with a single base mutation. (Figure 1-36) The most efficient ribozyme was cloned into an rAAV construct (p21Newhp) for further analysis. (Figure 1-37) The second step of the project was to develop in vitro assays to examine the ability of the ribozyme to cleave the mRNA. These assays were used to determine if the ribozymes would be effective for reducing pre-retinal neovascularization in an oxygen-induced mouse model of retinopathy.

To test the ribozyme in vivo, the A_{2B} Rz2 was intravitreally injected to the mouse model. Several models for oxygen-induced retinopathy have been developed. Dembinska[169] and Chowers[170] both used a rat model. The rats were placed in alternating hypoxic and hyperoxic environments. The alternating environments lead to severe retinal complications, which were not representative of retinopathy in human babies. Since the timing and duration of the hypoxia was inadequate, it gave inconsistent results. In our study we used a mouse model developed by Louis Smith.[171] An advantage of using the mouse retina is that in the newborn mouse the retinal vessel development stage is the same as that of premature human babies. Also, normal retinal vascular development in mice occurs within two weeks of birth, thus illustrating the evolution

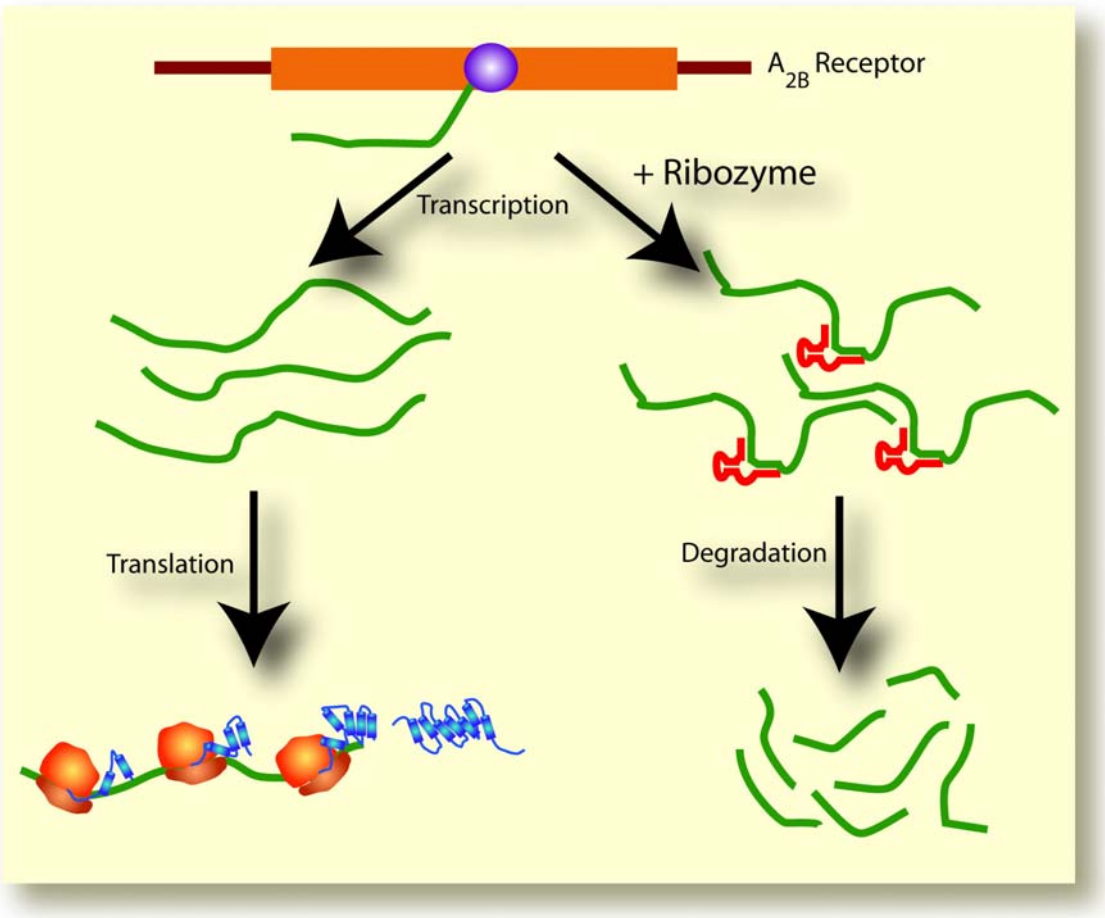

Figure 1-34. Cleavage of the A_{2B} receptor by a ribozyme prevents translation of the protein.

Species	A_{2B} Rz1 Target	A_{2B} Rz2 Target
Mouse	ACAUGUCUCUUUG	CAUUGUCUAUGCC
Human	AAGUGUCUCUUUG	CAUUGUCUAUGCU

Figure 1-35. Target sequences of the human and mouse A_{2B} ribozymes 1 and 2. Red indicates a difference in sequence between the human and mouse species.

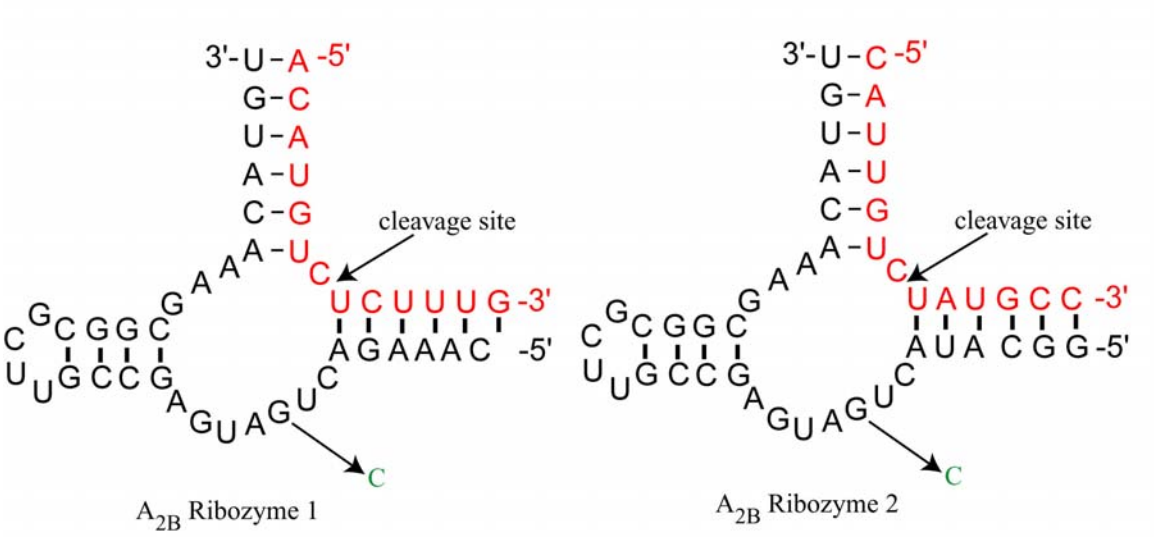

Figure 1-36. Hammerhead ribozymes for the A_{2B} Rz1 and Rz2. The target sequences are indicated in red. For each ribozyme an inactive version of the ribozyme was made with a C replaced by the G (arrow).

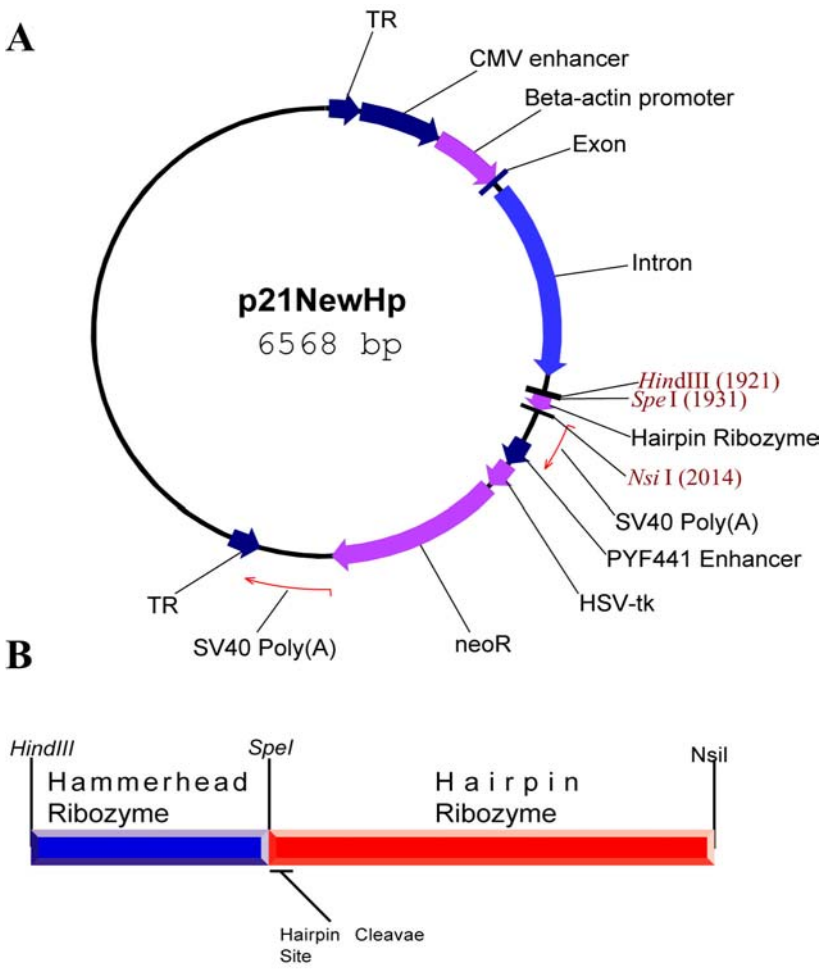

Figure 1-37. A)The p21Newhp Vector with the CMV enhancer and beta actin promoter. The hammer head ribozyme was cloned between the HindIII and SpeI sites. B) The hammerhead and the hairpin cleavage sites.

of the vascular bed. Mouse retinal vessels develop from spindle-cell precursors, which are found in the superficial layer of the retina and the deeper retinal vessels develop later. The same developmental pattern is observed in the human retina. Thus the similarities between the mouse retinal vasculature and that of the human premature babies makes it amenable for use in a model of ROP to better understand the human form of the disease.

In the Smith model, seven day old mouse pups are placed in a 75% oxygen chamber for 5 days. Upon return to normal air, these mice developed retinal neovascularization. Five days following return to normoxia (day 17), the animals are sacrificed and the eyes removed (Figure 1-38). Smith described two methods to quantify the neovascularization in the mice retina while minimizing the error and making the model applicable to retinopathy.[171] First, Smith recommended fluorescein labeled dextran perfusion of the animals into the left ventricle followed by flat mounting of the retinas. The perfusion technique delineated the blood vessels, however, it was not permanent as the fluorescein is sensitive to light. Thus, perfusion was recommended for a quick survey of the blood vessels present in the retina following exposure to hyperoxia. A second method that Smith recommended was counting the vascular nuclei in paraffin cross sections of the retina. Serial cross sections were stained with hematoxylin and eosin and the blood vessels were quantified by counting the number of vascular cell nuclei on the vitreal side of the inner limiting membrane. This method is more time consuming, however, it was reported by Smith to be more sensitive, reliable and reproducible.[171] This model has also been used by our lab for other studies pertaining to retinal development. For example, Mino et al used this model to examine the effects of various adenosine antagonists on neovascularization. [95]

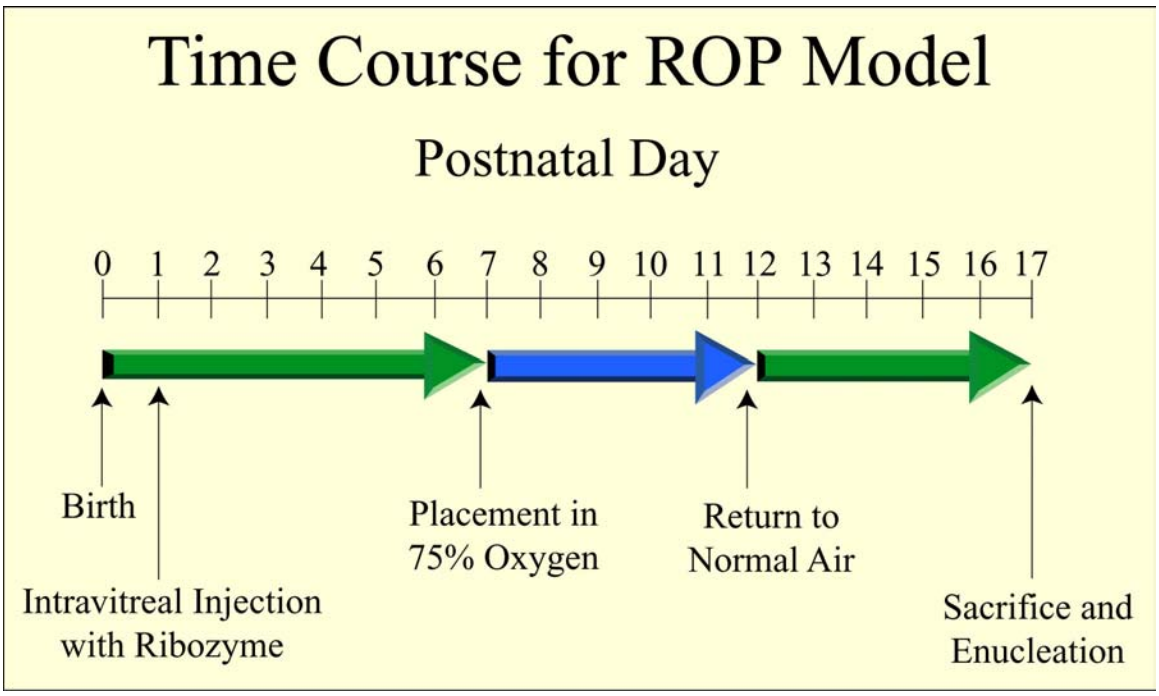

Figure 1-38. Time course for the ROP model. Seven day old pups are placed in a 75% oxygen chamber for 5 days. On day 12, the mice are returned to normal air and their eyes enucleated on day 17.

CHAPTER 2
METHODS AND MATERIALS

Defining Location of the Target Sequence

It is important to define the region of target mRNA where the ribozyme will bind and cleave. For hammer head ribozymes the highest k_{cat} (enzymatic rate of catalysis) has been observed for a GUC ribonucleotide sequence. Thus, it is important to locate all the GUC triplets within the target mRNA.

To decide where in the mRNA to target the ribozyme, Genbank was used to obtain sequences for the human A_{2B} receptor and for the mouse A_{2B} receptor. The results were transferred into Vector NTI and all of the GUC sequences identified. All the sites containing the GUC triplet were considered to be potential target regions, however, additional criteria were used to narrow these potential sites. Target regions with six nucleotides on either side of the arms consisting of a 50% GC content were selected since an ideal length for the target region is between 6-7 nucleotides. The presence of a U/A at the 3' cleavage site also enhances the k_{cat} ten fold. Therefore, application of these criteria reduced the potential number of target sequences to those containing GUCU/GUCA regions. Selected target regions were examined using the RNA folding algorithum designed by Micheal Zucker.[172] The folding program was used to fold 00-200 nucleotides on either side of the GUC target to determine whether the ribozyme binding location was acceptable.

A blast search was also conducted to ensure that the ribozyme did not cleave another known mRNA sequence within the known mouse or human sequences.

Preparation of the Target Oligo-Nucleotide.

The target oligonucleotide to be used in the cleavage reactions was radioactively labeled at the 5'end using T4 polynucleotide kinase (New England Biochmeicals; Beverly, MA). The reactions were set up as follows: 2µl of the RNA oligo (10pmol/µl, 20pmol total) was added to a mixture containing 1ul of 10X polynucleotide kinase buffer (Promega, Madison, WI), 1ul RNASin (Promega, Madison, WI), 1ul 0.1M DTT (Sigma, St. Louis, MO), 3µl water, 1µl (gamma ^{32}P) dATP (10uci) (ICN, Santa Clara CA) and 1µl of polynucleotide kinase (5 units) (Sigma, St. Louis, MO). The reaction was incubated at 37 °C for 30 minutes. 90µl of TE (Fisher, Swanee, GA) was added to the reaction prior to extraction of the unincorporated nucleotides.

A spin column (1ml syringe) was prepared with sterile glass wool and loaded with sephadex (Sigma, St. Louis, MO) saturated in water. The column was centrifuged at 1000 RPM for 5 minutes to remove any excess water and to further pack the sephadex. The ^{32}P labeled target (100µl) was loaded on to the column. The column was sealed with parafilm and centrifuged again at 1000 RPM for 5 minutes. The labeled elute was collected in a 1.5ml Eppendorf tube (Fisher, Swanee, GA) and was stored at -20 °C.

Time Course of Cleavage Reactions for Mouse and Human Targets (Hammerhead Ribozymes)

To evaluate the time course of cleavage of the ribozyme for the target, a cleavage reaction was set up as follows: 13µl of 400mM Tris-HCL (Fisher, Swanee, GA), pH 7.4-7.5 was added to 1ul ribozyme (2pmol) and 88ul of water. The mixture was incubated at 65 °C for 2 minutes and then left at room temperature for 10 minutes. 13µl of a 1:10 ratio of RNASEin:0.1M DTT was added to the reaction mixture along with 13µl of 200mM Magnesium chloride (20mM final) (Sigma, St. Louis, MO). The reaction was

then incubated at 37 °C for 10 minutes. 1µl of the ^{32}P labeled target (0.2 pmol) and 1µl of the cold target (20pmol total) were premixed and added to the reaction mixture at 37ºC. Time points were taken at 0, 1, 2, 3, 4, 5, 10, 15, and 30 minutes , and at 1, 2, and 3 hours and overnight. For each time point, 10 µl of the reaction mixture was removed from 37 °C and added to a tube containing 10ul of formamide dye mix (90% formamide (Sigma, St. Louis, MO), 50mM ehtylenediamine tetra acetic acid (EDTA) pH 8 (Fisher, Swanee, GA), 0.05% bromophenol blue (Sigma, St. Louis, MO), and 0.05% xylene cyanol (Sigma, St. Louis, MO). The samples were initially placed on ice and then heat denatured at 90 °C for 3 minutes. The denatured samples were cooled on ice before loading 6 µl onto a 10% PAGE-8M urea gel to separate the products. Bromophenol blue was run about 2/3 down the gel. The gels were analyzed on a molecular dynamics phosphoimager.

Multiple Turnover Kinetics

Multiple turnover kinetics were performed on the ribozymes. Reactions were performed in a final volume of 20 µl. Ribozyme (0.3 picomol, 15nM final) in 40mM Tris –HCL (pH 7.5) was incubated at 65 °C for 2 minutes and then incubated at 25 °C for 10 minutes. DTT (20mM final) and magnesium chloride (20mM final) and 4 units of RNasin were added. The reactions were incubated at 37 °C for 10 minutes, and cleavage was initiated by the addition of increasing concentrations of the target oligonucleotide (0-300 picomol; 0-1500 nM final). The reactions were incubated at 37 °C for a fixed interval determined in the time course analysis of cleavage. A variation on this protocol was incubation at 25 °C in 1mM $MgCl_2$. Reactions were terminated by the addition of 20 µl of formamide stop buffer and held on ice. The samples were then heat denatured at 95

°C for 2 minutes, placed on ice and the reaction products separated on 10% polyacrylamide-8M urea gels. The gels were analyzed on a molecular dynamics phosphoimager.

Cloning of the Hammerhead Ribozymes into the rAAV Expression Vector

Two complimentary DNA oligonucleotides (Invitrogen, Carlsbad, CA) were annealed in order to produce a double stranded DNA fragment coding for each hammerhead ribozyme. All DNA oligonucleotides were synthesized with 5'phosphate groups. The DNA oligonucleotides were designed to generate a cut HindIII site at the 5' end and a cut SpeI site at the 3' end after annealing. The DNA oligonucleotides were incubated at 65 °C for 2 minutes and annealed by slow cooling to room temperature for 30 minutes. The resulting double stranded DNA fragment was ligated into the HindIII and SpeI sites of the rAAV vector pTRUF-21 (UF vector Core, http://www.gtc.ufl.edu/gtc-home.htm). A self cleaving hairpin ribozyme has been cloned downstream of the inserted hammerhead ribozymes into the SpeI and NsiI sites. This vector has the cytomegalovirus (CMV) beta-actin chimeric enhancer-promoter and results in the hairpin ribozyme cleaving eight bases downstream of the 3'end of the hammerhead ribozymes. The ligated plasmids were transformed into SURE electroporation competent cells (Stratagene, La Jolla, CA) in order to maintain the integrity of the inverted terminal repeats. The ribozyme clones were verified by sequencing.

Sequencing of the Clones

Prior to sequencing the hammerhead inserts, the integrity of the inverted terminal repeats (TR's) was verified by digestion with the restriction endonuclease SmaI. This

digest also served to determine the approximate concentration of the plasmid. The hammerhead inserts were verified by sequencing using the Ladderman Dideoxy sequencing kit (TaKaRa Shuzo Co, Japan) according to the manufacturers protocol.

Human Retinal Endothelial Cell (HREC) Tissue Culture

HREC were isolated from human donor eyes within 24 hours of death. The eyes were placed on a sterile gauze pad (Johnson and Johnson Medical Supplies, Arlington, Texas) in a laminar flow hood and washed with 5ml betadine (Courtesy, Shands Hospital, Gainesville, Fl). Sterile scalpels (No. 1, Feather Industries limited, Japan) and tweezers were used to dissect the eyes and remove the neural retina from the posterior portion of both eyes. The RPE layer was not included in the harvested retina. The retinae were placed on a 53 micron mesh nylon membrane (Tetko Inc, Lab Pack, Kansas City, MO) and the remainder of the ocular components discarded. The retinas were washed with phosphate buffered saline (PBS) containing 2% antibiotic/antimycotic mix (ABAM) (Sigma, St. Louis, MO). A sterile wooden spatula was used to grind the retina over the nylon membrane while washing. The remaining retinae were aspirated into a sterile 10ml pipette and added to a 20ml Erlenmeyer flask containing 10ml of PBS with antibiotics. Approximately 1mg of collagenase (342 u/mg, Worthington Biomedical Corporation, Lakewood, NJ) was added to the flask and placed in a 37 °C water bath for 15 minutes. The flask contents were mixed every 5 minutes to keep the collagenase dissolved. Following the 15 minute incubation in the 37 °C water bath, 20ml of complete endothelial cell media was added to the flask. (250ml Dulbelco's Modified Eagle Medium (DMEM) low glucose, 250 ml HAM's F12, 10% fetal bovine serum, 15% endothelial cell growth supplement, 15% insulin/transferring/selenium, 2% L-glutamic

acid, 2% antibiotic/antimycotic mix). The cells were washed twice with media and plated onto a T25 flask (Fisher, Springfield, NJ) coated with 1% gelatin (Sigma, St. Louis, MO). The cells were allowed to grow and attach for 48-72 hours before changing the media and adding fresh antibiotics. Once the T25 flask was confluent, the cells were passed and split into T75 flasks using 5ml of trypsin EDTA solution for endothelial cells (Sigma, St. Louis, MO). For passing the cells, the cells were washed twice with PBS and then 5ml of trypsin added. The flask was placed into the CO_2 incubator for 45 seconds. The trypsin was neutralized using 2x volume of the complete endothelial cell media. The cells were centrifuged at 1000 RPM in an Eppendorf CT 5810R. The pellet was re-suspended in 6ml of complete endothelial cell media and plated in a T75 flask (Fisher, Swanee, GA) containing 15ml of complete endothelial cell growth media and fresh antibiotics.

LDL Uptake of the HREC

HREC were seeded in a 6 well tissue culture plate (Corning Incorporated, Corning, NY) and allowed to attach and grow to about 80-85% confluency. Morphology of the HRECs was observed and recorded using a Carl Zeiss Microscope (Zeiss, Goettingen, Germany).

The HREC were washed twice with Hanks Balanced salt solution (HBSS) (Sigma, St. Louis, MO). 50 μg/ml of Dil labeled (1,1'-dioctdycl-3,3,3',3'-tetramethyl-indocarbocyanin perchlorate) acetylated LDL (Molecular probes, Eugene, OR) was added to the cells overnight in serum free medium. The cells were then washed with HBSS and examined by fluorescence microscopy for the uptake of the label. The cells were quantified as a percentage of labeled cells/total cells.

Transfection of HREC using DEAE-Dextran

HREC were transfected at 70% confluency on an 150 mm tissue culture dish (Bio-Rad, Hercules, CA). The cells were washed twice with PBS (Biowhittaker, Walkersville, Maryland) and 10.5ml of 10% Nuserum (Bio-Rad, Bedford, MA) was added to the culture dish. (10% Nuserum has all the ingredients of endothelial cell complete media except for the fetal bovine serum). 10 μg of DNA in Tris buffered saline (TBS) (Bio-Rad, Hercules, CA) (total volume of 108 μl) was prepared in an eppendorf tube. 216 ul of DEAE dextran (diethylaminoethyl-dextran) (Sigma, St. Louis, MO) (10mg/ml) were added dropwise to the tube while constantly mixing on a vortex mixer. 324 μl of this mixture was added to the 150mm tissue culture dish containing 10.5ml of 10% Nuserum. The mixture was added dropwise across the plate and the plate swirled to distribute completely. Immediately, 8.1μl of chloroquine (100 mM) (Sigma, St. Louis, MO) was added to the plate and swirled. Chloroquine prevents the lysosmes from releasing DNAses that would destroy the DNA. The plates were incubated at 37 °C for 4 hours in a CO_2 incubator and the plates were mixed every 15 minutes to ensure even distribution of the plasmid. After incubation, the cells were treated with 15ml of 10% dimethly sulfoxide (DMSO) (Sigma, St. Louis, MO) in PBS for 1 minute. The cells were then washed twice with PBS. 20ml of complete endothelial cell media was added to the plates and the plates held in a CO_2 incubator at 37 °C. Media with fresh antibiotics was replaced after 24 hours. The cells were then allowed to grow for about 48 hours following replacement of media before harvesting the cells for further analysis.

Transfection Efficiency using DEAE Dextran for HREC's

To determine the efficiency of HREC transfection, HREC were transfected as described above, using a plasmid expressing GFP (PTRUF11) obtained from the Vector Core at the University of Florida. The level of GFP expression was observed using a Carl Zeiss fluorescent microscope (Zeiss, Goettingen, Germany).

Cell Migration Assay

HREC were grown in 150mm tissue culture dishes and transfected using the DEAE dextran method. The HREC were washed twice with PBS. 7ml of trypsin was added to the culture dish and incubated at 37 °C in a CO_2 incubator for 45 seconds. The cells were observed during this period to ensure maximal detachment of the cells. The trypsin was neutralized using 14ml of complete endothelial cell media containing fetal bovine serum. The cells were then centrifuged at 1000 RPM for 5 minute. The supernatant was discarded and the cells washed three times with basal media.

The number of cells was determined with a hemacytometer (Hausser Scientific Horsham, PA). The cells were suspended in 50 µl of PBS to a final concentration of 10,000 cell/µl. 30ul of the resuspended cells were loaded into the wells of a Chemotaxis Chamber (Neuro Probe Inc, Gaithersburg, MD). The wells were covered with a 12uM porous polycarbonate membrane (Neuro Probe Inc, Gaithersburg, MD) pre-coated with 10% bovine collagen. The chemotaxis chamber was then sealed and placed upside down in a 37 °C CO_2 incubator. This allowed the cells to attach to the lower side of the 12 µM porous membrane. After 4 hours, the chamber was removed, and the cells stimulated with 1, 10 or 100 µM concentrations of NECA (dissolved in endothelial cell basal media (serum free). 50ul of the positive control (complete endothelial cell media), negative

control (endothelial cell basal media), or NECA concentrations were added to the top of the chamber. The chamber was then incubated at 37 °C in a CO_2 incubator for 12 hours, to allow the attached cells to migrate through the porous membrane.

The chamber was disassembled and the porous membrane removed from the chamber. The dull side of the membrane (containing all the attached cells) was scraped using a cell scraper. The membrane was then stained using a diff Quik R stain set (Dade Behring Inc, Newark, DE) and mounted onto a glass slide. The migrated cell nuclei per well were counted per high power field.

Morphology of HEK Cells

HEK 293 cells were obtained from American Type Culture Collection (ATCC) (Manassas, VA) and plated onto a 150 mm tissue culture dish. The cells were allowed to attach and grow to about 80% confluency. To ensure a homogenous population of HEK cells, the morphology of the HEK cells was recorded using a Zeiss microscope (Zeiss, Goettingen, Germany).

Transfection using Lipofectamine on HEK 293 cells

HEK 293 cells (ATCC, Manassas, VA) were seeded onto a 150mm tissue culture dish and allowed to attach and grow to 85-90% confluency. The HEK cells were fed with 1X high glucose Dubellco's modified Eagle medium (Gibco, Carlsbad, CA) containing 2% fetal bovine serum and 2% ABAM. Prior to transfection, the media was removed and 20.1 ml of high glucose DMEM with 2% FBS was added to the cultured cells. The antibiotics were not added for the duration of the transfection assay.

33.5µg of DNA was dissolved in 2,010 µl of optimem I reduced serum media (Gibco, Carlsbad, CA) (final volume). 134ul of lipofectamine 2000 reagent (Invitrogen,

Carlsbad, CA) was also diluted in 2,010 µl of optimem (final volume) and incubated at room temperature for 5 minutes. The diluted DNA was then added to the diluted lipofectamine reagent and incubated at room temperature for a further 20 minutes. The entire mixture was then added to the cultured HEK 293 cells and gently swirled. The cells were incubated at 37 °C in a CO_2 incubator. After 24 hours, the media was changed and the antibiotics replaced.

Transfection Efficiency for HEK Cells using Lipofectamine Reagent

The HEK cells were transfected as above with the plasmid pTRUF-11 which expresses GFP. GFP expression was determined using a fluorescence microscope at: 6hr, 24 hr, 48hr, 72 hr, 96hr, P1 and P2.

cAMP Assay on Transfected HEK 293 Cells

HEK cells transfected with the plasmids expressing either the active or inactive ribozymes, or the control plasmid were harvested for the cAMP assay. A Bradford protein assay (Bio-Rad) was used to determine the amount of protein in the transfected cells. A stock solution of 1mg/ml of BSA (Sigma, St. Louis, MO) was used to prepare the standard curve. 100ul final volume of protein standards containing 50 µg, 100 µg, 200 µg and 300 µg of BSA were prepared in water. The unknown samples were diluted 1:10 with water to a final volume of 100 µl. 2ml of protein assay dye reagent (Bio-Rad, Hercules, CA) diluted 1:5 with water was added to all the standards and unknown samples. The absorbance of standards and samples at 595nm was determined using a Beckman spectrophotometer. The concentration of protein in the unknown samples was determined by comparison to the linear regression plot of the standard curve. Based on the protein concentration in the unknown samples, the unknowns were diluted to a final

concentration of 1.5mg/ml with Hanks balanced salt solution (HBSS) (Gibco, Carlsbad, CA.). Unknown samples were diluted immediately prior to the addition of the adenosine agonist.

For each transfected dish, a total of 16 Eppendorf tubes were set up and the cells stimulated with NECA. Basal levels were determined in duplicate in the absence of NECA. Seven concentrations of NECA were prepared from a $1x10^{-2}$ stock solution ($1x10^{-4}$, $5x10^{-5}$, $1x10^{-5}$, $5x10^{-6}$, $1x10^{-6}$, $1x10^{-7}$, $1x10^{-8}$ (final concentrations in HBSS). Each concentration of NECA was done in duplicate. Tubes contained 150ul of HBSS and 50ul of cells (1.5mg/ml). Cells were pre-warmed in a 37 °C water bath for 5 minutes. Following the incubation, 50ul of a phosphodiesterase inhibitor (10 μM roliprom (Sigma, RBI, St. Louis, MO) (100 mM final concentration) was added to all the tubes including the basal tubes. 5ul of the NECA concentrations were added in duplicate to all 16 tubes. No NECA was added to the basal tubes. The tubes were incubated for a further 10 minutes at 36°C water bath. To end the reaction, all tubes were placed in a boiling water bath for minutes. The tubes were cooled to room temperature and centrifuged at 2000 rpm for 2 minutes. The supernatants were then assayed for cAMP content.

A cAMP standard curve ranging from 1 nmol to 25 pmol was prepared using a stock solution of $1x10^{-3}$ M cAMP (Sigma, St Louis, MO). Each unknown was assayed in duplicate. Additional tubes used to determine total binding and non-specific binding were also included. The resultant cAMP standard curve ranged from the non-specific to the total binding and was a sigmoidal curve. The samples were expected to fall within the linear range of the sigmoidal curve.

For samples, 50µl of the supernatant was added to a glass test tube. To the non-specific tube, 50µl of the highest cAMP concentration was added. 50µl of (^{125}I) ScAMP (adenosine 3'5' cyclic phosphoric acid 2') -succinyl (^{125}I) iodotyrosine methyl ester, courtesy Dr. John Shyrock, Dept of Pharmacology and Therapeutics, University of Florida, Gainesville) was added to all the tubes including the cAMP standard curve. 50µl of the cAMP antibody (Accurate Chemical Company, Westburg, NY) was also added to all tubes including the standard curve. The tubes were then covered with parafilm and incubated at 4 °C overnight for at least 12 hours.

Next, 75µl of a hydroxyapatite solution (Biomedical Research and Development Laboratories), diluted 1:3 with water, was added to the tubes. The cAMP and the antibody bound to the hydroxyapatitie. The tubes were then washed with cold 10mM Tris-HCl pH 7.0 using a cell harvester (Brandell, Gathersburg, Maryland). A glass fiber filter, grade No.32 (pore size 2.3 um) (Schleicher and Schuell, Keena, NH) was used to trap the complexes bound to the hydroxyapatite. The individual filters were then placed in a Beckman G5500 counter which measured the ^{125}I emissions in a one minute window.

The results were analyzed with the statistical analysis and Graphics software, Prism (Graphpad software, San Diego, CA) was used. The unknown sample concentrations were determined from the standard curve as pmole per sample of cAMP accumulated. The cAMP per mg of protein was determined. Basal values were subtracted from the NECA stimulated tubes to obtain a net response of NECA. Based on these values, a dose response graph was plotted. Maximum binding was determined by the (^{125}I) ScAMP bound in the absence of additional non-radioactive cAMP. Non-specific binding was

determined by the addition of 500 pmoles cAMP and was subtracted from all the other readings before plotting the standard curve. By subtracting non specific binding from the total binding, specific binding for the assay was determined. The percent inhibition of (^{125}I) ScAMP binding to the antibody by additional cAMP (1nmol to 25 pmoles) was graphed. As the cAMP concentraion increased, less ^{125}I was detected. An EC 50 for the effect of NECA was also calculated. EC 50 is the effective concentration that displays a 50% response in cAMP production.

Total Retinal RNA Extraction for PCR

Total retinal RNA was isolated from HEK 293 cells using TRizol LS reagent (Invitrogen, Carlsbad, CA) following the manufacturers protocol.

Real Time PCR

The cDNA was synthesized using either 2 or 4μg of total RNA and TaqMan ^{R} reverse transcription reagents (PE Applied Biosystems, Foster City, CA) in 100μl RT reactions. TaqMan ^{R} real time PCR analysis was applied using 1ul cDNA per reaction and SYBR R Green PCR core reagents on ABI prism sequence detection system 5700 (PE Applied Biosystem, Foster City, CA). In each experiment, a standard curve for each primer pair was obtained using a serial dilution of total RNA samples prepared from cells that over expressed A_{2B} adenosine receptor. At the end of the PCR cycle, a dissociation curve was generated to ensure the amplification of a single product and the threshold cycle time (ct values) for each gene was determined. Relative mRNA levels were calculated based on the ct values and normalized to a house-keeping gene: cyclophilin (100%).

Animals

All animals were treated in accordance with the IACUC of the University of Florida and the ARVO statement for the use of animals in ophthalmic and vision research. All animal protocols were approved by the IACUC at the University of Florida prior to experimentation. C5BL6/J pregnant mice on gestation day 14 were obtained from Jackson Laboratory (Bar harbor, ME). The mice were housed in the University of Florida Health Science Animal Resources facilities. A Total of 24 animals were used (8 animals per plasmid) Animals were sacrificed by injecting a lethal dose of ketamine followed by spinal dislocation.

Intraocular Injection into the Mouse Model of Oxygen Induced Retinopathy

One day following birth, the mouse pups received a 0.5ul intravitreal injection of plasmid (2mg/ml) OD (right eye). In the neonatal mouse model of oxygen induced retinopathy, 7 day old mice were placed with their nursing dams in a 75% oxygen atmosphere for 5 days. The oxygen chamber was monitored with an oxygen sensor within the closed chamber. The chamber oxygen level was maintained for 5 days at 75%. After the fifth day, the oxygen chamber was slowly returned to 21% oxygen over a period of one hour. The animals were removed from the oxygen chamber and placed in clean bedding. Upon return to normal air, these mice developed retinal neovascularization, with peak development occurring 5 days after their return to normoxia. After the fifth day following return to normoxia (day 17), the animals were sacrificed and the eyes removed and fixed in 4% paraformaldehyde and embedded in paraffin. Three hundred serial sections (6 μm) were cut sagitally through the cornea parallel to the optic disc. Every thirtieth section was placed on slides and stained with hematoxylin and eosin (H&E). This resulted in ten sections from each eye being scored in a masked fashion

using light microscopy by counting endothelial cell nuclei extending beyond the inner limiting membrane into the vitreous. The efficacy of treatment with each plasmid was then calculated as the percent average nuclei per section in the injected eye versus the un-injected control.

Statistical Analysis.

Student T-test was used to evaluate the data generated for all the experiments. A p value of less than 0.05 was considered to be significant.

CHAPTER 3
RESULTS

The expression of the A_{2B} receptor upregulates VEGF expression which in turn leads to angiogenesis. The hypothesis underlying this research project was that a decrease in the A_{2B} receptor expression may prevent or decrease the severity of the angiogenesis. In this study, two different ribozymes were designed to cleave the A_{2B} receptor mRNA. Two corresponding inactive versions of the ribozyme were also made.

Determining Accessibility of the Target Site

Success of ribozyme therapy depends on the identification of an RNA target site. The m-fold program analysis was used to determine if the chosen target would be accessible to the ribozyme for binding. Figure 3-1 shows the theoretical tertiary structure of the active A_{2B} Rz1 and Figure 3-2 shows the active A_{2B} Rz2 mRNA under cellular conditions.

Ribozymes generally fold into one of four secondary structure types. Type A, B, C and D. Type A structures have the highest activity based on the delta G values. The targeting arms in the type A structure do not interact to form a secondary structure and thus are readily available for target binding. Types B and C compete with the type A structure and reduce the activity of the ribozyme. However, these structures are catalytically active in vitro and should thus be effective in vivo. Ribozymes that form

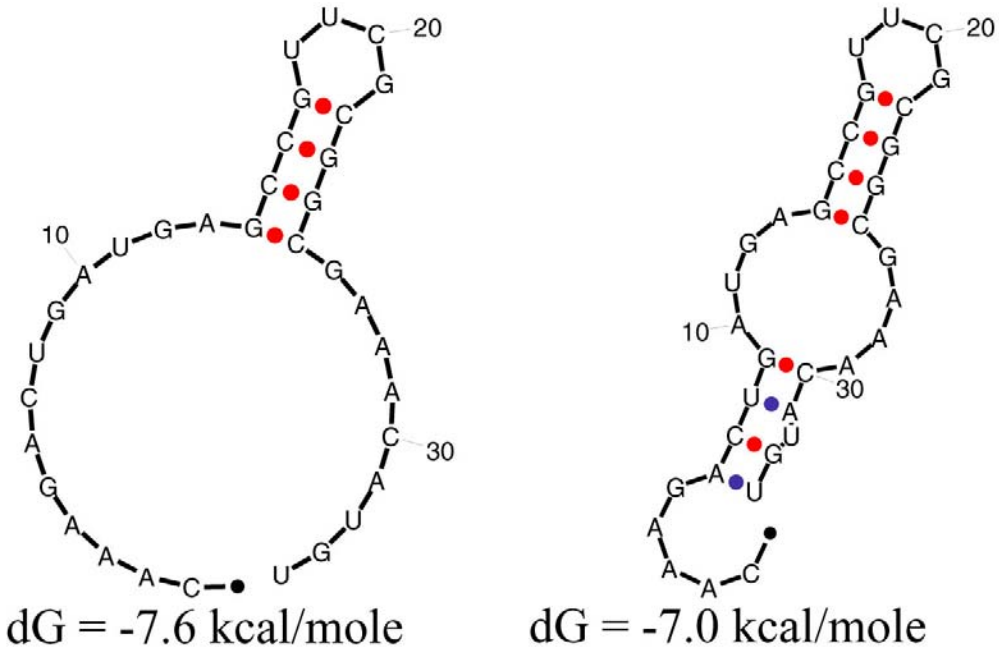

Figure 3-1. Theoretical tertiary structures of the active A_{2B} Rz1 generated by the mfold program.

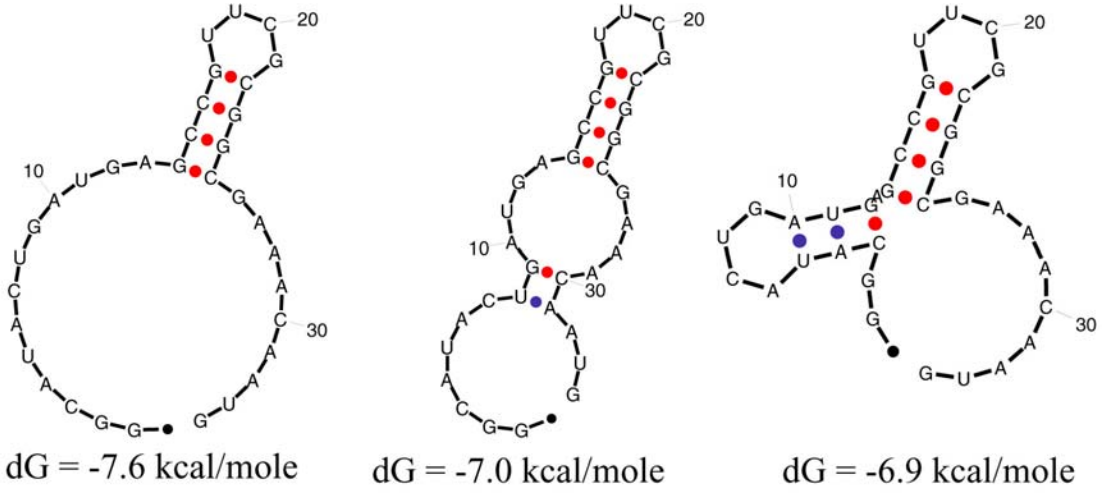

Figure 3-2. Theoretical tertiary structures of the active A_{2B} Rz2 generated by the mfold program.

structures which are significantly more stable than the type A, such as type D, can completely inhibit the ribozymes catalytic activity and should not be considered for in vitro and in vivo studies.

The m-fold analysis showed that the A_{2B} Rz1 could fold into two structures, types A and C, with dG's of -7.6 and -7.0 kcal/moles respectively. The A_{2B} Rz2 analysis by m-fold produced three structures, types A, B and C with dG's of -7.6, -7.0 and -6.9 kcal/mol respectively. Based on this analysis both of the A_2B ribozymes should be effective in vitro, and, therefore we decided to test both ribozymes.

Time Course of Ribozyme cleavage

Time course of cleavage analysis was done for the A_{2B} Rz1 and the A_{2B} Rz 2 as described in the Methods section. Figure 3-3 is an autoradiograph from a 10% polyacrylamide-8M urea gel used to separate the products of cleavage of the A_{2B} Rz2 on the mouse target for reactions performed at 37 °C and at 20 mM $MgCl_2$. The autoradiograph shows an increase in the 5'cleaved product over time and a corresponding decrease in the target. Significant product accumulation was found at 1 minute after the addition of the target to the ribozyme. Figure 3-4 shows the graphical representation of the data in Figure 3-3 in addition to the data for the A_2B Rz1 on the mouse target. The A_{2B} Rz2 appears to have the higher rate of cleavage.

Kinetic analysis on the hammerhead ribozymes is performed at the time point where no more than 15% of the target has been cleaved. We select this point because the ribozyme cleavage rate is at a maximum and is linear at this point and the ribozyme is saturated by the target. Figure 42 shows that this time point is less than one minute for the A_{2B} Rz2. Since we do our kinetic analysis manually, as opposed to using a flow

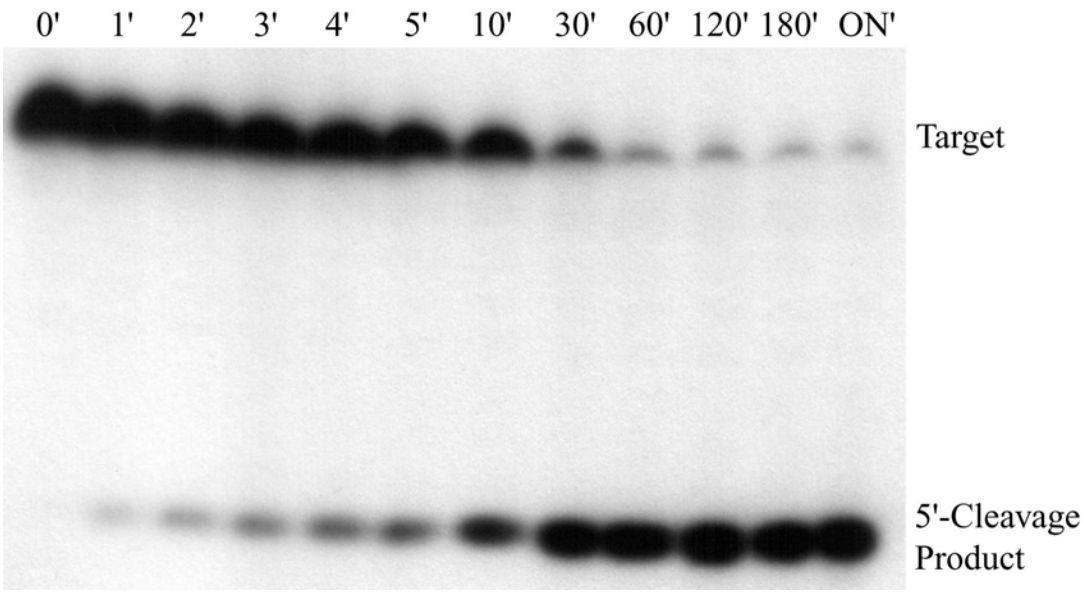

Figure 3-3. Time course autoradiograph of a 10% polyacrylamide 8M urea gel showing products of cleavage of the A_{2B} Rz2 on the mouse target. The autoradiogarph shows an increase in the 5' cleavage product over time and a corresponding decrease in target.

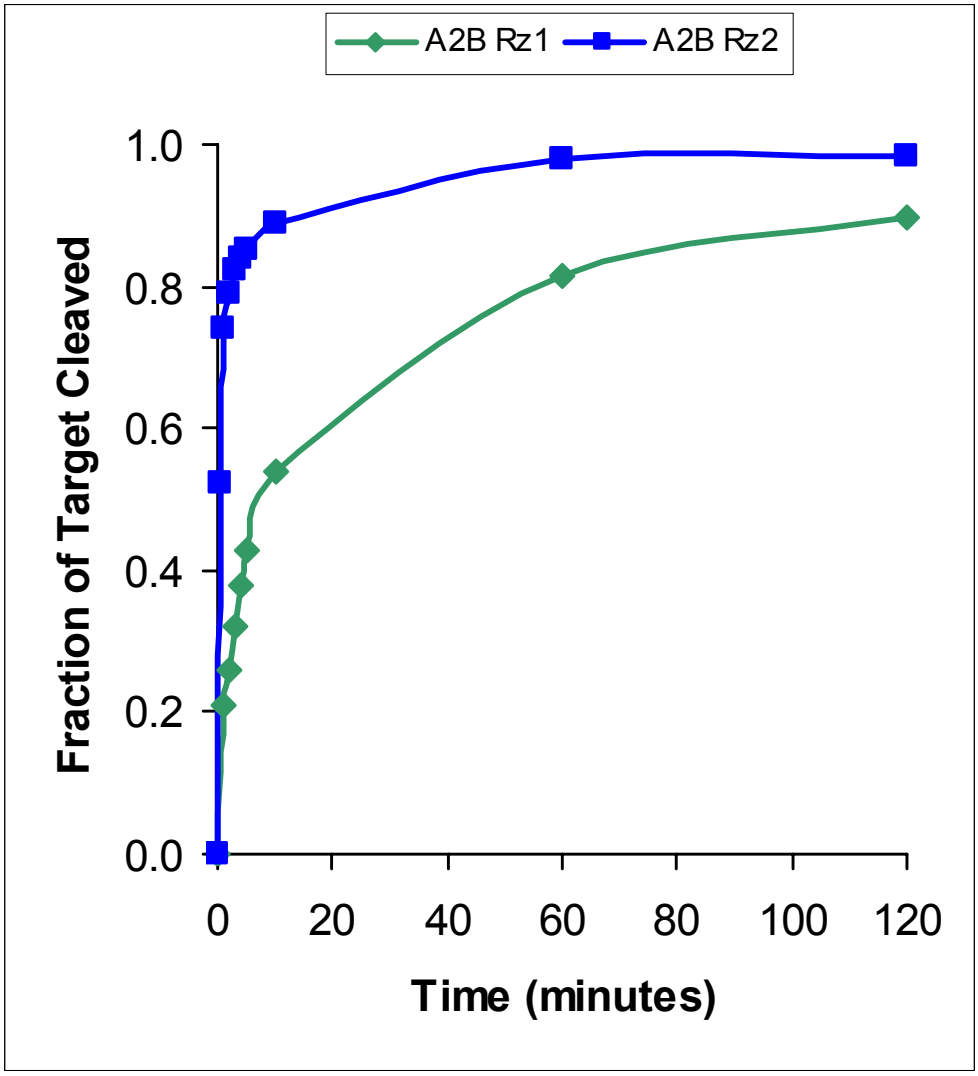

Figure 3-4 Time course analysis data. Graphical representation of the cleavage for the A_{2B} Rz1 and A_{2B} Rz2 appears to have a higher rate of cleavage with 15% of the target being cleaved in less than one minute.

cytometer, we decided to reduce the rate of cleavage of both ribozymes in order to find a time point where manual kinetic analysis could be easily completed.

Time course reactions were performed with increasing concentrations of the target (1:10, 1:40, 1:66, 1:100; Rz:Tar). (Figure 3-5) Increasing the target concentrations also did not slow the ribozyme down enough to assess the time point at which 15% of the cleavage occurs. Next the temperature and MgCl2 concentration were varied for the time course of cleavage reactions. Figure 3-6 shows the results of this analysis for the A2B Rz2 which yielded a time point of about 1 minute where the amount of target was reduced by 15%. Based on this type of analysis we did kinetic analysis on the A2B Rz1 at 37 ºC at 20mM MgCl2 at a time point of 6 minutes, and on the A2B Rz2 at 25 ºC at 1 mM MgCl2 at a time point of 1 minute.

Multiple Turnover Kinetics

To ensure cleavage of the RNA substrate in vivo, it is important to design ribozymes with the highest possible catalytic activity and therefore this turnover number (k_{cat}) and the Michaelis constant (Km) of the ribozymes were determined. This analysis relies on several assumptions: first, measurement of the initial rate of the reaction ensures that changes in the formation of the product and depletion of substrate do not affect the rate of reaction. Conventionally, kinetic measurements are made when no more than 15% of the substrate is converted to the products. A second assumption is that the concentration of the ribozyme is lower than the Km. A low ratio of the ribozyme to target ensures that the

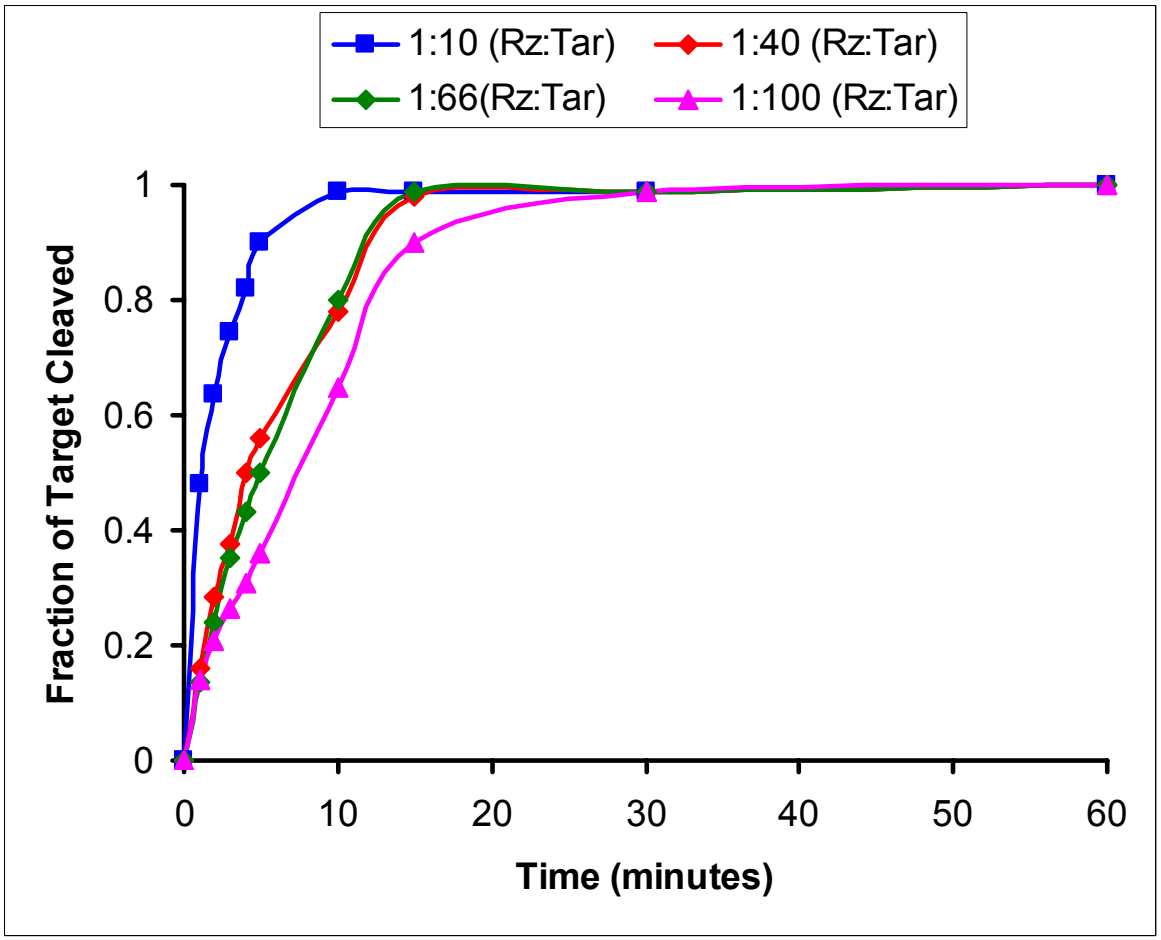

Figure 3-5. Time course of the ribozyme with increasing target concentrations.

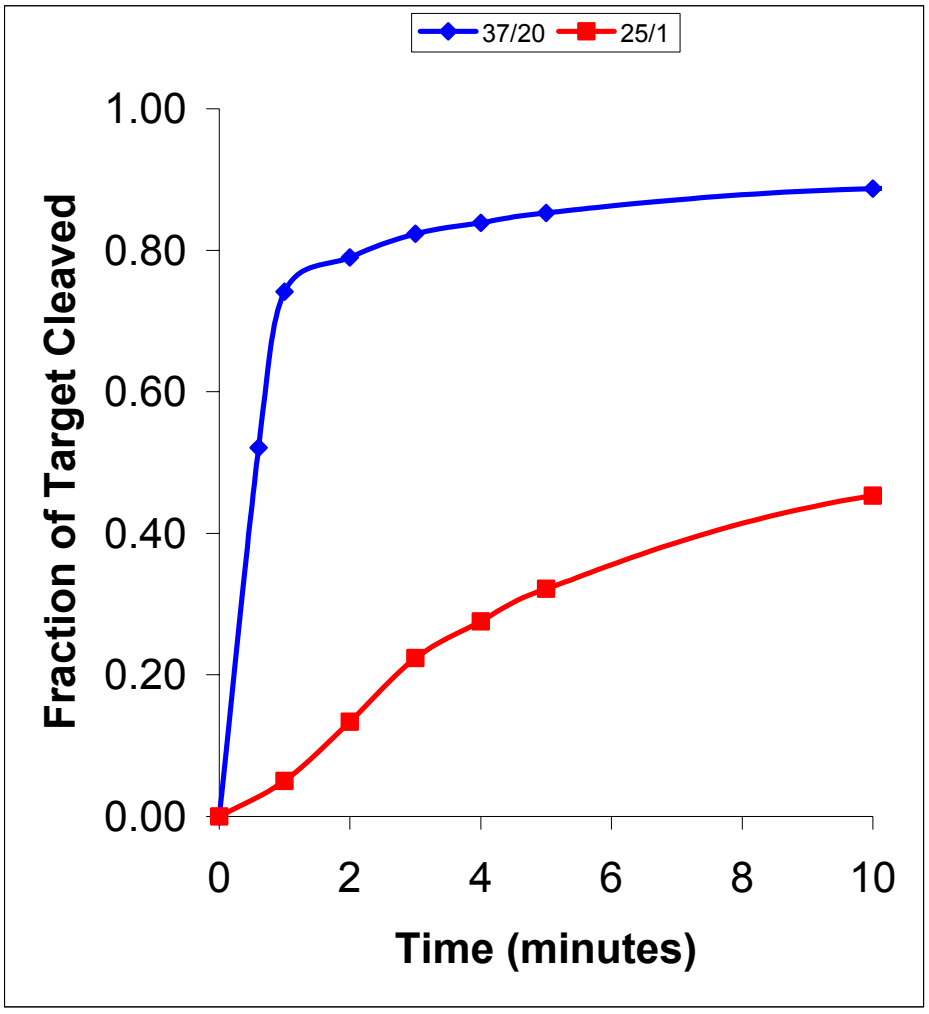

Figure 3-6. Time course cleavage reaction with varying temperatures (37 ºC/25ºC) and magnesium concentrations of 20mM/1mM.

velocity of the reaction is proportional to the concentration of the ribozyme thus allowing the turnover rate of the reaction to be determined. The initial rate (v_0) is determined by dividing the concentration of the reaction product over time. A liner regression curve is then plotted of 1/v vs 1/s and the kinetic parameters (Figure 3-7) can thus be determined from the equation for the line generated from the data ($1/V_{MAX}$=abs/y at X=0, $1K_m$= abs/X at y=0). Each analysis was performed a minimum of 3 times. The reactions were done at 37ºC and terminated at 6 minutes for the A_{2B} Rz1 and at 1 minute for the A_{2B} Rz2. At 37 ºC and 20 mM $MgCl_2$, the A_{2B} Rz1 has a V_{max} of 27.3 nM/min, k_m of 8.3 μM and a k_{cat} of 1.8/min. Under the same conditions, the A_{2B} Rz2 had a V_{max} of 515 nM/min, K_m of 4.3 μM and a k_{cat} of 36.1/min. At 25 °C and 1mM $MgCl_2$, the A_{2B} Rz2 had a V_{max} of 16.9 μM/min, a km of 14.4 μM, and a k_{cat} of 1.1/min. At 37°C and 20 mM $MgCl_2$, the A_{2B} Rz2 had the highest catalytic activity of the two ribozymes and based on these results we dropped the A_{2B} Rz1 and only cloned the A_{2B} Rz2 for further testing.

Cloning of the Hammerhead Ribozyme into an rAAV Expression Vector

Ribozymes injected directly into an in vivo model are susceptible to endonuclease attack. Modification of the ribozyme by adding phosphorothioate groups would protect the ribozyme from the endonucleases. However, modifications such as these are expensive and potentially toxic. Therefore, the A_{2B} Rz2 was cloned into an rAAV vector, p21Newhp. These vectors are suitable for injection of the plasmid directly into an in vivo model and for the HREC transfection. This vector allows us the option to package into AAV for subsequent experiments in vitro and in vivo.

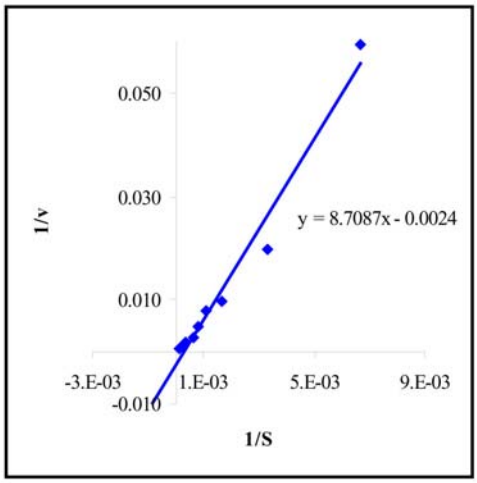

Conditions	$37^{o}C/20mM\ MgCl_2$	$37^{o}C/20mM\ MgCl_2$	$25^{o}C/1mM\ MgCl_2$
Ribozyme	A_{2B} Rz1	A_{2B} Rz2	A_{2B} Rz2
V_{max} (nM/min)	27.30 ± 3.2	515 ± 125	16.9 ± 2.8
K_M (μM)	8.3 ± 0.2	4.3 ± 0.7	14.4 ± 1.1
k_{cat} (min^{-1})	1.8 ± 0.06	36.1 ± 8.3	1.1 ± 0.06

Figure 3-7. Kinetic analysis of the ribozymes.

Sequencing of the Clones

Once the A_{2B} Rz2 was cloned into the rAAV vector, it was sequenced to confirm the sequences of the active A_{2B} Rz2 ribozyme, inactive Rz2 and the p21Newhp vector alone. Figure 3-8 shows the sequencing results. The C/G base difference between the active and the inactive ribozyme are indicated.

Cell Cultures

Human retinal endothelial cells (HREC) were grown and assesed for purity of culture. A special mesh pore nylon membrane was used to isolate these cells. This membrane retains the retinal endothelial cells but allows passage of the retinal components. Morphologically, the HREC usually have a 'pebble stone' morphology (Figure 3-9). The pebble stone morphology is not always easily distinguishable. If the culture flask is coated with 1% gelatin, it helps the cells to adhere to the culture flask and display their morphological characteristics. They have a rounded nucleus which fills up most of the cell and a scanty cytoplasm. It is not always possible to have a 100% pure culture of the retinal endothelial cells, and the presence of some pericytes is not unusual.

To confirm the purity of the HREC the ability of the endothelial cells to take up acetylated LDL was assesed. The human LDL complex delivers cholesterol to the cells by receptor mediated endocytosis. The complex consists of a core of ester and triglycerides surrounded by a thick shell of phospholipids, unesterified cholesterol and an apoprotein B unit. Once internalized, LDL dissociates from its receptors and appears in lysosomes. The lysine residues of LDL's apoprotein B can be acetylated to form acetylated LDL. Once acetylated, the LDL complex no longer binds to the LDL receptor

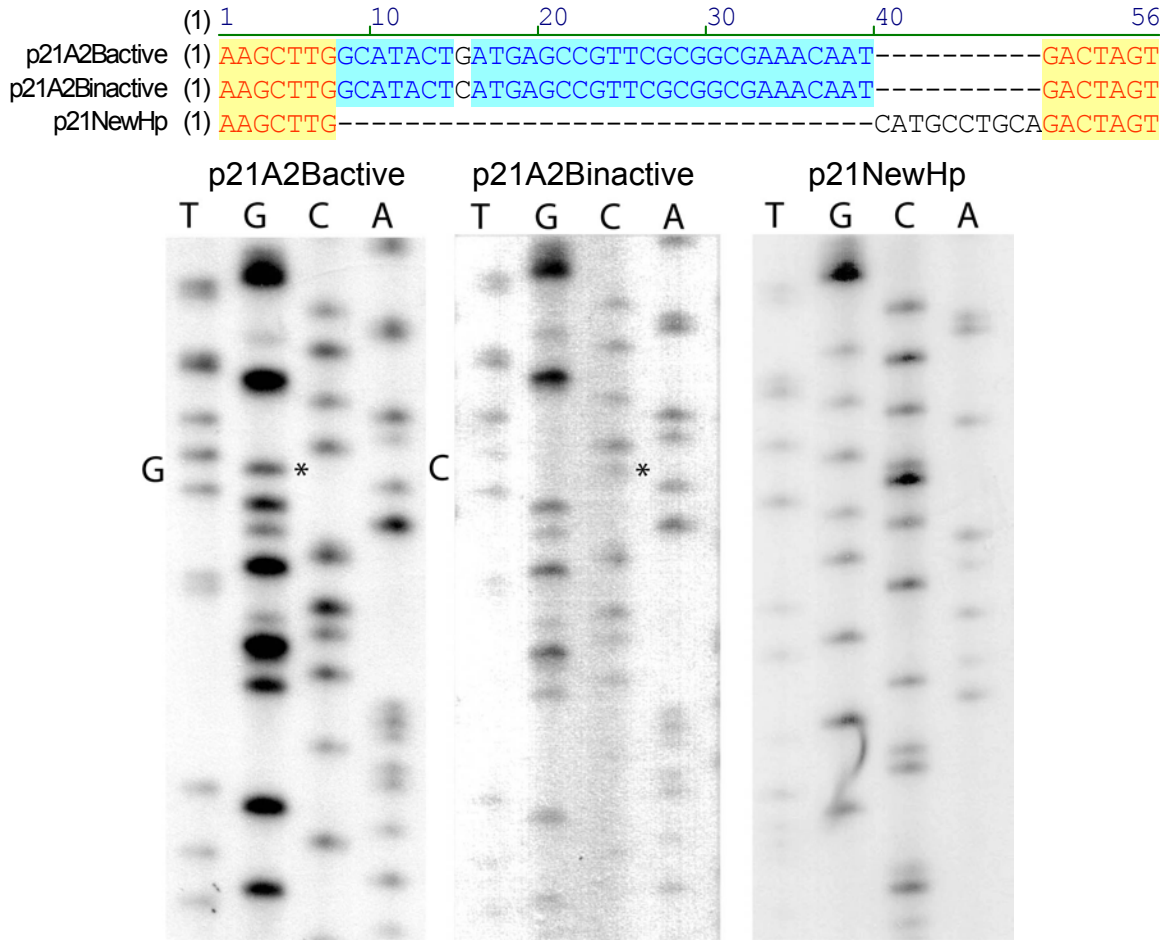

Figure 3-8. Sequence of the active and inactive versions of the A_{2B} ribozymes at the site of insertion within the p21NewHp vector. The G to C change in the catalytic core at position 15 in the upper panel is also noted on the 6% polyacrylamide-8M urea gel in the lower panel. The yellow sequences indicate the HindIII and SpeI sites. The blue sequences indicate the target.

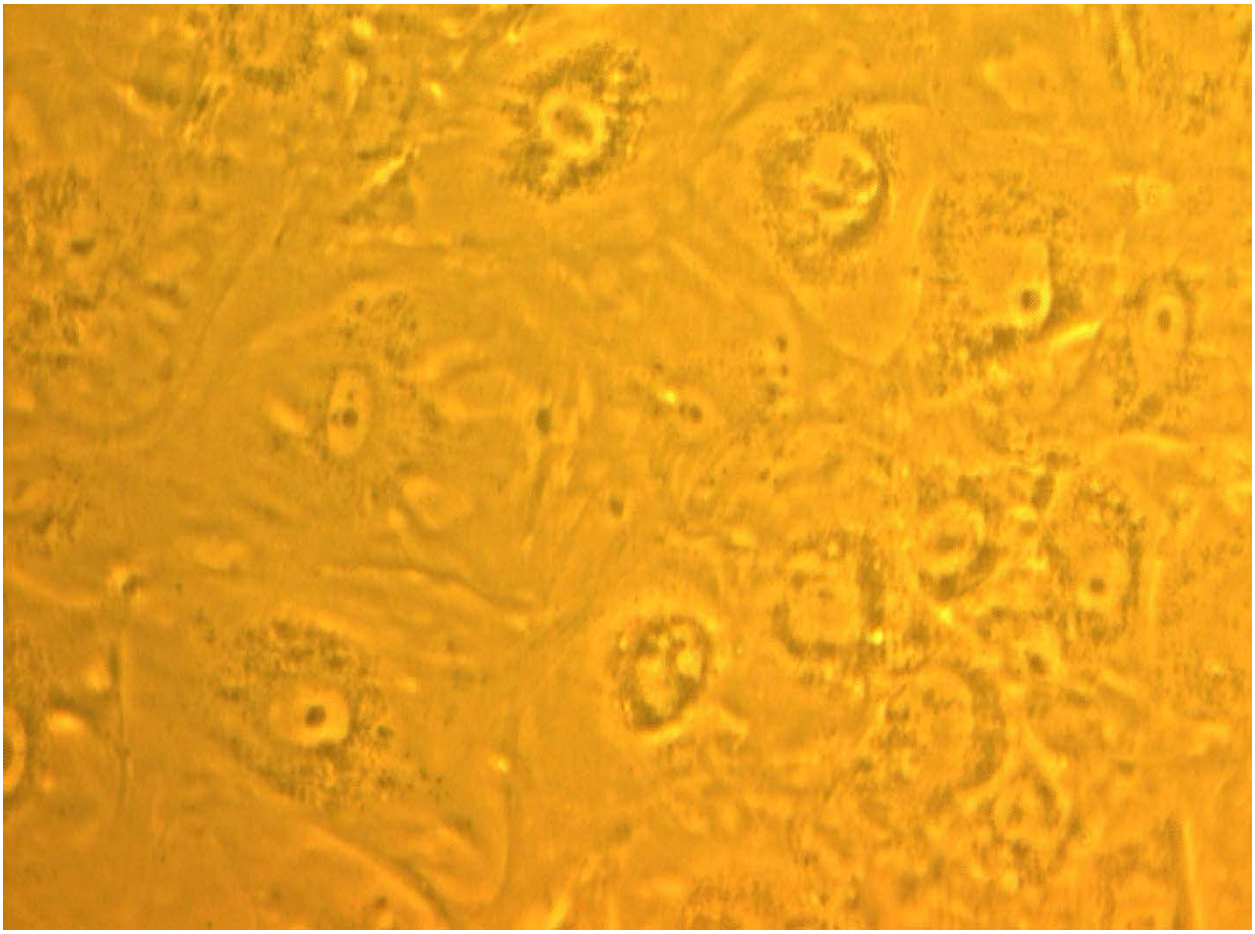

Figure 3-9. Pebble stone morphology of the HREC

and is taken up by scavenger receptors specific for modified LDL. Endothelial cells and macrophages have these scavenger receptors. The acetylated LDL complexes accumulate within the cells diffusely in the cytoplasm (Figure 3-10). To asses the purity of the culture, the number of cells that take up the LDL are expressed as a percentage of the total cells.

Transfection of HREC

The HREC were transfected with the ribozyme constructs to asses the ribozymes ability to cleave the target mRNA. HREC were initially transfected with a rAAV vector PTRUF11. This plasmid is similar to the p21NewHp, and, it expresses GFP downstream of a beta-actin CMV promoter (Figure 3-11). HREC were transfected with this plasmid to determine the transfection efficiency using the DEAE dextran protocol. The cells were transfected and observed under a fluorescent microscope for expression of GFP in the HREC over time. The number of cells expressing GFP increased with time as expected. However, the maximal expression of GFP was not seen until 3 weeks post transfection. (Figure 3-12).

Once the efficiency of the protocol was established, HREC were transfected with the active and inactive versions of the A_{2B} Rz2, and the vector control (p21Newhp) using the DEAE dextran protocol. Following transfection, the cells were allowed to grow for 72 hours. After 72 hours, the cells were not able to sustain normal morphology or characteristics of HRECs. Thus, the cells were harvested at 72 hours post transfection for further analysis.

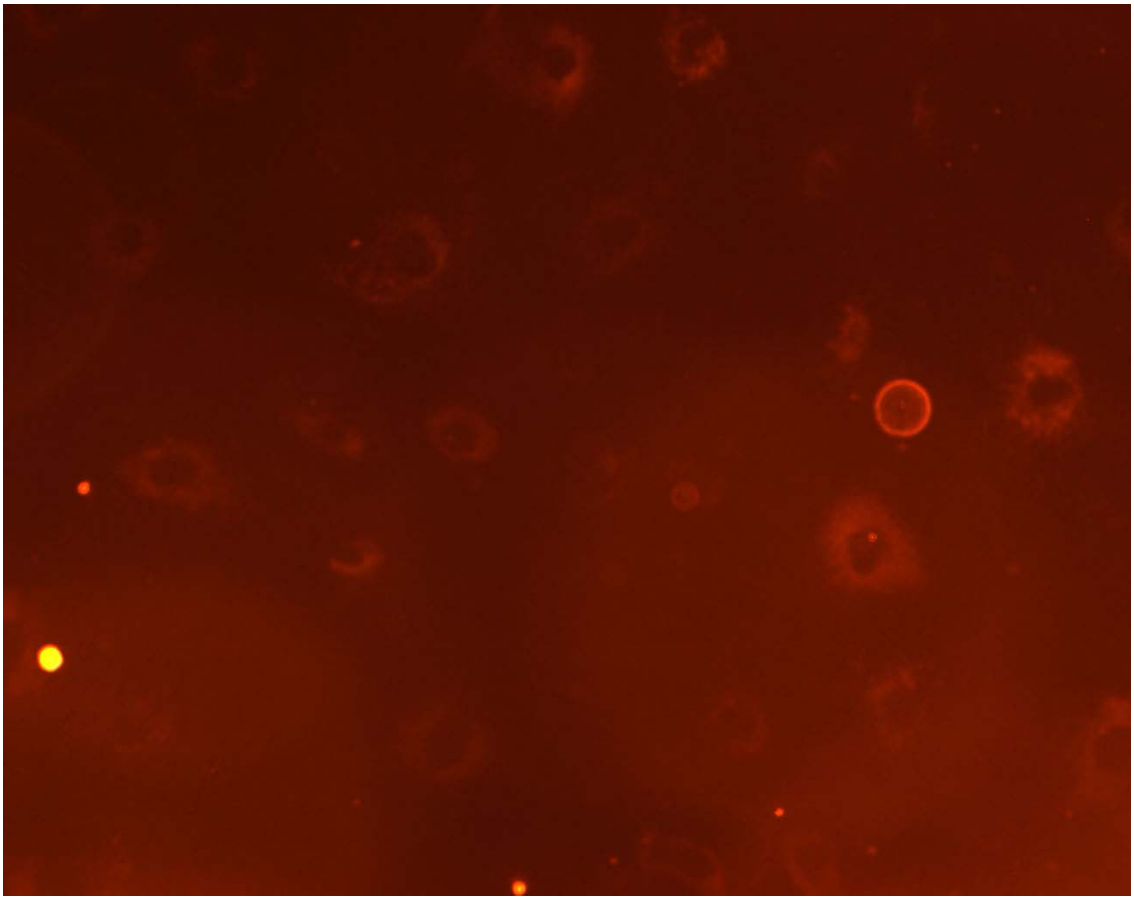

Figure 3-10. LDL uptake of HREC.

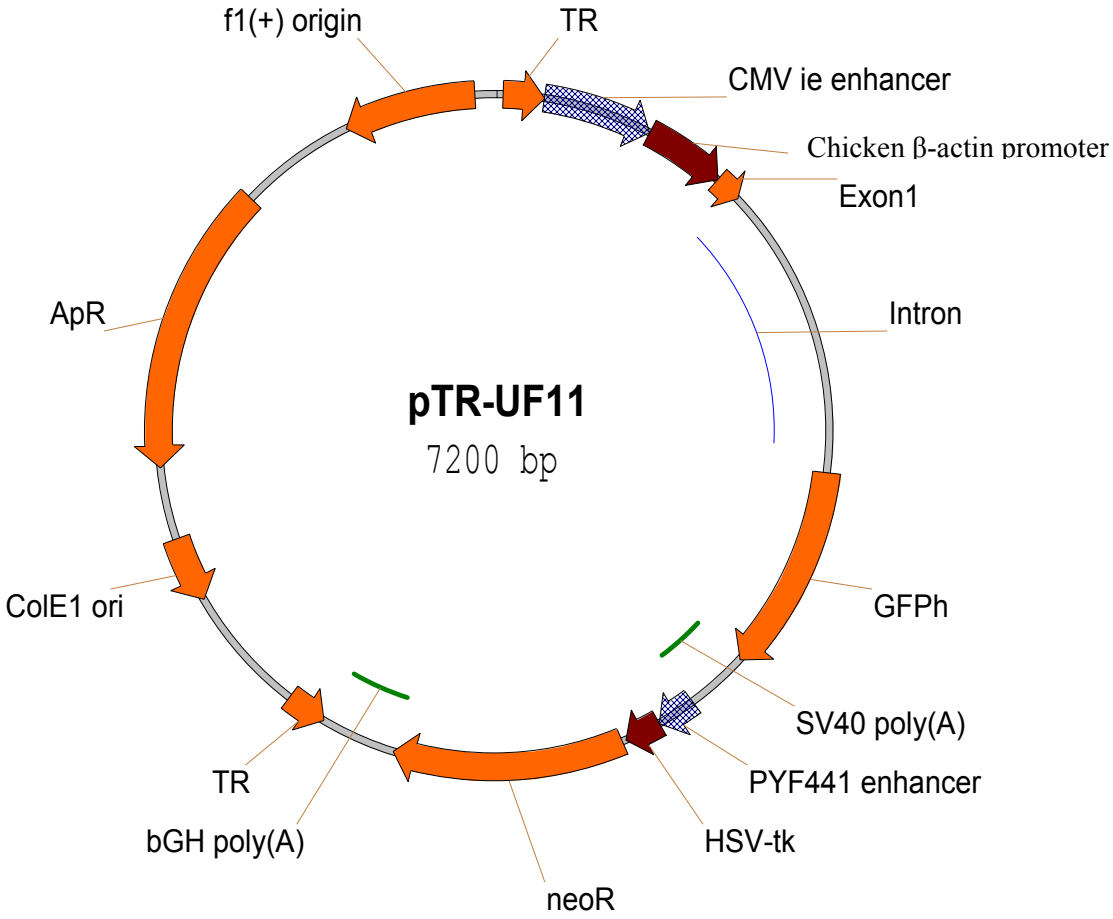

Figure 3-11. The GFP plasmid. This plasmid was driven by a CMV enhancer and a chicken beta actin promoter

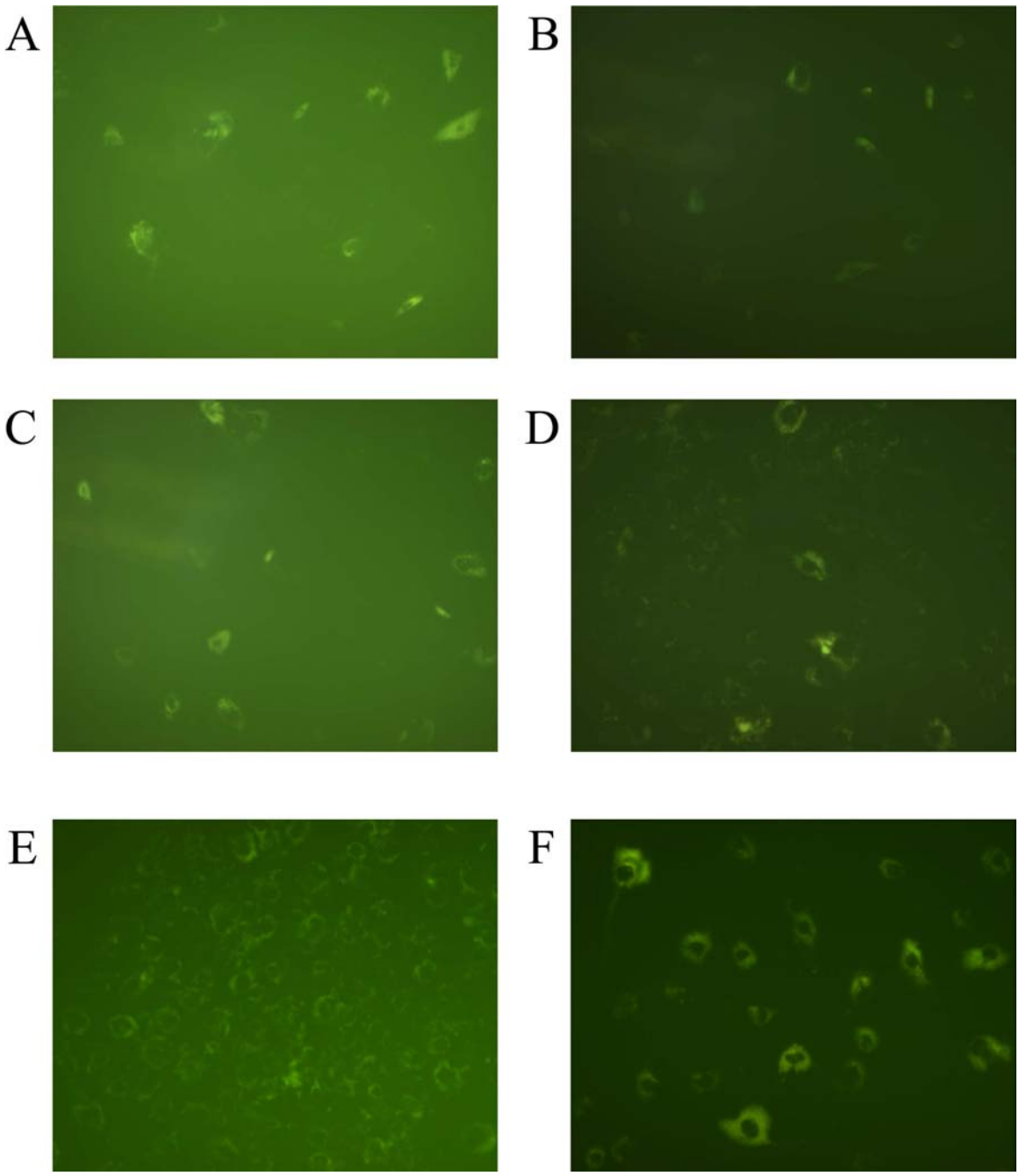

Figure 3-12. Transfection efficiency of the HREC. A)24hrs. B)48hrs. C)72hrs. D)96hrs. E)3 weeks and F)Passage 1 post transfection.

A migration assay was used to assess the levels of the A_{2B} receptor in the transfected HRECs. For a migration assay, cells are placed in a chemotaxis chamber and covered with a porous membrane and allowed to attach to the lower side of this membrane. A stimulus is provided to the cells. The cells respond to the stimulus and migrate through the pores of the membrane. For this experiment, we placed the transfected cells into the wells of the chemotaxis chamber and stimulated the cells with increasing concentrations of NECA. NECA is an adenosine analogue and cells transfected with the active A_{2B} Rz2 were not expected to respond to NECA as readily as the inactive transfected, or the vector transfected cells. The cells transfected with the active A_{2B} Rz2 are expected to have the A_{2B} receptor mRNA cleaved and thus have a decreased dose-dependent response to NECA than the other cells. (Figure 3-13) Cells transfected with the plasmid coding for active A_{2B} Rz 2 reduced migration of cells by an average of 39% when compared to the p21NewHp control at increasing concentrations of NECA (10 and 100ng/ml), and cells transfected with plasmid coding for the inactive A_{2B} Rz2 reduced migration of cells by an average of 15%. (Figure 3-14)

Transfection Using Lipofectmaine on HEK Cells

Human embryonic kidney cells (HEK) 293 cells were also transfected with the same plasmids for further in vitro analysis. Since these cells were transfected using a different protocol than the HREC the transfection efficiency had to be determined for these cells also.

To assess the transfection efficiency, the HEK cells were transfected with the GFP plasmid and the cells observed for expression of GFP under the fluorescence

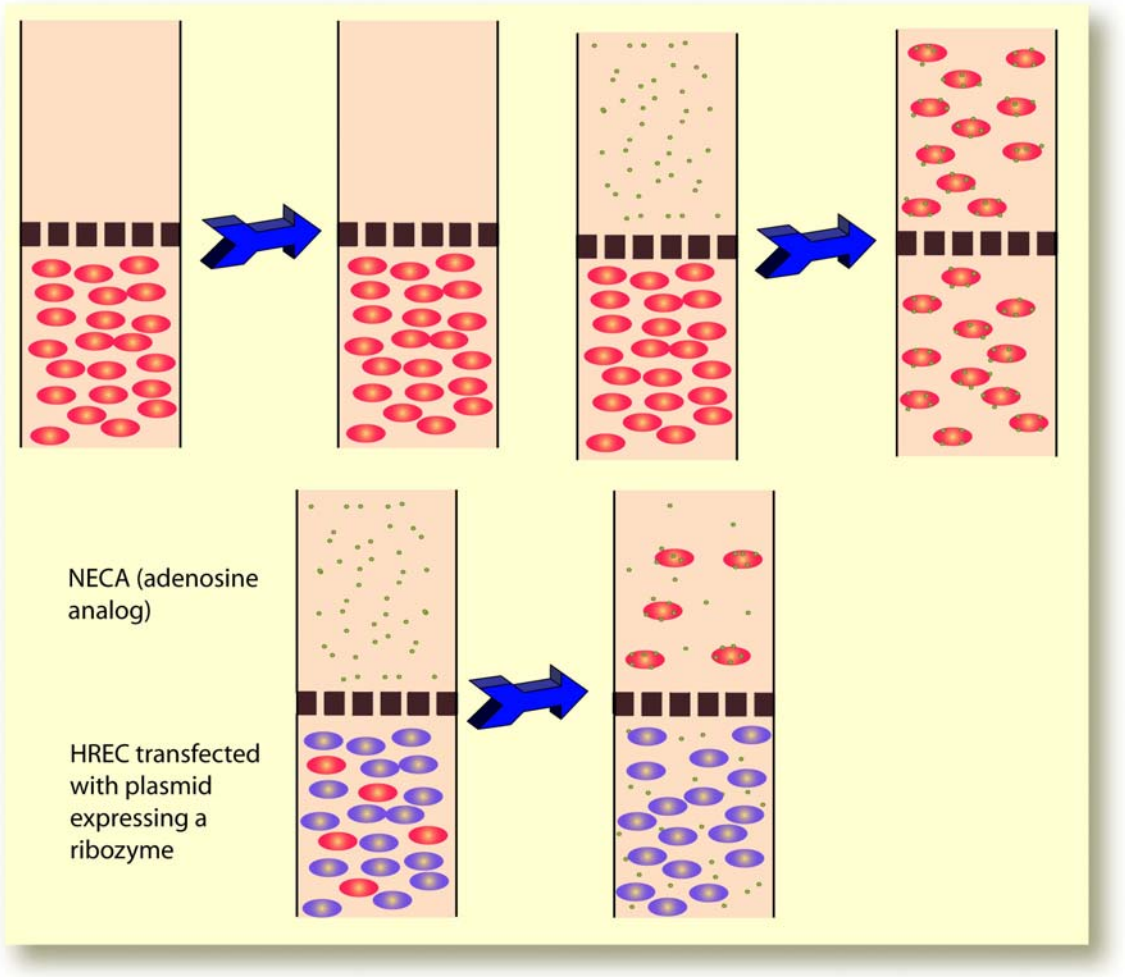

Figure 3-13. Theory of migration assay. Cells are plated into a well and covered with a porous membrane. Cells migrate through the membrane in response to a stimulus (eg. NECA). When A_{2B} Rz2 transfected cells are placed in the well, fewer cells respond to the same stimulus.

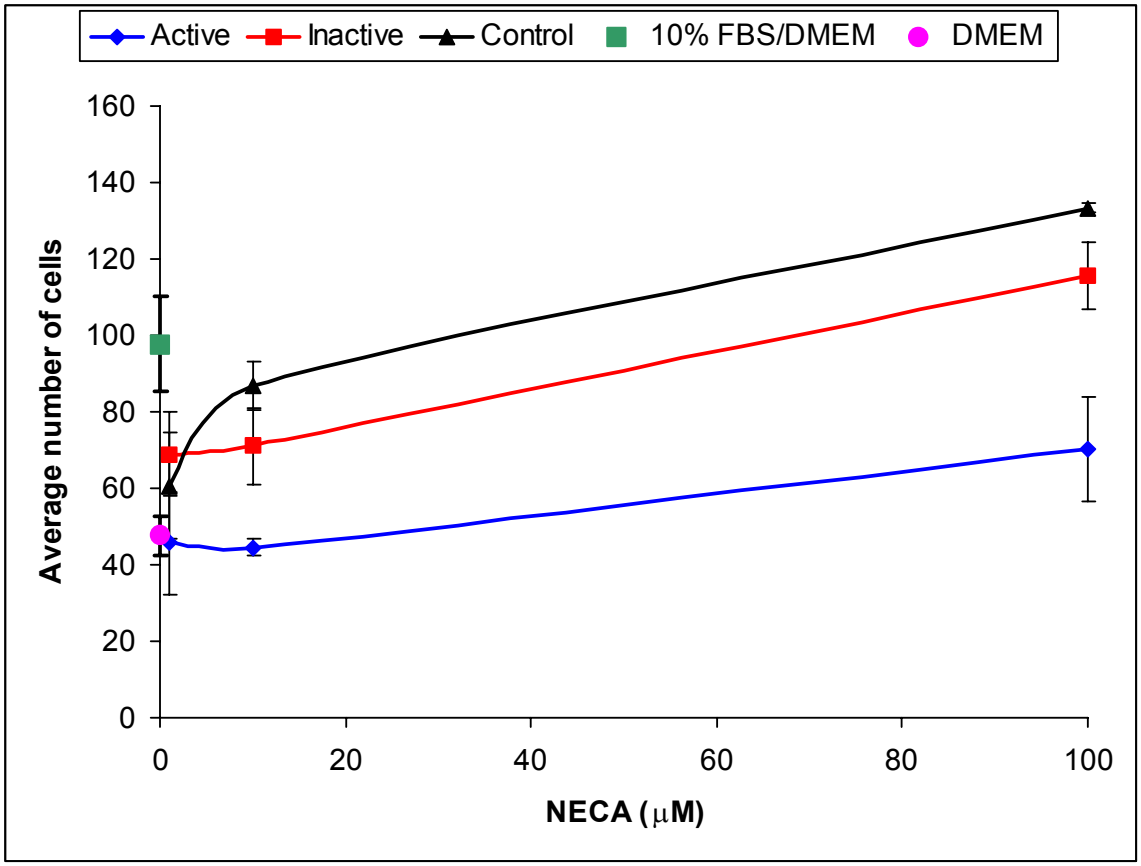

Figure 3-14. Migration data for the cells transfected with the active and inactive versions of the A_{2B} receptor and the vector control. 10% FBS/DMEM is the positive control and DMEM alone is the negative control

microscope. In this case, expression of the GFP plasmid was observed within 24 hours of transfection. The number of cells expressing the GFP increased with time. (Figure 3-15) After 96 hours post-transfection, the cells were passaged to assess the level of expression. The HEK cells continued to express GFP following passage P1. (Figure 3-16) The level of expression of GFP also continued to increase with time. Ninety six hours after the first passage, the cells were passaged again to determine if the GFP expression was maintained with repeated passaging.

The HEK cells showed a considerably different pattern of expression of the same GFP plasmid used for the transfection of the HRECs. There are a number of possible explanations for this observation. First and foremost, the HEK cells were obtained from an established cell line and the purity of their culture guaranteed. The HEK cells are much smaller than the HRECs and the transfection protocol of the HEK cells was completely different from that of the HRECs.

CAMP Assay on Transfected HEK Cells

Once the transfection efficiency of the HEK cells was established, the A_{2B} RZ2 plasmids were used to transfect the cells. Seventy two hours post-transfection, the cells were harvested for a cAMP assay. The transfected cells were stimulated with NECA, the adenosine analogue. Adenosine binding to receptors leads to production of cAMP. Figure 3-17 shows the results of the cAMP assay. There is a significant reduction of cAMP production in the HEK cells transfected with the active A_{2B} Rz2. However, this effect was not reproducible.

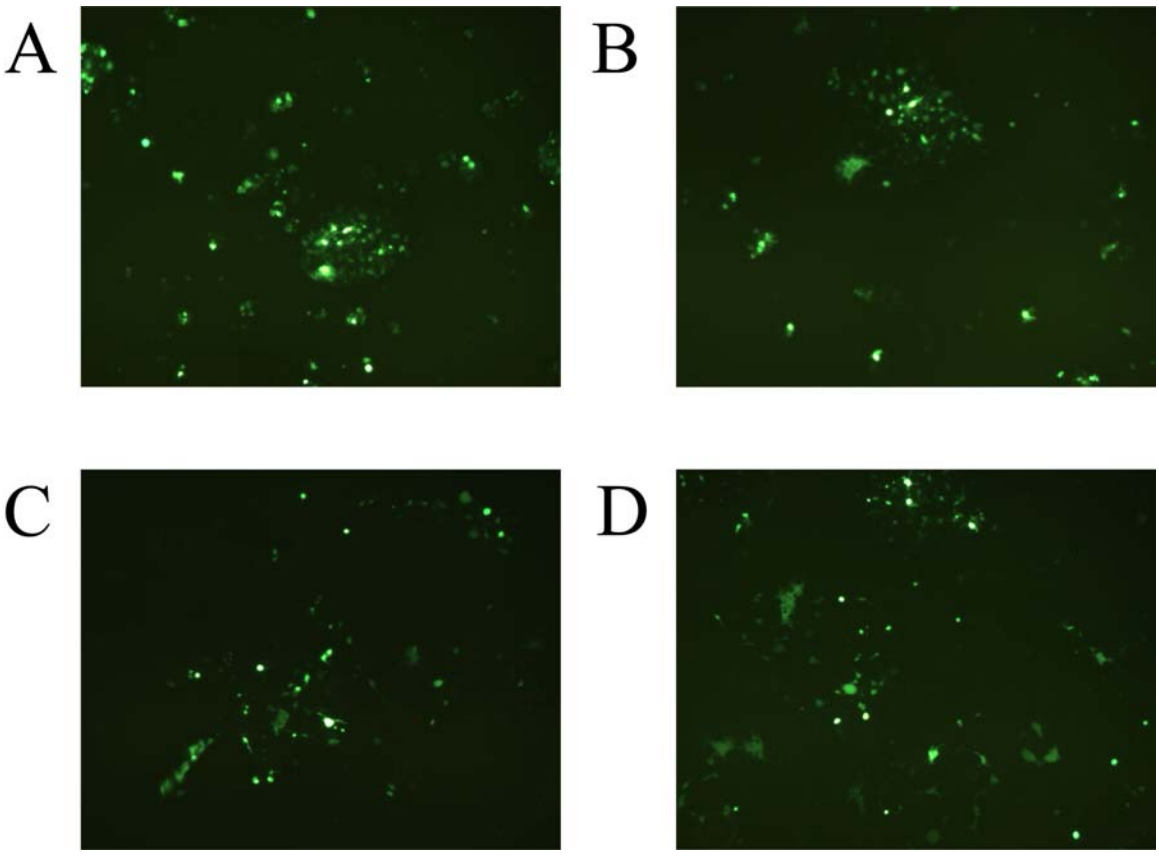

Figure 3-15. Transfection Efficiency of HEK cells. A)6hrs, B)24hrs, C)48hrs, D)72hrs and E)96hrs post transfection.

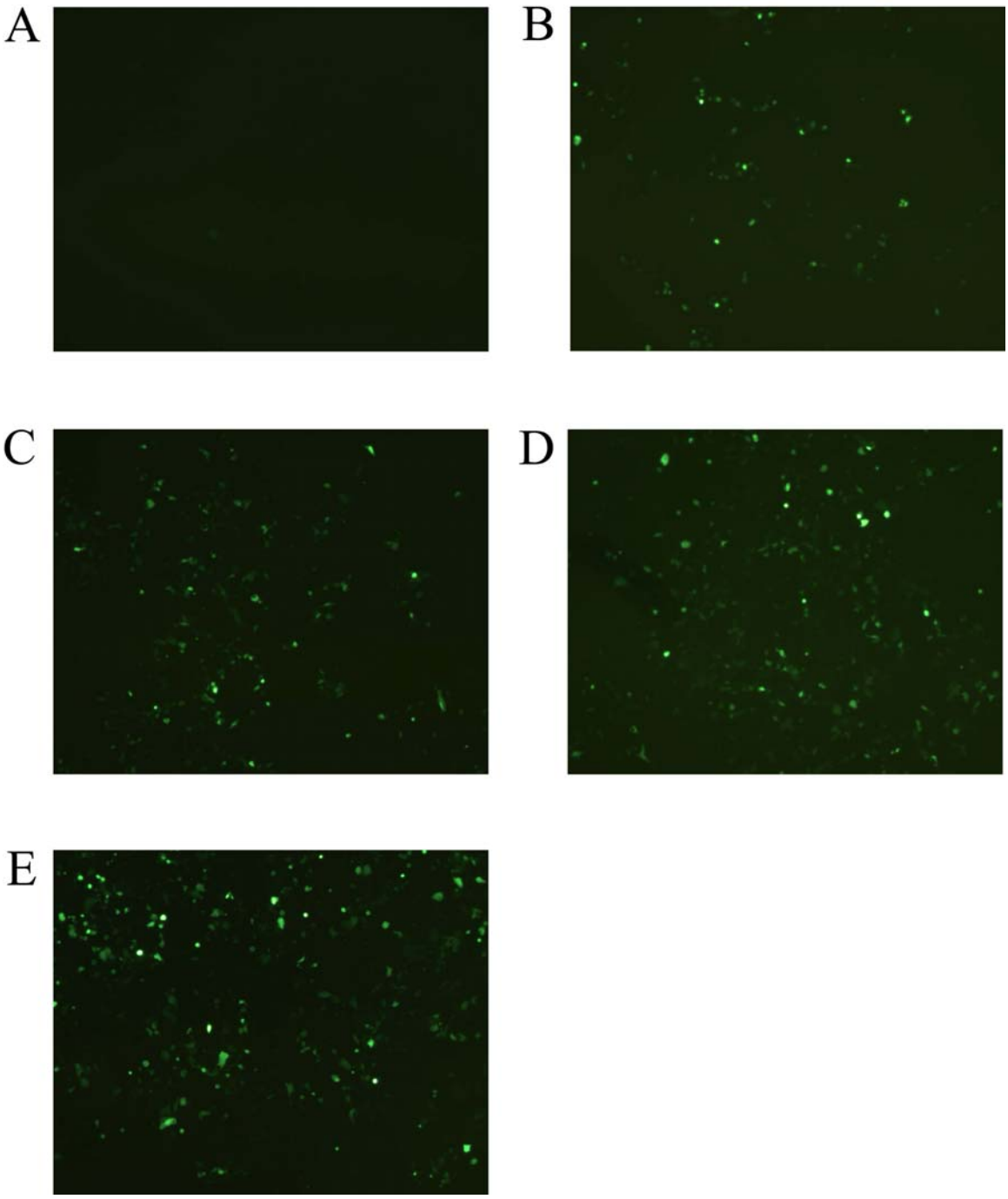

Figure 3-16. HEK cells transfection efficiency following passage 1. A)24hrs, B)48hrs, C)72hrs, and D)96hrs following passage 1.

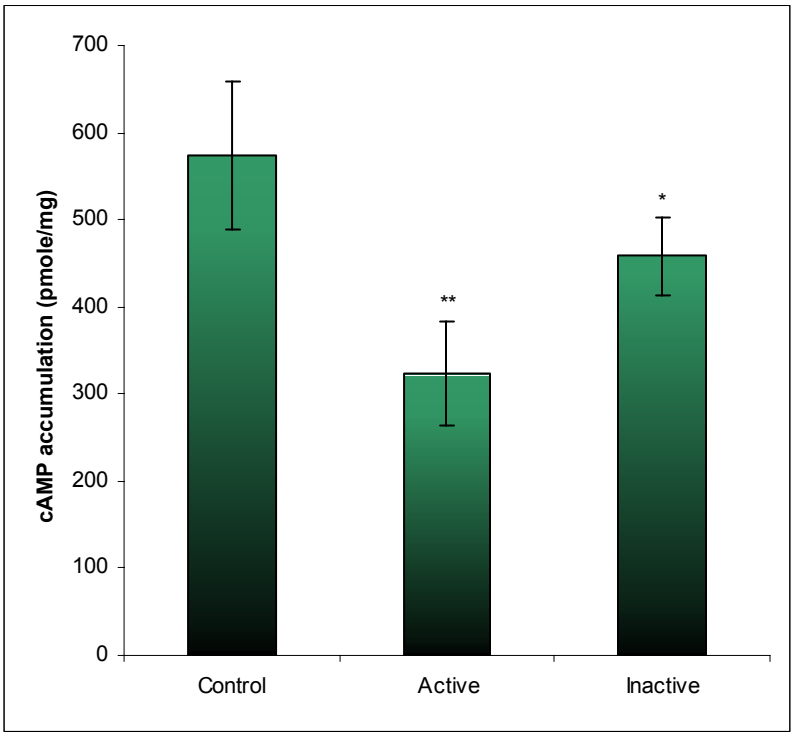

Figure 3-17. cAMP accumulation in HEK cells transfected with the control, active A_{2B} Rz2 and inactive A_{2B} Rz 2.

Real Time PCR

Figure 3-18 shows the results of TaqMan real time RT-PCR on mRNA isolated from HEK cells transfected with the active and inactive versions of the A_{2B} Rz2, and with the control plasmid. The active A_{2B} Rz2 reduces mRNA levels by 43%. The inactive A_{2B} ribozyme shows no significant reduction in mRNA levels as expected for the catalytically inert ribozyme. The level of mRNA detected were normalized to cyclophilin.

Effect of A_{2B} Ribozymes on Neovascularization in the ROP Mouse Model

Active and inactive A_{2B} ribozymes and the cloning vector p21NewHp were injected intra-ocularly on post natal day one in the right eye of mouse pups. There was no injection in the left eyes (which served as controls), and the pups and their dams were taken through the oxygen-induced model of retinopathy. On day 17 the mice were euthanized and their eyes enucleated and fixed in 4% paraformaldehyde. The eyes were embedded in paraffin and three hundred serial, 6uM sections were done. Every thirtieth section was placed on a slide and stained with hematoxylin and eosin. (Figure 3-19). The extent of angiogenesis was determined by counting the pre-retinal endothelial cell nuclei surrounding a blood vessel lumen. The cloning vector p21NewHp showed marked angiogenesis. (Figure 3-20) The active A_{2B} Rz2 reduced the average number of nuclei per section on average by 55%. (Figure 3-21) The inactive A_{2B} Rz2 reduced the average number of nuclei on average by 5%. (Figure 3-22)

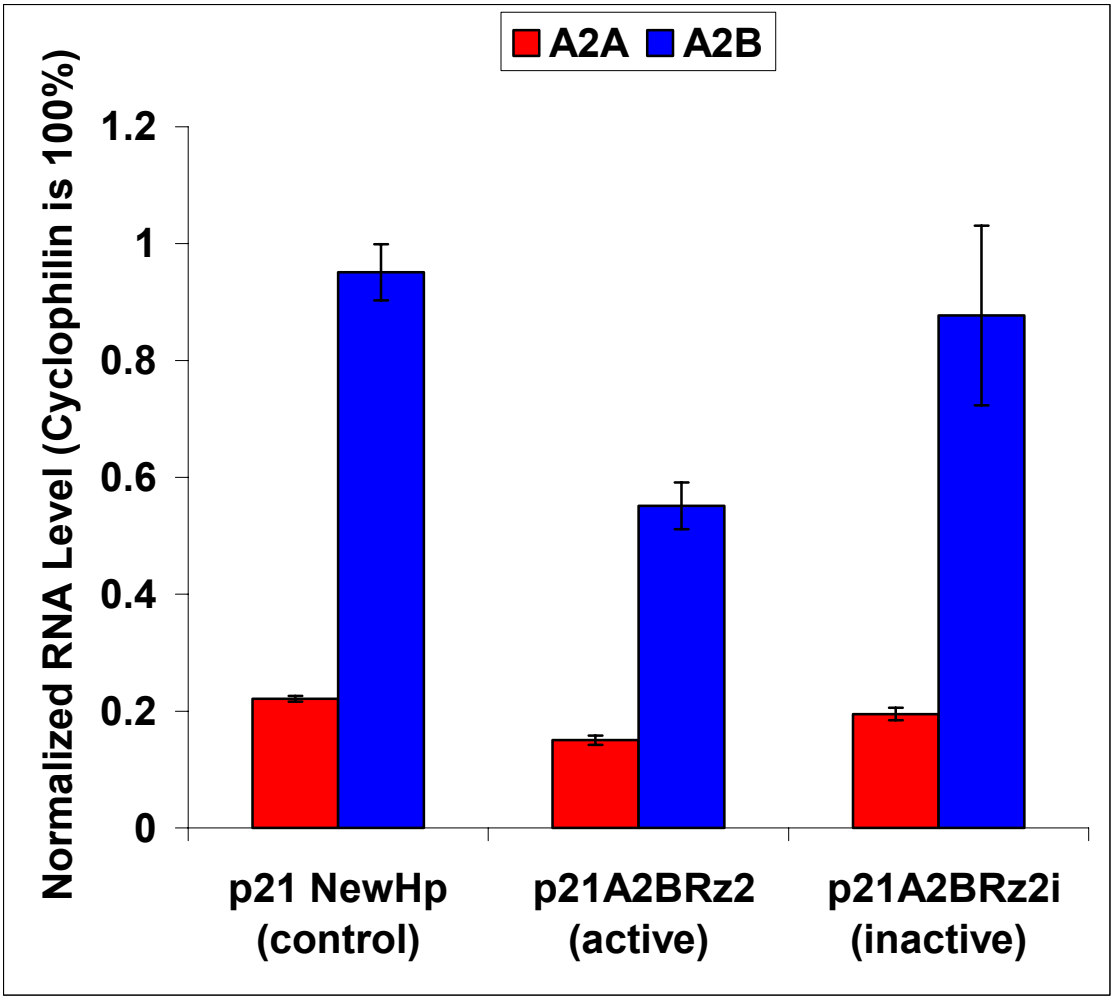

Figure 3-18. Real time RT-PCR results showing relative levels of the adenosine A_{2A} and A_{2B} receptor mRNAs isolated from HEK cells transfected with plasmid DNA.

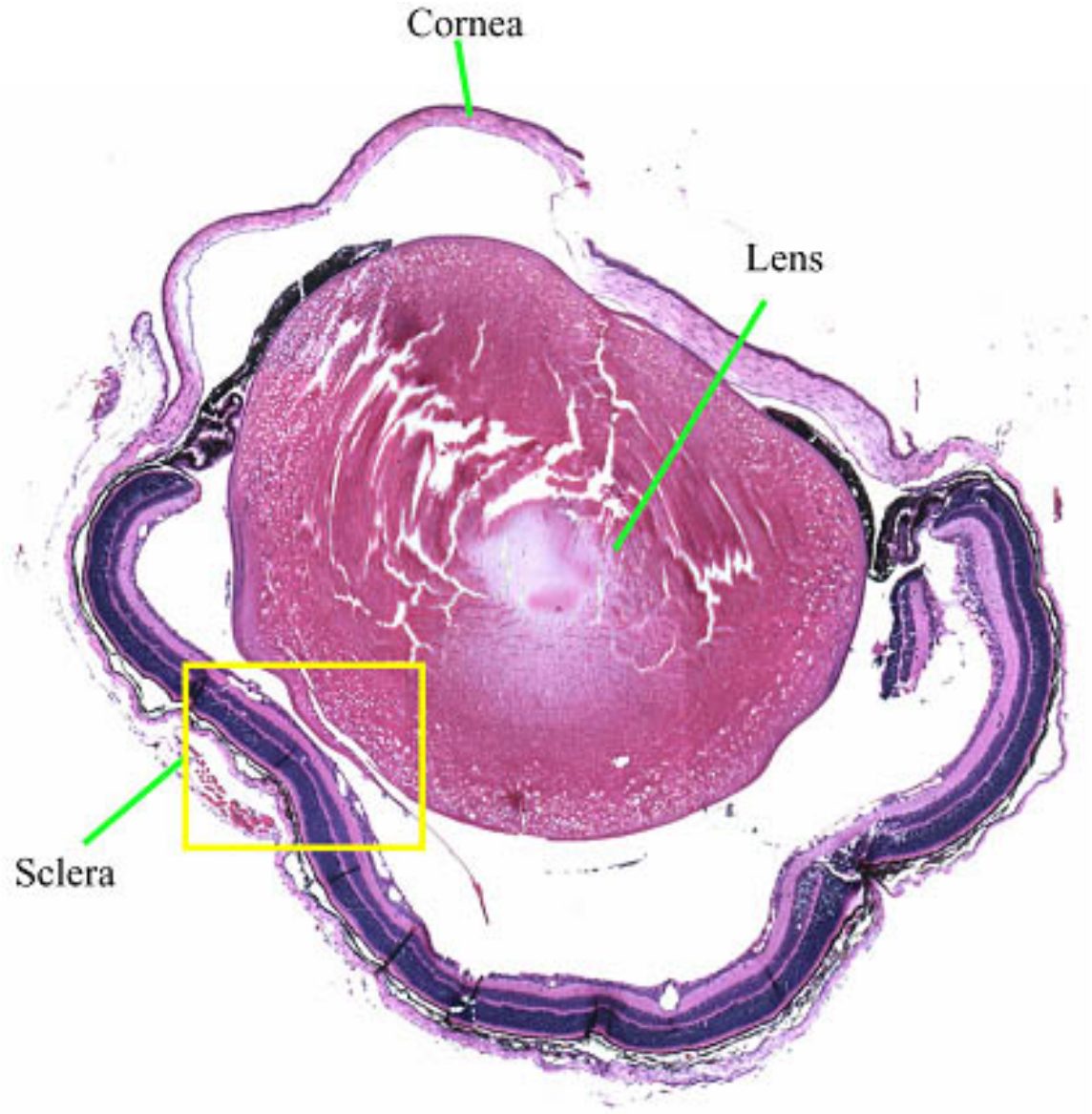

Figure 3-19. The mice eyes were embedded in paraffin and three hundred serial sections were done. Every thirtieth section was placed on a slide and stained with hematoxylin and eosin. This figure shows a representative mouse eye that was stained. Arrows indicate the cornea, sclera and the lens of the mouse eye.

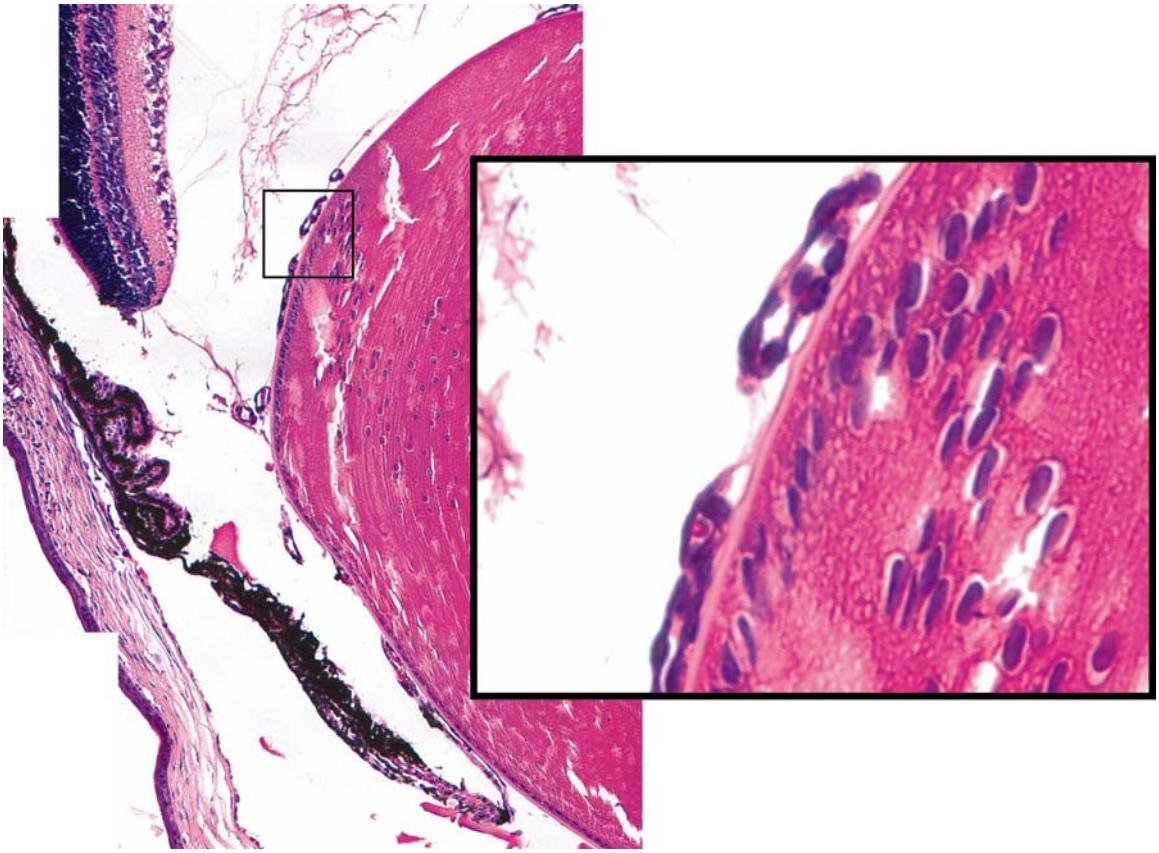

Figure 3-20. Injection with the control plasmid prior to exposure to high oxygen shows a high number of endothelial cell nuclei surrounding blood vessel lumen. This indicates that the control plasmid did not reduce the amount of pre-retinal angiogenic vessels.

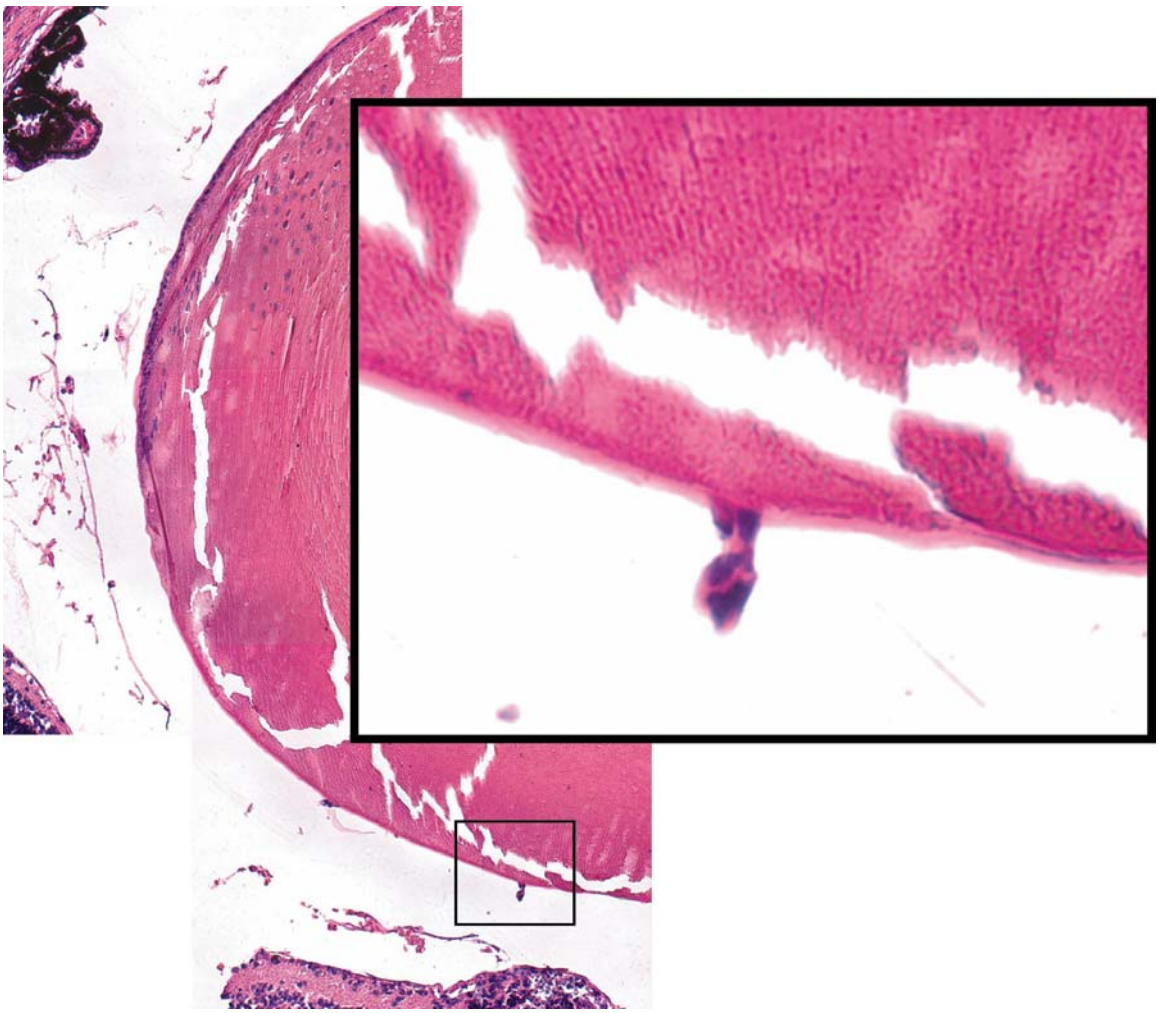

Figure 3-21. Injection with the active A_{2B} ribozyme prior to high oxygen exposure significantly reduced the pre-retinal neovascularization.

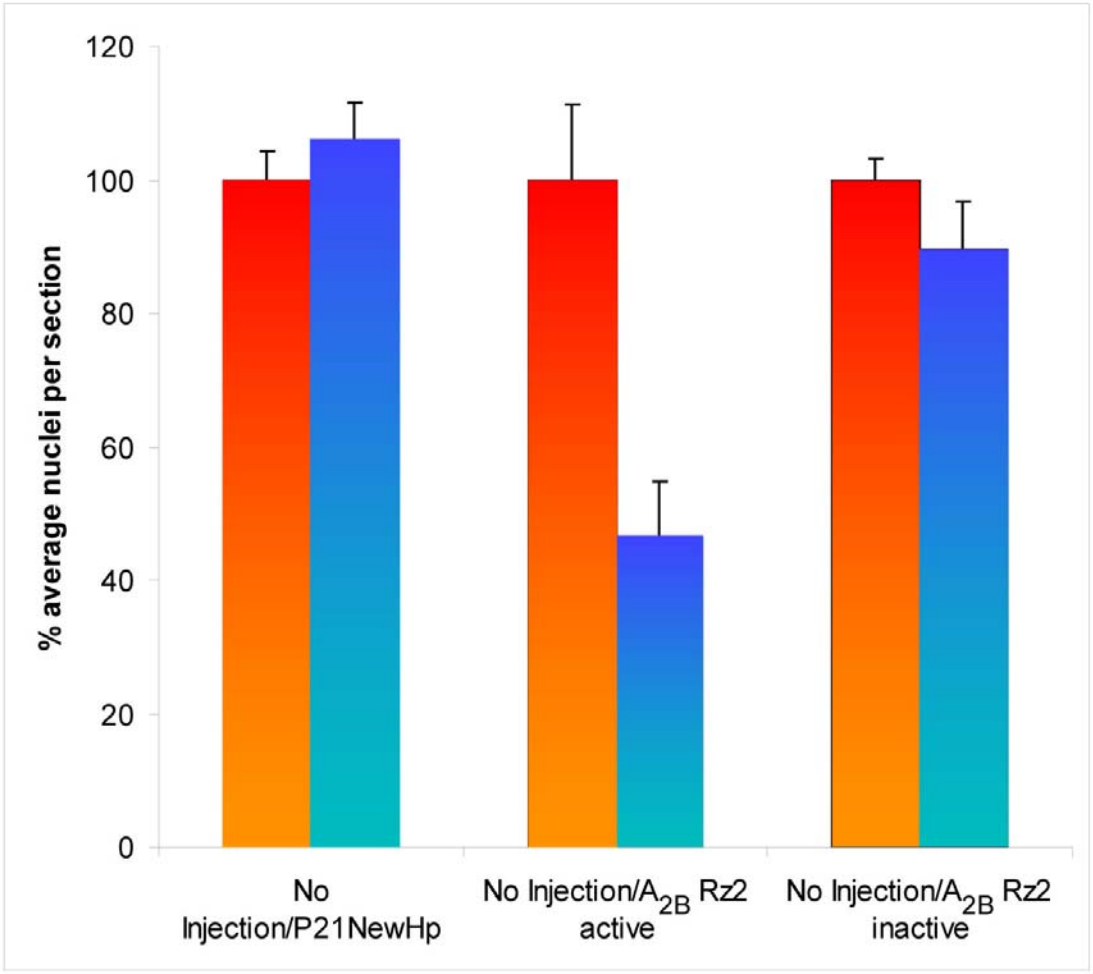

Figure 3-22. Injection of the active and inactive versions of the A_{2B} Rz2 and the vector control in the ROP mouse model

CHAPTER 4
DISCUSSION

The overall goal of this project was to develop a hammerhead ribozyme targeted against the adenosine A_{2B} receptor that would cleave the A_{2B} mRNA and reduce the expression of this receptor in cell culture and in a mouse model of oxygen-induced retinopathy. The value of this ribozyme is that it allows us to study the involvement of the A_{2B} receptor in the complex physiological pathway of angiogenesis. Secondary to this is the potential of using this ribozyme as a therapy in the treatment of pathologies that produce abnormal neovascularization such as retinopathies and tumorogenesis.

Our results demonstrate that we have developed a hammerhead ribozyme that specifically cleaves the mouse and human adenosine A_{2B} receptor mRNA. We have demonstrated that this ribozyme reduces the expression and function of the A_{2B} receptor in HREC and HEK cells and we have shown that this ribozyme reduces abnormal retinal neovascularization in the mouse model of oxygen-induced retinopathy.

The ability of the active ribozyme to inhibit the expression of the A_{2B} mRNA in HEK cells was clearly shown. Reduction in A_{2B} mRNA signal in cells transfected with the active ribozyme was 43% compared to cells transfected with the control plasmid. The chemotactic migration of HRECs across a porous membrane toward solutions containing increasing concentrations of NECA is dependent on the presence of A_{2B} receptors on the cell surface. The reduction of this migration in HREC transfected with a plasmid expressing the active A_{2B} ribozyme suggests that cell surface levels of the A_{2B} receptor have been reduced due to inhibition of expression of the A_{2B} mRNA by the

ribozyme. A reduction of 39% in the number of migrating cells was found in cells expressing the active ribozyme. Our results show that approximately 60% of this reduction in expression is due to cleavage of the message while the remaining inhibition results from an antisense effect of ribozyme binding to the target. These results also show that ribozyme cleavage of the A_{2B} mRNA reduces expression of the protein in cultured cells to a level that significantly inhibits the cellular function of the A_{2B} receptor. Therefore, inhibition of the A_{2B} receptor as it affects other components of this pathway can be quantitatively examined.

In addition this ribozyme inhibits pre-retinal neovascularization in vivo in a mouse model of oxygen-induced retinopathy, where a reduction in pre-retinal neovascularization of 55% in eyes injected with the plasmid expressing the active ribozyme was achieved and only a small portion of this reduction, approximately 5%, is due to an anti-sense effect. These results suggest that the reduction in neovascularization is the result of ribozyme inhibition of the expression of the A_{2B} receptor and demonstrate that this ribozyme will also be useful for in vivo studies of A_{2B} receptor function including studies on retinopathies.

Ribozymes As Tools To Study Gene Expression

There are a number of reports on the ability of the hammerhead ribozymes to control expression of specific genes in cell culture. For example, a hammerhead ribozyme designed to cleave mRNA encoding C-Ha Ras mutation inhibited formation of foci of transformed cells by 50%.[173] Hammerhead ribozymes have also been used to target anticancer therapies. For example, hammerhead ribozymes were used to target mRNA of a BCR/ABL fusion protein, which is responsible for chronic myelogenous leukemia. The hammerhead ribozyme eliminated expression of the protein in K562

cells.[174] Hammerhead ribozymes targeted to survivin, which is expressed in carcinoma cells were also able to reduce survivin mRNA by 74%.[175] In another study, a hammerhead ribozyme was used to target bcl-2 mRNA in tumors, which overexpress the protein. The ribozyme was tested in a lymphoma cell line and showed a decrease in the bcl-2 mRNA and protein following transfection with the ribozyme.[176] In yet another study, ribozymes were designed as HIV therapies by a number of groups. A hammerhead ribozyme expressed in Hum7 cells decreased the hepatitis B viral production by 83%.[177]

Naturally occurring RNAs have distinct advantages over DNA. RNA has a 2'OH group associated with the sugar moiety of RNA which participates directly in a chemical reaction which enhances the reactivity of the adjacent 3'OH group. The 2'OH group is also a hydrogen donor and acceptor, thus rendering RNA more versatile then DNA in tertiary structure formation.[178] DNA is predominantly a base paired duplex of complementary strands and RNA is folded from a single strand. RNA, can thus form extensive secondary structures due to pairing of imperfect complementary sequences in the RNA strand. Single stranded regions punctuate through this secondary structure leading to a variety of RNA conformations. RNA also has a uridine base instead of a thymidine allowing it to form unique secondary structures. For example, a uridine turn in tRNA and hammerhead ribozymes causes an abrupt turn in direction of the polynucleotide backbone and allows formation of complex tertiary interactions. The uridine turn is stabilized by hydrogen bonding and Van Der Waals interactions between uridine and the surrounding nucleotides.

Antisense therapy has been used by a number of investigators to inhibit angiogenesis. For example, Robinson et al used an antisense oligonucelotide against the

mouse VEGF to inhibit retinal neovascularization.[179] The oligos were injected into the mouse eye intravitreally and then exposed to hypoxia. Treatment with the anti-sense oligo's resulted in a 25% decrease in angiogenic vessel growth. This study was able to confirm the importance of VEGF in the angiogenic pathway, however, the antisense. olinucleotides were not successful at potently inhibiting the growth of abnormal vessels. [179] Another study used an oligonucleotide targetting the human and rat VEGF forms and were only able to lower the incidence of choroidal neovascularization by 30%. Antisense therapy is effective when the targeted mRNA is not abundant. Antisense nucleotides are complementary DNA or RNA sequences which hybridize to specific mRNA. These nucleotides are specific to the target, easy to design and synthesize. However, antisense nucleotides used for therapy of disease have a poor uptake, are unstable. The nucleotides are also sensitive to degradation by exogenous and endogenous nucleases. Antisense nucleotides are toxic to cells because a higher concentration of nucleotides is required to significantly affect the expression of a gene. The stability of anti sense oligonucleotides is enhanced by phosphorothioate bonds, which are toxic to mammalian cells. [180,181]

An advantage of using ribozymes instead of antisense oligonucleotides is their small size making them inexpensive and easy to produce. Their small size allows them to be inserted into gene encoding ribozymes into viral vectors used for their delivery to cells in vivo. Trans acting ribozymes inactivate or modify multiple mRNA molecules, which is a distinct advantage over anti-sense oligonucleotides, which act stoichiometrically. Ribozymes also do not require host cellular machinery to degrade the substrate. Therefore trans-acting ribozymes inactivate target RNA more efficiently than anti-sense oligonucleotides. In comparison to the conventional antisense RNAs, ribozymes provide

the potential of turnover, with a single molecule being able to inactivate multiple target RNAs. [181]

Ribozymes and protein enzymes share similarities in their mode of action. Both, ribozymes and protein enzymes require a complex secondary and tertiary structure for catalysis.[166,182,183] They also share similar mechanisms of acid base catalysis to carry out a reaction[184] and stabilize a transition state between substrate and product formation. Catalysis is driven by intrinsic binding energy resulting from interactions between enzyme and its substrate at sites different from the catalytic core.[185] Ribozymes can recognize RNA substrates via base pairing, thus their specificity is easy to manipulate. Ribozymes also do not evoke an immune response to the same degree as (foreign) proteins evoke. RNA is a natural component of the cell and has a low half-life, thus low toxicity. Proteins, on the other hand require the host cell machinery to degrade the substrate.

Delivery Of The Ribozyme In vivo

The plasmid used for the expression of the A_{2B} Rz2 has inverted terminal repeats (ITRs) at either ends of the ribozyme. ITRs contain the sequences, which are required for replication, packaging and integration of the plasmid into an rAAV vector. AAV is a single stranded, encapsulated DNA virus. AAV contains ITRs, which flank the AAV genome. This region of the genome is replaced with the gene of interest to generate the rAAV. [186] rAAV has been successfully used to deliver transgenes into the eyes. While the A2B ribozyme was cloned into this vector for potential packaging into AAV, we have demonstrated a significant response of the Active A_{2B} Rz2 naked plasmid and thus did not proceed to packing the ribozyme into an rAAV virus to enhance the effect.

There are several advantages to using plasmid DNA versus rAAV. The plasmid DNA is easier to propagate and is usually of higher quality. [187] Plasmids can also carry larger DNA sequences as compared to limited 5kb capacity of rAAVs.[188] Plasmid DNA can also be repeatedly administered due to its low immunogenicity and toxicity. [189,190]

Another method for the delivery of the ribozyme involves packaging the plasmid into a liposomal mixture that would bind to cell surface receptors and enhance uptake of the plasmid. [191,192] Liposomes are microscopic vessels composed of an aqueous compartment surrounded by a lipid layer. The transferrin receptor can be used as a vehicle to carry liposome/DNA complex into the cell. Transferrin binds to iron extracellulary and subsequently binds to the transferrin receptor on the cell surface. The receptor and transferrin are taken up by endocytosis into the cell. The iron is released and the transferrin and the receptor are recycled out of the cell. The transferrin helps the uptake of plasmid DNA by the cell. (Figure 4-1) Transferrin complexes can also be used to deliver cancer chemotherapeutic drugs to the tumor directly. For example, doxorubin, a cytotoxic drug was complexed with transferrin in liposomes and delivered to the site of tumor development. In another study, liposomal mediated delivery of the alpha interferon to murine bladder tumor cell line MBT2 was shown to increase the uptake of alpha interferon and enhance proliferative activity. Liposomal mediated delivery is safe, non-immunogenic, can be re-administered without harm and an unlimited size of DNA can be delivered. However, a major drawback using the liposome/transferrin route of delivery is the poor transfection efficiency of liposomal vectors. [193]

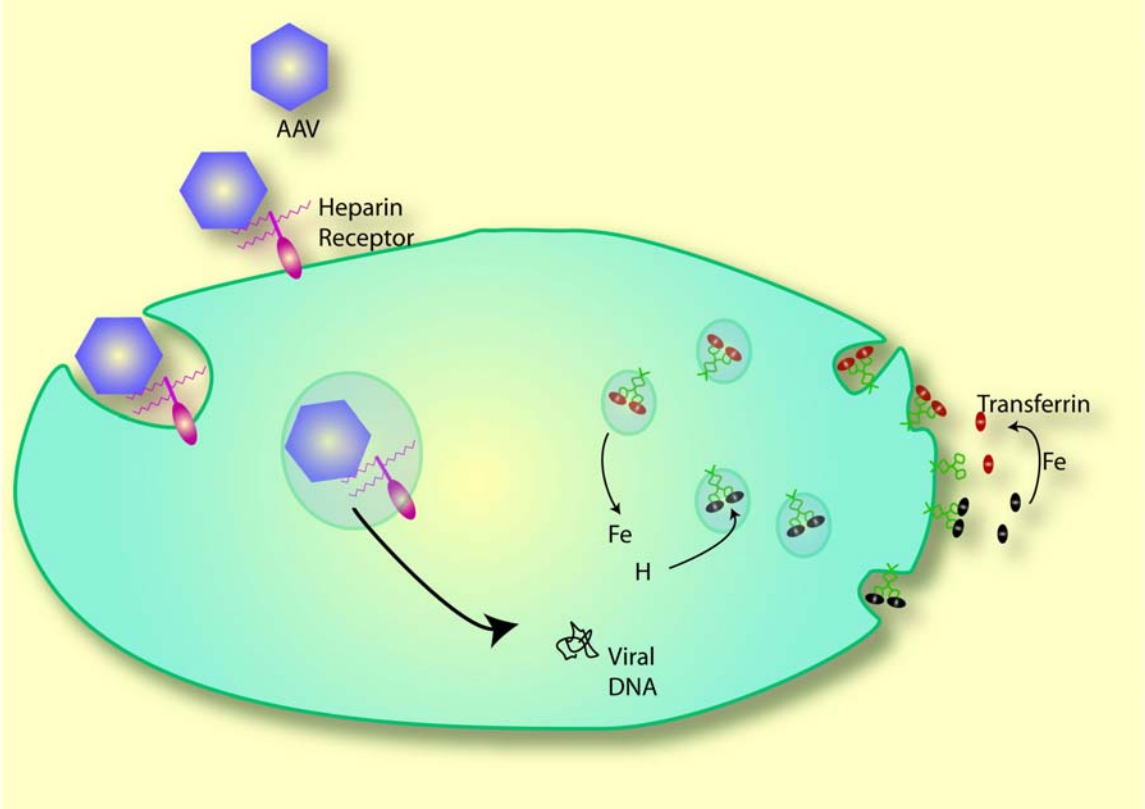

Figure 4-1. Entry of the AAV into the cell involves binding of the virus particle to heparan receptors on the cell surface followed by uptake of the virus into the cell and eventual release of viral DNA. In the transferrin cycle, transferrin after binding to the cell, it binds to the transferrin receptor on the cell surface and is taken into the cell where the iron is released and transferrin and its receptor are recycled out of the cell.

Our lab has also tested the delivery of liposomes versus the naked DNA in an ROP model. A GFP plasmid was packed into a liposome with transferrin and suspended in HEPES buffer. Naked DNA resuspended in HEPES buffer was also used. Both formulations were tested in an ROP model of retinopathy in the mice. The mice were sacrificed and their eyes flat mounted to observe the expression of GFP. Results showed that the naked plasmid DNA injection had higher levels of GFP expression, thus supporting the results that naked DNA plasmid injection is sufficient.

Use of the ribozyme in tissue cultures has shown a decrease in the expression of the A_{2B} receptor in HREC. However, the efficiency of the transfection might be improved with increasing the amounts of the ribozyme. The transfection efficiency was determined by the transfection efficiency of a similar plasmid containing a GFP expression site. GFP is a unique fluorophore, which forms intracellulary. It does not require additional co-factors and the emitted fluorescent intensity is proportional to the GFP expression levels within the cells. Thus GFP intensity can be measured at a single cell level. The GFP plasmid is also driven by a CMV promoter and thus would be taken up by any type of cell present in the culture. Using this GFP plasmid it was shown that the cells expressed GFP for up to three passages in the HEK cells and up to two passages in the HREC. However, this plasmid was not exactly the same as the one used to carry the ribozyme. To further enhance the chance of transfecting more cells, it would be better to place GFP upstream of the ribozyme and then transfect the cells. The tissue culture can then be monitored for cells that express the GFP. Any cells expressing the GFP can be analyzed by flow cytometry which, can simultaneously measure and analyze multiple physical characteristics of cells as they flow in a fluid stream through a beam of light. Properties

it can measure include cell size, granularity and relative fluorescence. The cells can also be separated by a fluorescence activated cell sorter (FACS) and subsequently grown as pure culture. The pure culture would allow better characterization of the effects of the ribozyme. Sorenson et al [194] transfected H9 cells with a GFP marker located upstream of a retroviral vector. They were able to sort cells into two distinct populations by measuring the expression and the intensity of GFP expression. The sorted cells were viable for culture following sorting and the presence of GFP did not affect the cells.

Promoter Considerations

A CMV promoter was used to drive the expression of the plasmid, which carried the ribozyme. The CMV promoter is used for mammalian promoter strength to enhance the level of transient transgene expression in a majority of mammalian cells. The promoter is ubiquitous and affects most cells types. To better understand the pathophysiology of retinal angiogenesis, the CMV/beta actin promoter needs to be replaced with a proliferating endothelial cell specific promoter, which is under the control of cell cycle gene switch. Such a promoter would only be expressed in proliferating endothelial cells in animals undergoing angiogenesis. A promoter has been designed with a cdc6 cell cycle promoter and endothelin elements. Cdc6 is expressed in proliferating cells[195,196] and the expression of endothelin on mainly endothelial cells makes it an attractive target for endothelial cells.[197,198,199] The cdc6 promoter was inserted into a plasmid and a mouse multimerized endothelin enhancer was inserted upstream of the cdc6 promoter. A five-fold increase in the expression of activity for the endothelin enhancer/cdc6 promoter was observed in diving cells versus the non-diving endothelial cells. However, this promoter was not found to be sufficient for adequately expressing ribozymes. Therefore a GAL4 DNA binding protein was used. The trans-

activating protein was fused to the NF-kB p65 transactivation domain. Expression of the fusion protein was driven by a CMV enhancer promoter (Figure 4-2). To test the specificity of the endothelin/cdc6 promoter for endothelial proliferating cells, mice were implanted with SCCVII tumor cells. The tumor was allowed to develop for a few days following and IV injection with liposome/plasmid complexes. The tumor and lung tissues were harvested at 18 hours and 4 days post injection and assayed for CAT expression. At 18hours post injection, the tumor did not have any Cat activity present, and the lung tissue had detectable levels of CAT. However, at 4 days post injection, the tumor had ten times the activity of CAT and the lung tissue had less amounts. These results indicated that the CAT expressing promoter was repressed in non-dividing endothelial cells of the lung but was very high in the dividing cells of the tumor. It was however, interesting to note that there was no expression of CAT following 18hours of injection into the tumor. It is possible that endothelial cells need time to pass through at least one round of cell division for the promoter to become activated. Experiments are currently underway to clone the A_{2B} Rz2 downstream of this promoter.

Thus far the distribution of the A_{2B} receptors in different tissues has been based on the characterization of the receptors based on agonist binding. Antagonists would have been more preferable to determine the localization of these receptors, however, none are available. The A_{2B} receptor has also been shown to be present in fibroblasts, which are present at sites of angiogenesis. Therefore, the widespread pattern of A_{2B} receptor distribution, based on agonist binding studies, may be misleading.[200] Cloning of the A_{2B}

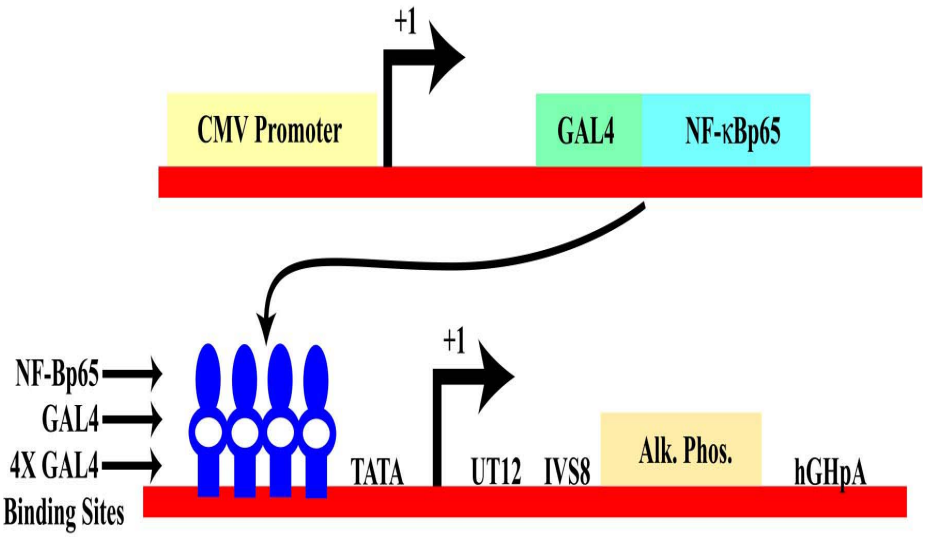

Figure 4-2. Diagram of the expression cassettes fusion protein and alkaline phosphatase (Alk Phos). UT12 refers to the consensus untranslated region of the message. IVS8 is a consensus splice site for mRNA processing. HGHpA is the human growth hormone poly A sequence. +1 is the transcriptional start site.

Rz2 into the cdc6/endothelin promoter would allow better localization and distribution patterns of the A_{2B} receptor.

The purity of the HRECs was important for the success of this project and for determining the presence of contaminating cells such as pericytes. The purity of the culture was assessed either based on the morphology of the cells or the uptake of acetylated LDL by scavenger receptors. Both of these techniques are reliable for assessing the purity of the cultures. In addition, a functional assay, Matrigel, can also be performed. This assay involves plating the cells onto a commercially available Matrigel. Matrigel is a basement membrane composed of collagens, laminin and proteoglycans. It also contains matrix degrading enzymes, TIMPs and growth factors. Endothelial cells plated onto a Matrigel helps them to form tube like structures. The Matrigel assay is time consuming and would not have provided any additional information to help in determining the purity of the HRECs culture.

Future Studies

Transfection with the active A_{2B} ribozyme showed a 43% decrease in the levels of the A_{2B} receptor by real time PCR. VEGF is a potent contributor to the process of angiogenesis and it has already been shown that the A_{2B} receptor works upstream of VEGF. Hypoxia has been shown to upregulate the expression of the VEGF receptor and the production of VEGF. Therefore, cells transfected with the active form of the A_{2B} ribozyme should also show a decrease in the levels of VEGF receptor and VEGF production. Therefore, it would be important to assess how down regulation of the A_{2B} receptor affects the subsequent growth factors, which also play an important role in angiogenesis.

It also remains to be ascertained whether down-regulation of the A_{2B} receptor affects the other adenosine receptors. It is possible that down-regulation of one of the receptors causes the other receptors to enhance their effects to compensate for the deficiency. The data from the real-time PCR shows that the levels of the A_{2A} receptor mRNA remain unaffected following transfection with the A_{2B} Rz2. Even though the mRNA for the A_{2B} receptor has been shown to be decreased, it is possible that the amount of protein being produced is unaffected. Therefore, it would be useful to measure the A_{2B} receptor protein by western blotting to confirm that a reduction in the amount of mRNA corresponds to a reduction in the amount of protein. Currently, however, a suitable antibody for western blotting purposes is unavailable for the A_{2B} receptor. Since a suitable antibody is available for the A_{2A} receptor, it would be interesting to see if transfection of HRECs with the A_{2B} Rz2 affects the level of protein production of the A_{2A} receptor.

Our lab has also made ribozymes to other components of the angiogenesis pathway, for example, VEGF and the integrins. These ribozymes are made similar to the methods described for the A_{2B} ribozymes. Sufficient in vivo and in vitro testing of the ribozymes has also been carried out. It would be interesting to see the effect of a combination of the ribozymes might have on the angiogenesis pathway. Theoretically, a combination of ribozymes targeting various aspects of the angiogenic pathway would have a more potent effect. However, it is also possible that down regulation of too many of the growth factors may also hinder the development of normal blood vessels too.

Downstream signaling of the A_{2B} receptors is not well established. For example, the A_{2B} receptors in xenopus have been shown to stimulate PLC, which in turn can

activate calcium dependent chloride conductance. [201] This effect has not been shown in the retinal endothelial cells. The A_{2B} receptor also leads to the activation of the MAPK pathway, which may stabilize HIF-1 α which, in turn may lead to the mitogenic effects of VEGF.[108] The MAPK pathway may also stabilize hypoxia inducible factor (HIF-1α) by preventing its proteasomal degradation. HIF-1 is a heterodimeric protein, which is activated by hypoxia and regulates the transcription of many genes. It consists of constitutive HIF-1β and the rate limiting HIF-1α.[202-204] Under normoxia, HIF-1 is regulated by the removal of the HIF-1α subunit by ubiquination and proteasomal degradation. HIF-1β is the aryl hydrocarbon receptor nuclear translocator (ARNT) which heterodimerizes with the aryl hydrocarbon receptor. [204] Hypoxia inhibits the removal of the HIF-1α subunit by the proteasome thus preventing HIF-1α destruction. The prevention of proteasomal degradation of HIF-1α is poorly understood. However, it is thought that the hydroxylation of two proline residues in the HIF-1α subunit prevent its degradation by the proteasome.[203] The stabilized HIF-1α translocates to the nucleus and dimerizes with the HIF-1β (ARNT). The stabilized HIF-1α /β subunit subsequently binds to the hypoxia response element (HRE). The HRE is a gene promoter which upregulates the expression of VEGF.[205] Hypoxia also leads to the stabilization of the short lived VEGF mRNA directly, thereby augmenting the effect of HIF-1 alpha.[206]

Glycogen synthase kinase-3 (GSK-3) is an enzyme, which catalyzes the breakdown of glycogen synthase. It is a pro-apoptotic enzyme and is constitutively active in cells. Phosphorylation of GSK-3 inhibits its activity. [207] The PI3 kinase pathway has been shown to phosphorylate GSK-3 and hence inhibit its activity. The A_{2B} receptor couples to $G_{\alpha q}$ and activates the PI-3 kinase pathway. However, it has not been shown yet

whether the PI-3 kinase pathway leads to the phosphorylation of GSK-3 by the A_{2B} receptor. [207]

Coupling of the A_{2B} receptor to $G_{\alpha q}$ also leads to the activation of the MAPK pathway. It is possible that the MAPK pathway stabilizes HIF-1α by preventing its proteasomal degradation. [207] Therefore it may also be hypothesized that phosphorylation of GSK-3 and subsequent inhibition of its activity also stabilizes the HIF-1 α subunit. This pathway would contribute to the upregulation of VEGF and angiogenic blood vessel growth. (Figure 4-3) It is important to be able to dissect the signaling pathway of the receptor to better understand the angiogenic pathway. The active A_{2B} ribozyme in combination with inhibitors of some of the common kinases may be an important tool in studying this pathway.

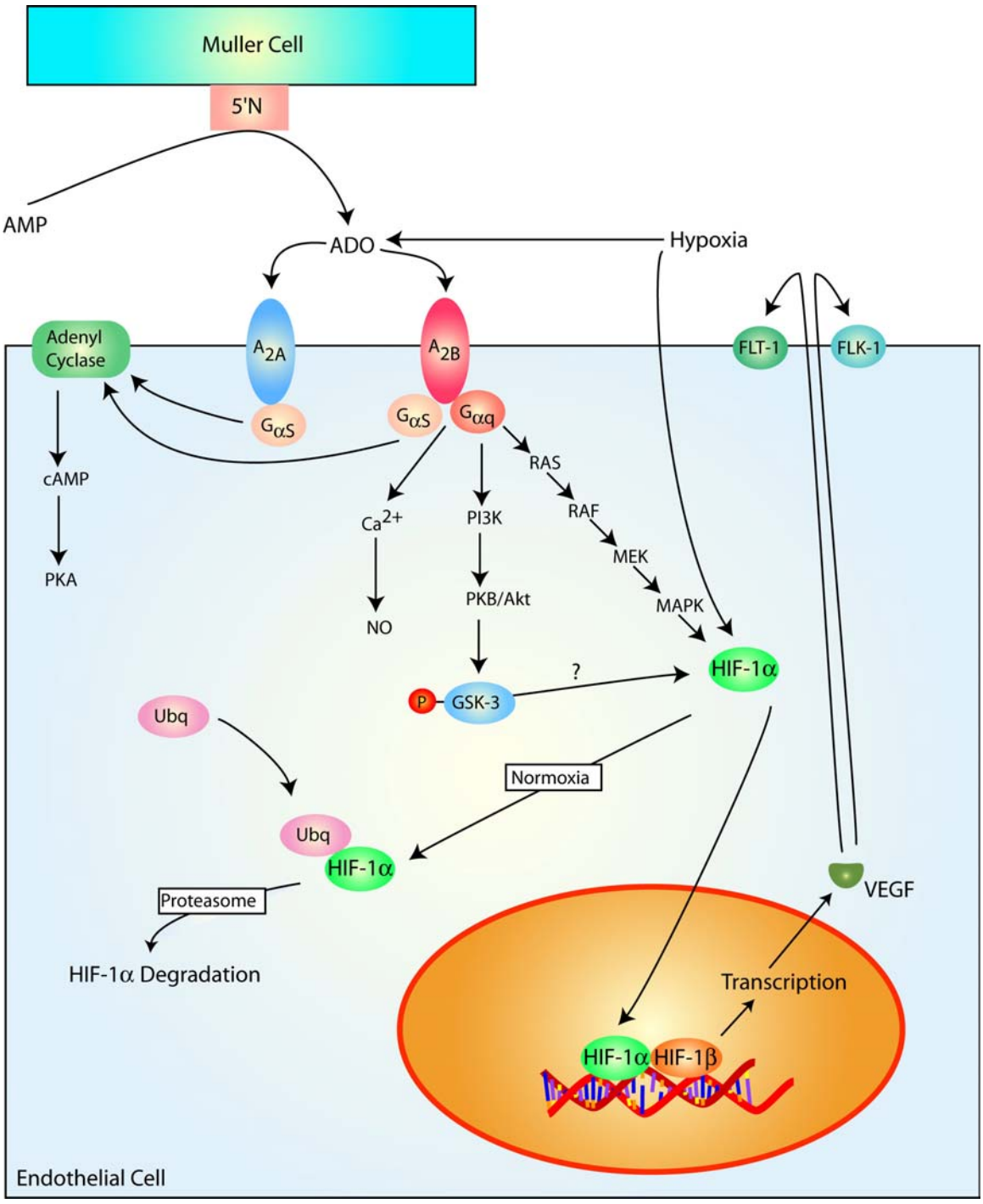

Figure 4-3. A_{2B} signaling pathway with theoretical downstream effects, which have yet to be confirmed

LIST OF REFERENCES

1. Hogan M. *Histology of theHuman Eye*. Philadelphia: WB Saunders Co; 1976.

2. Snell R, Lemp, MA. *Clinical Anatomy of the Eye*. Chicago, IL: Blackwell Scientific Publications.; 1989.

3. Gelatt K. *Veterinary Ophthalmology*. NY: Lippincott and Williams; 1996.

4. Forrester J. *The eye. Basic Sciences inPpractice*. Philadelphia, PA: WB Saunders Co Ltd; 1996.

5. Wise G, Dollery CT, Henkind P. *The Retinal Circulation.* NY: Harper & Row Publishers; 1971.

6. Hart W. *Adler's Physiology of the Eye.* 9th. ed. NY: Blackwell Scientific publications.; 1992.

7. Rubin LL, Staddon JM. The cell biology of the blood-brain barrier. *Annu Rev Neurosci*. 1999;22:11-28.

8. Hyman L, Neborsky R. Risk factors for age-related macular degeneration: an update. *Curr Opin Ophthalmol*. 2002;13:171-5.

9. Stone EM, Sheffield VC, Hageman GS. Molecular genetics of age-related macular degeneration. *Hum Mol Genet*. 2001;10:2285-92.

10. Gottlieb JL. Age-related macular degeneration. *Jama*. 2002;288:2233-6.

11. Harvey PT. Common eye diseases of elderly people: identifying and treating causes of vision loss. *Gerontology*. 2003;49:1-11.

12. Campochiaro PA. Retinal and choroidal neovascularization. *J Cell Physiol*. 2000;184:301-10.

13. Cai J, Boulton M. The pathogenesis of diabetic retinopathy: old concepts and new questions. *Eye*. 2002;16:242-60.

14. Aiello LP. The potential role of PKC beta in diabetic retinopathy and macular edema. *Surv Ophthalmol*. 2002;47 Suppl 2:S263-9.

15. Sulochana K, Ramakrishnan, S., Rajesh M., Coral, K., and Badrinath, SS. Diabetic retinoapthy:moelcular mechanism, present regime of treatment and future perspectives. *Current Science*. 2001;80:133-142.

16. Gardner TW, Antonetti DA, Barber AJ, LaNoue KF, Levison SW. Diabetic retinopathy: more than meets the eye. *Surv Ophthalmol*. 2002;47 Suppl 2:S253-62.

17. Rosenbaum JT. Sugar creates a sticky business: round up the usual suspects. *Am J Pathol*. 2002;160:1547-50.

18. Gardner TW, Antonetti DA, Barber AJ, Lieth E, Tarbell JA. The molecular structure and function of the inner blood-retinal barrier. Penn State Retina Research Group. *Doc Ophthalmol*. 1999;97:229-37.

19. Miller JW, Adamis AP, Aiello LP. Vascular endothelial growth factor in ocular neovascularization and proliferative diabetic retinopathy. *Diabetes Metab Rev*. 1997;13:37-50.

20. Weinberger B, Laskin DL, Heck DE, Laskin JD. Oxygen toxicity in premature infants. *Toxicol Appl Pharmacol*. 2002;181:60-7.

21. McColm JR, Fleck BW. Retinopathy of prematurity: causation. *Semin Neonatol*. 2001;6:453-60.

22. Wesolowski E, Smith LE. Effect of light on oxygen-induced retinopathy in the mouse. *Invest Ophthalmol Vis Sci*. 1994;35:112-9.

23. Hack M, Flannery DJ, Schluchter M, Cartar L, Borawski E, Klein N. Outcomes in young adulthood for very-low-birth-weight infants. *N Engl J Med*. 2002;346:149-57.

24. Wheatley CM, Dickinson JL, Mackey DA, Craig JE, Sale MM. Retinopathy of prematurity: recent advances in our understanding. *Br J Ophthalmol*. 2002;86:696-700.

25. Kotecha S. Oxygen therapy for infants with chronic lung disease. *Arch Dis Child Fetal Neonatal Ed.* 2002;87:F11-4.

26. An international classification of retinopathy of prematurity. The Committee for the Classification of Retinopathy of Prematurity. *Arch Ophthalmol*. 1984;102:1130-4.

27. Katz X, Kychenthal A, Dorta P. Zone I retinopathy of prematurity. *J Aapos*. 2000;4:373-6.

28. Ellis A. Phot essay: regression of severe retinopathy of prematurity after laser treatment. *Arch Ophthalmol*. 2002;120:1404-5.

29. Banach MJ, Berinstein DM. Laser therapy for retinopathy of prematurity. *Curr Opin Ophthalmol*. 2001;12:164-70.

30. Weinberger B, Laskin DL, Heck DE, Laskin JD. Oxygen toxicity in premature infants. *Toxicol Appl Pharmacol*. 2002;181:60-7.

31. Fielder AR, Reynolds JD. Retinopathy of prematurity: clinical aspects. *Semin Neonatol*. 2001;6:461-75.

32. Mintz-Hittner HA, Kretzer FL. The rationale for cryotherapy with a prophylactic scleral buckle for Zone I threshold retinopathy of prematurity. *Doc Ophthalmol*. 1990;74:263-8.

33. Connolly B, McNamara JA, Regillo CD, Vander JF, Tasman W. A comparison of laser photocoagulation with cryotherapy for threshold retinopathy of prematurity at 10 years: part 2 refractive outcome. *Ophthalmology*. 2002;109:936-41.

34. Whitfill CR, Drack AV. Avoidance and treatment of retinopathy of prematurity. *Semin Pediatr Surg*. 2000;9:103-5.

35. Mintz-Hittner HA, Prager TC, Kretzer FL. Visual acuity correlates with severity of retinopathy of prematurity in untreated infants weighing 750 g or less at birth. *Arch Ophthalmol*. 1992;110:1087-91.

36. Kretzer FL, Mehta RS, Brown ES, Mintz-Hittner HA. The pathogenesis of retinopathy of prematurity as it relates to surgical treatment. *Doc Ophthalmol*. 1990;74:205-11.

37. Hinz BJ, de Juan E, Jr., Repka MX. Scleral buckling surgery for active stage 4A retinopathy of prematurity. *Ophthalmology*. 1998;105:1827-30.

38. Chuang Y. Scleral buckeling for stage 4 ROP. *Ophthalmic Surg Lasers*. 2002;31.

39. McPherson AR, Hittner HM, Lemos R. Retinal detachment in young premature infants with acute retrolental fibroplasia. Thirty-two new cases. *Ophthalmology*. 1982;89:1160-9.

40. Aggarwal R, Agarwal R, Deorari AK, Paul VK. Retinopathy of prematurity. *Indian J Pediatr*. 2002;69:83-6.

41. Fielder AR, Reynolds JD. Retinopathy of prematurity: clinical aspects. *Semin Neonatol*. 2001;6:461-75.

42. Agarwal R AR, Deorari AK, Paul VK. Retinopathy of prematurity. *Indian J Pediatr*. 2002;69:83-6.

43. Bhushan M, Young HS, Brenchley PE, Griffiths CE. Recent advances in cutaneous angiogenesis. *Br J Dermatol*. 2002;147:418-25.

44. Bussolino F, Mantovani A, Persico G. Molecular mechanisms of blood vessel formation. *Trends Biochem Sci*. 1997;22:251-6.

45. Liekens S, De Clercq E, Neyts J. Angiogenesis: regulators and clinical applications. *Biochem Pharmacol*. 2001;61:253-70.

46. Jekunen A, Kairemo K. Inhibition of angiogenesis at endothelial cell level. *Microsc Res Tech*. 2003;60:85-97.

47. Fajardo LF. The complexity of endothelial cells. A review. *Am J Clin Pathol*. 1989;92:241-50.

48. Hirschi KK, D'Amore PA. Pericytes in the microvasculature. *Cardiovasc Res*. 1996;32:687-98.

49. Vestweber D. Molecular mechanisms that control endothelial cell contacts. *J Pathol*. 2000;190:281-91.

50. Diaz-Flores L, Gutierrez R, Varela H, Rancel N, Valladares F. Microvascular pericytes: a review of their morphological and functional characteristics. *Histol Histopathol*. 1991;6:269-86.

51. Alexander JS, Elrod JW. Extracellular matrix, junctional integrity and matrix metalloproteinase interactions in endothelial permeability regulation. *J Anat*. 2002;200:561-74.

52. Ingber D. Extracellular matrix and cell shape: potential control points for inhibition of angiogenesis. *J Cell Biochem*. 1991;47:236-41.

53. Nicosia RF, Villaschi S. Autoregulation of angiogenesis by cells of the vessel wall. *Int Rev Cytol*. 1999;185:1-43.

54. Mignatti P, Rifkin DB. Plasminogen activators and matrix metalloproteinases in angiogenesis. *Enzyme Protein*. 1996;49:117-37.

55. Mignatti P, Rifkin DB. Plasminogen activators and angiogenesis. *Curr Top Microbiol Immunol*. 1996;213 (Pt 1):33-50.

56. Sternlicht MD, Werb Z. How matrix metalloproteinases regulate cell behavior. *Annu Rev Cell Dev Biol*. 2001;17:463-516.

57. Cao Y, Ji RW, Davidson D, Schaller J, Marti D, Sohndel S, McCance SG, O'Reilly MS, Llinas M, Folkman J. Kringle domains of human angiostatin. Characterization of the anti-proliferative activity on endothelial cells. *J Biol Chem*. 1996;271:29461-7.

58. Juliano RL. Signal transduction by cell adhesion receptors and the cytoskeleton: functions of integrins, cadherins, selectins, and immunoglobulin-superfamily members. *Annu Rev Pharmacol Toxicol*. 2002;42:283-323.

59. Shattil SJ, Ginsberg MH. Integrin signaling in vascular biology. *J Clin Invest*. 1997;100:S91-5.

60. Plow EF, Haas TA, Zhang L, Loftus J, Smith JW. Ligand binding to integrins. *J Biol Chem*. 2000;275:21785-8.

61. Harris ES, McIntyre TM, Prescott SM, Zimmerman GA. The leukocyte integrins. *J Biol Chem*. 2000;275:23409-12.

62. Mizejewski GJ. Role of integrins in cancer: survey of expression patterns. *Proc Soc Exp Biol Med*. 1999;222:124-38.

63. Uhm JH, Gladson CL, Rao JS. The role of integrins in the malignant phenotype of gliomas. *Front Biosci*. 1999;4:D188-99.

64. Boudreau NJ, Jones PL. Extracellular matrix and integrin signalling: the shape of things to come. *Biochem J*. 1999;339 (Pt 3):481-8.

65. Coppolino MG, Dedhar S. Bi-directional signal transduction by integrin receptors. *Int J Biochem Cell Biol*. 2000;32:171-88.

66. Calderwood DA, Shattil SJ, Ginsberg MH. Integrins and actin filaments: reciprocal regulation of cell adhesion and signaling. *J Biol Chem*. 2000;275:22607-10.

67. Senger DR, Ledbetter SR, Claffey KP, Papadopoulos-Sergiou A, Peruzzi CA, Detmar M. Stimulation of endothelial cell migration by vascular permeability factor/vascular endothelial growth factor through cooperative mechanisms involving the alphavbeta3 integrin, osteopontin, and thrombin. *Am J Pathol*. 1996;149:293-305.

68. Eliceiri BP, Cheresh DA. The role of alphav integrins during angiogenesis: insights into potential mechanisms of action and clinical development. *J Clin Invest*. 1999;103:1227-30.

69. Cheng N, Brantley DM, Chen J. The ephrins and Eph receptors in angiogenesis. *Cytokine Growth Factor Rev*. 2002;13:75-85.

70. Gale NW, Yancopoulos GD. Ephrins and their receptors: a repulsive topic? *Cell Tissue Res*. 1997;290:227-41.

71. Holmberg J, Frisen J. Ephrins are not only unattractive. *Trends Neurosci*. 2002;25:239-43.

72. Kalo MS, Pasquale EB. Signal transfer by Eph receptors. *Cell Tissue Res*. 1999;298:1-9.

73. Papetti M, Herman IM. Mechanisms of normal and tumor-derived angiogenesis. *Am J Physiol Cell Physiol*. 2002;282:C947-70.

74. Dora KA. Cell-cell communication in the vessel wall. *Vasc Med*. 2001;6:43-50.

75. Dejana E, Corada M, Lampugnani MG. Endothelial cell-to-cell junctions. *Faseb J*. 1995;9:910-8.

76. Loughna S, Sato TN. A combinatorial role of angiopoietin-1 and orphan receptor TIE1 pathways in establishing vascular polarity during angiogenesis. *Mol Cell*. 2001;7:233-9.

77. Chavakis E, Dimmeler S. Regulation of endothelial cell survival and apoptosis during angiogenesis. *Arterioscler Thromb Vasc Biol*. 2002;22:887-93.

78. Ortega N, Hutchings H, Plouet J. Signal relays in the VEGF system. *Front Biosci*. 1999;4:D141-52.

79. Suhardja A, Hoffman H. Role of growth factors and their receptors in proliferation of microvascular endothelial cells. *Microsc Res Tech*. 2003;60:70-5.

80. Dow JK, deVere White RW. Fibroblast growth factor 2: its structure and property, paracrine function, tumor angiogenesis, and prostate-related mitogenic and oncogenic functions. *Urology*. 2000;55:800-6.

81. Klint P, Claesson-Welsh L. Signal transduction by fibroblast growth factor receptors. *Front Biosci*. 1999;4:D165-77.

82. Gabrilove JL. Angiogenic growth factors: autocrine and paracrine regulation of survival in hematologic malignancies. *Oncologist*. 2001;6 Suppl 5:4-7.

83. Stice LL, Vaziri C, Faller DV. Regulation of platelet-derived growth factor signaling by activated p21Ras. *Front Biosci*. 1999;4:D72-86.

84. Campochiaro PA, Chang M, Ohsato M, Vinores SA, Nie Z, Hjelmeland L, Mansukhani A, Basilico C, Zack DJ. Retinal degeneration in transgenic mice with photoreceptor-specific expression of a dominant-negative fibroblast growth factor receptor. *J Neurosci*. 1996;16:1679-88.

85. Pepper MS. Transforming growth factor-beta: vasculogenesis, angiogenesis, and vessel wall integrity. *Cytokine Growth Factor Rev*. 1997;8:21-43.

86. Itoh S, Itoh F, Goumans MJ, Ten Dijke P. Signaling of transforming growth factor-beta family members through Smad proteins. *Eur J Biochem*. 2000;267:6954-67.

87. Attisano L, Wrana JL. Signal transduction by the TGF-beta superfamily. *Science*. 2002;296:1646-7.

88. Burridge K, Chrzanowska Wodnicka M. Focal adhesions, contractility, and signaling. *Ann Rev Cell Dev Biol*. 1996;12:463-518.

89. Aplin AE, Howe A, Alahari SK, Juliano RL. Signal transduction and signal modulation by cell adhesion receptors: the role of integrins, cadherins, immunoglobulin-cell adhesion molecules, and selectins. *Pharmacol Rev*. 1998;50:197-263.

90. Hanahan D. Signaling vascular morphogenesis and maintenance. *Science*. 1997;277:48-50.

91. Ghiardi GJ, Gidday JM, Roth S. The purine nucleoside adenosine in retinal ischemia-reperfusion injury. *Vision Res*. 1999;39:2519-35.

92. Takagi H, King GL, Robinson GS, Ferrara N, Aiello LP. Adenosine mediates hypoxic induction of vascular endothelial growth factor in retinal pericytes and endothelial cells. *Invest Ophthalmol Vis Sci*. 1996;37:2165-76.

93. Takagi H, King G, Ferrara N, Aiello L. Hypoxia regulates vascular endothelial growth factor receptor KDR/Flk gene expression through adenosine A2 receptors in retinal capillary endothelial cells. *Invest Ophthalmol Vis Sci*. 1996;37:1311-1321.

94. Ash JD, Overbeek PA. Lens-specific VEGF-A expression induces angioblast migration and proliferation and stimulates angiogenic remodeling. *Dev Biol*. 2000;223:383-98.

95. Mino RP, Spoerri PE, Caballero S, Player D, Belardinelli L, Biagionni I, Grant MB. Adenosine receptor antagonists and retinal neovascularization in vivo. *Invest Ophthalmol Vis Sci*. 2001;43:3320-4.

96. Grant MB TR, Caballero S, Ozeck MJ, Davis MI, Spoerri PE, Feoktistov I, Biaggioni I, Shryock JC, Belardinelli L. Adenosine receptor activation induces vascular endothelial growth factor in human retinal endothelial cells. *Circ Res*. 1999;85:699-706.

97. Smith LE, Kopchick JJ, Chen W, Knapp J, Kinose F, Daley D, Foley E, Smith RG, Schaeffer JM. Essential role of growth hormone in ischemia-induced retinal neovascularization. *Science*. 1997;276:1706-1709.

98. Bussolino F, Mantovani A, Persico G. Molecular mechanisms of blood vessel formation. *Trends Biochem Sci*. 1997;22:251-6.

99. Daniel TO, Abrahamson D. Endothelial signal integration in vascular assembly. *Annu Rev Physiol*. 2000;62:649-71.

100. Feoktistov I, Biaggioni I. Adenosine A2B receptors. *Pharmacol Rev*. 1997;49:381-402.

101. Linden J. Molecular approach to adenosine receptors: receptor-mediated mechanisms of tissue protection. *Annu Rev Pharmacol Toxicol*. 2001;41:775-87.

102. Lutty GA, Merges C, McLeod DS. 5' nucleotidase and adenosine during retinal vasculogenesis and oxygen- induced retinopathy. *Invest Ophthalmol Vis Sci*. 2000;41:218-29.

103. Braun N, Lenz C, Gillardon F, Zimmermann M, Zimmermann H. Focal cerebral ischemia enhances glial expression of ecto-5'-nucleotidase. *Brain Res*. 1997;766:213-26.

104. van Calker D, Muller M, Hamprecht B. Adenosine regulates via two different types of receptors, the accumulation of cyclic AMP in cultured brain cells. *J Neurochem*. 1979;33:999-1005.

105. Londos C, Cooper DM, Wolff J. Subclasses of external adenosine receptors. *Proc Natl Acad Sci U S A*. 1980;77:2551-4.

106. Daly JW, Butts-Lamb P, Padgett W. Subclasses of adenosine receptors in the central nervous system: interaction with caffeine and related methylxanthines. *Cell Mol Neurobiol*. 1983;3:69-80.

107. Bruns RF, Lu GH, Pugsley TA. Characterization of the A2 adenosine receptor labeled by [3H]NECA in rat striatal membranes. *Mol Pharmacol*. 1986;29:331-46.

108. Gao Z, Chen T, Weber MJ, Linden J. A2B adenosine and P2Y2 receptors stimulate mitogen-activated protein kinase in human embryonic kidney-293 cells. cross-talk between cyclic AMP and protein kinase c pathways. *J Biol Chem*. 1999;274:5972-80.

109. Rivkees S, Reppert, S. M:RFL9 encodes and A2B adenosine receptor. *Mol Endocrinol*. 1992;6:1598-1604.

110. Pierce KD, Furlong TJ, Selbie LA, Shine J. Molecular cloning and expression of an adenosine A2b receptor from human brain. *Biochem Biophys Res Commun*. 1992;187:86-93.

111. Palmer TM, Stiles GL. Adenosine receptors. *Neuropharmacology*. 1995;34:683-94.

112. Montesinos MC, Gadangi P, Longaker M, Sung J, Levine J, Nilsen D, Reibman J, Li M, Jiang CK, Hirschhorn R, Recht PA, Ostad E, Levin RI, Cronstein BN. Wound healing is accelerated by agonists of adenosine A2 (G alpha s-linked) receptors. *J Exp Med*. 1997;186:1615-20.

113. Ongini E, Fredholm BB. Pharmacology of adenosine A2A receptors. *Trends Pharmacol Sci*. 1996;17:364-72.

114. Marquardt DL, Walker LL, Heinemann S. Cloning of two adenosine receptor subtypes from mouse bone marrow-derived mast cells. *J Immunol*. 1994;152:4508-15.

115. Linden J, Thai T, Figler H, Jin X, Robeva AS. Characterization of human A(2B) adenosine receptors: radioligand binding, western blotting, and coupling to G(q) in human embryonic kidney 293 cells and HMC-1 mast cells. *Mol Pharmacol*. 1999;56:705-13.

116. Olah ME. Identification of A2a adenosine receptor domains involved in selective coupling to Gs. Analysis of chimeric A1/A2a adenosine receptors. *J Biol Chem*. 1997;272:337-44.

117. Palmer TM, Stiles GL. Structure-function analysis of inhibitory adenosine receptor regulation. *Neuropharmacology*. 1997;36:1141-1147.

118. Bruns RF. Adenosine antagonism by purines, pteridines and benzopteridines in human fibroblasts. *Biochem Pharmacol*. 1981;30:325-33.

119. Brackett LE, Daly JW. Functional characterization of the A2b adenosine receptor in NIH 3T3 fibroblasts. *Biochem Pharmacol*. 1994;47:801-14.

120. Feoktistov I, Biaggioni I. Characterization of adenosine receptors in human erythroleukemia cells and platelets: further evidence for heterogeneity of adenosine A2 receptor subtypes. *Mol Pharmacol*. 1993;43:909-14.

121. Webb R, Sillis, MA., Chovan, JP., Blawierczak, JL., Francis, JE. CGS 21680: a potent selective adenosine A2 receptor agonist. *Cardiovasc Drug Rev*. 1992;10:26-53.

122. Hide I, Padgett WL, Jacobson KA, Daly JW. A2A adenosine receptors from rat striatum and rat pheochromocytoma PC12 cells: characterization with radioligand binding and by activation of adenylate cyclase. *Mol Pharmacol*. 1992;41:352-9.

123. Chern Y, Lai HL, Fong JC, Liang Y. Multiple mechanisms for desensitization of A2a adenosine receptor-mediated cAMP elevation in rat pheochromocytoma PC12 cells. *Mol Pharmacol*. 1993;44:950-8.

124. van der Ploeg I, Ahlberg S, Parkinson FE, Olsson RA, Fredholm BB. Functional characterization of adenosine A2 receptors in Jurkat cells and PC12 cells using adenosine receptor agonists. *Naunyn Schmiedebergs Arch Pharmacol*. 1996;353:250-60.

125. Feoktistov I, Biaggioni I. Adenosine A2b receptors evoke interleukin-8 secretion in human mast cells. An enprofylline-sensitive mechanism with implications for asthma. *J Clin Invest*. 1995;96:1979-86.

126. Jarvis MF, Schulz R, Hutchison AJ, Do UH, Sills MA, Williams M. [3H]CGS 21680, a selective A2 adenosine receptor agonist directly labels A2 receptors in rat brain. *J Pharmacol Exp Ther*. 1989;251:888-93.

127. Nakane T, Chiba S. Adenosine constricts the isolated and perfused monkey coronary artery. *Heart Vessels*. 1990;5:71-5.

128. Alexander SP, Cooper J, Shine J, Hill SJ. Characterization of the human brain putative A2B adenosine receptor expressed in Chinese hamster ovary (CHO.A2B4) cells. *Br J Pharmacol*. 1996;119:1286-90.

129. Kenakin TP, Bond RA, Bonner TI. Definition of pharmacological receptors. *Pharmacol Rev*. 1992;44:351-62.

130. Stehle JH, Rivkees SA, Lee JJ, Weaver DR, Deeds JD, Reppert SM. Molecular cloning and expression of the cDNA for a novel A2-adenosine receptor subtype. *Mol Endocrinol*. 1992;6:384-93.

131. Dixon K, Gubitz, AK., Sirinathsinghji, DJS., Richardson, PJ., Freeman, TC. Tissue distributions of adenosine recptors mRNAs in the rat. *Br J Pharmacol*. 1996;118:1461-1468.

132. Iwamoto T, Umemura S, Toya Y, Uchibori T, Kogi K, Takagi N, Ishii M. Identification of adenosine A2 receptor-cAMP system in human aortic endothelial cells. *Biochem Biophys Res Commun*. 1994;199:905-10.

133. Peakman MC, Hill SJ. Adenosine A2B-receptor-mediated cyclic AMP accumulation in primary rat astrocytes. *Br J Pharmacol*. 1994;111:191-8.

134. Peakman MC, Hill SJ. Adenosine A1 receptor-mediated inhibition of cyclic AMP accumulation in type-2 but not type-1 rat astrocytes. *Eur J Pharmacol*. 1996;306:281-9.

135. Mogul DJ, Adams ME, Fox AP. Differential activation of adenosine receptors decreases N-type but potentiates P-type Ca2+ current in hippocampal CA3 neurons. *Neuron*. 1993;10:327-34.

136. Liang BT, Morley JF. A new cyclic AMP-independent, Gs-mediated stimulatory mechanism via the adenosine A2a receptor in the intact cardiac cell. *J Biol Chem*. 1996;271:18678-85.

137. Strickler J, Jacobson KA, Liang BT. Direct preconditioning of cultured chick ventricular myocytes. Novel functions of cardiac adenosine A2a and A3 receptors. *J Clin Invest*. 1996;98:1773-9.

138. Murthy KS, McHenry L, Grider JR, Makhlouf GM. Adenosine A1 and A2b receptors coupled to distinct interactive signaling pathways in intestinal muscle cells. *J Pharmacol Exp Ther*. 1995;274:300-6.

139. Elfman L, Lindgren E, Walum E, Fredholm BB. Adenosine analogues stimulate cyclic AMP-accumulation in cultured neuroblastoma and glioma cells. *Acta Pharmacol Toxicol (Copenh)*. 1984;55:297-302.

140. Altiok N, Balmforth AJ, Fredholm BB. Adenosine receptor-induced cAMP changes in D384 astrocytoma cells and the effect of bradykinin thereon. *Acta Physiol Scand*. 1992;144:55-63.

141. Fiebich BL, Biber K, Gyufko K, Berger M, Bauer J, van Calker D. Adenosine A2b receptors mediate an increase in interleukin (IL)-6 mRNA and IL-6 protein synthesis in human astroglioma cells. *J Neurochem*. 1996;66:1426-31.

142. Blazynski C. Discrete distributions of adenosine receptors in mammalian retina. *J Neurochem*. 1990;54:648-55.

143. Schulte G, Fredholm BB. Human adenosine A(1), A(2A), A(2B), and A(3) receptors expressed in Chinese hamster ovary cells all mediate the phosphorylation of extracellular-regulated kinase 1/2. *Mol Pharmacol*. 2000;58:477-82.

144. Fredholm BB, Lindgren E, Lindstrom K, Nordstedt C. Alpha-adrenoceptor stimulation, but not muscarinic stimulation, increases cyclic AMP accumulation in brain slices due to protein kinase C mediated enhancement of adenosine receptor effects. *Acta Physiol Scand*. 1987;131:543-51.

145. Zamecnik PC, Stephenson ML. Inhibition of Rous sarcoma virus replication and cell transformation by a specific oligodeoxynucleotide. *Proc Natl Acad Sci U S A*. 1978;75:280-4.

146. Blake KR, Murakami A, Miller PS. Inhibition of rabbit globin mRNA translation by sequence-specific oligodeoxyribonucleotides. *Biochemistry*. 1985;24:6132-8.

147. Ohkawa J, Koguma T, Kohda T, Taira K. Ribozymes: from mechanistic studies to applications in vivo. *J Biochem (Tokyo)*. 1995;118:251-8.

148. Heuer TS, Chandry PS, Belfort M, Celander DW, Cech TR. Folding of group I introns from bacteriophage T4 involves internalization of the catalytic core. *Proc Natl Acad Sci U S A*. 1991;88:11105-9.

149. Inoue T, Cech TR. Secondary structure of the circular form of the Tetrahymena rRNA intervening sequence: a technique for RNA structure analysis using chemical probes and reverse transcriptase. *Proc Natl Acad Sci U S A*. 1985;82:648-52.

150. Zaug AJ, Been MD, Cech TR. The Tetrahymena ribozyme acts like an RNA restriction endonuclease. *Nature*. 1986;324:429-33.

151. Herschlag D, Cech TR. Catalysis of RNA cleavage by the Tetrahymena thermophila ribozyme. 2. Kinetic description of the reaction of an RNA substrate that forms a mismatch at the active site. *Biochemistry*. 1990;29:10172-80.

152. Tsui LC. The spectrum of cystic fibrosis mutations. *Trends Genet*. 1992;8:392-8.

153. Michel F, Hanna M, Green R, Bartel DP, Szostak JW. The guanosine binding site of the Tetrahymena ribozyme. *Nature*. 1989;342:391-5.

154. Michel F, Westhof E. Modelling of the three-dimensional architecture of group I catalytic introns based on comparative sequence analysis. *J Mol Biol*. 1990;216:585-610.

155. Kole R, Altman S. Properties of purified ribonuclease P from Escherichia coli. *Biochemistry*. 1981;20:1902-6.

156. Bothwell AL, Stark BC, Altman S. Ribonuclease P substrate specificity: cleavage of a bacteriophage phi80-induced RNA. *Proc Natl Acad Sci U S A*. 1976;73:1912-6.

157. Plehn-Dujowich D, Altman S. Effective inhibition of influenza virus production in cultured cells by external guide sequences and ribonuclease P. *Proc Natl Acad Sci U S A*. 1998;95:7327-32.

158. Yuan Y, Hwang ES, Altman S. Targeted cleavage of mRNA by human RNase P. *Proc Natl Acad Sci U S A*. 1992;89:8006-10.

159. Cedergren R. RNA--the catalyst. *Biochem Cell Biol*. 1990;68:903-6.

160. Perrotta AT, Been MD. A pseudoknot-like structure required for efficient self-cleavage of hepatitis delta virus RNA. *Nature*. 1991;350:434-6.

161. Perrotta AT, Been MD. Cleavage of oligoribonucleotides by a ribozyme derived from the hepatitis delta virus RNA sequence. *Biochemistry*. 1992;31:16-21.

162. Hampel A, Tritz R, Hicks M, Cruz P. 'Hairpin' catalytic RNA model: evidence for helices and sequence requirement for substrate RNA. *Nucleic Acids Res*. 1990;18:299-304.

163. Joseph S, Burke JM. Optimization of an anti-HIV hairpin ribozyme by in vitro selection. *J Biol Chem*. 1993;268:24515-8.

164. Esteban JA, Walter NG, Kotzorek G, Heckman JE, Burke JM. Structural basis for heterogeneous kinetics: reengineering the hairpin ribozyme. *Proc Natl Acad Sci U S A*. 1998;95:6091-6.

165. Haseloff J, Gerlach WL. Simple RNA enzymes with new and highly specific endoribonuclease activities. 1988. *Biotechnology*. 1992;24:264-9.

166. Pley HW, Flaherty KM, McKay DB. Three-dimensional structure of a hammerhead ribozyme. *Nature*. 1994;372:68-74.

167. Chowrira BM, Berzal-Herranz A, Burke JM. Ionic requirements for RNA binding, cleavage, and ligation by the hairpin ribozyme. *Biochemistry*. 1993;32:1088-95.

168. Hampel A, Tritz R. RNA catalytic properties of the minimum (-)sTRSV sequence. *Biochemistry*. 1989;28:4929-33.

169. Dembinska O, Rojas LM, Chemtob S, Lachapelle P. Evidence for a brief period of enhanced oxygen susceptibility in the rat model of oxygen-induced retinopathy. *Invest Ophthalmol Vis Sci*. 2002;43:2481-90.

170. Chowers I, Banin E, Hemo Y, Porat R, Falk H, Keshet E, Pe'er J, Panet A. Gene transfer by viral vectors into blood vessels in a rat model of retinopathy of prematurity. *Br J Ophthalmol*. 2001;85:991-5.

171. Smith LE, Wesolowski E, McLellan A, Kostyk SK, D'Amato R, Sullivan R, D'Amore PA. Oxygen-induced retinopathy in the mouse. *Invest Ophthalmol Vis Sci*. 1994;35:101-111.

172. Zucker M, Mathews, C.C. ,Turner D.H. *Algorithms and Thermodynamics for RNA Secondary Structure Prediction: A Practical Guide*: Kluwer Academic Publishers; 1999.

173. Kashani-Sabet M, Funato T, Florenes VA, Fodstad O, Scanlon KJ. Suppression of the neoplastic phenotype in vivo by an anti-ras ribozyme. *Cancer Res*. 1994;54:900-2.

174. Li X, Gervaix A, Kang D, Law P, Spector SA, Ho AD, Wong-Staal F. Gene therapy targeting cord blood-derived CD34+ cells from HIV-exposed infants: preclinical studies. *Gene Ther*. 1998;5:233-9.

175. Choi KS, Lee TH, Jung MH. Ribozyme-mediated cleavage of the human survivin mRNA and inhibition of antiapoptotic function of survivin in MCF-7 cells. *Cancer Gene Ther*. 2003;10:87-95.

176. Luzi E, Papucci L, Schiavone N, Donnini M, Lapucci A, Tempestini A, Witort E, Nicolin A, Capaccioli S. Downregulation of bcl-2 expression in lymphoma cells by bcl-2 ARE-targeted modified, synthetic ribozyme. *Cancer Gene Ther*. 2003;10:201-8.

177. Beck J, Nassal M. Efficient hammerhead ribozyme-mediated cleavage of the structured hepatitis B virus encapsidation signal in vitro and in cell extracts, but not in intact cells. *Nucleic Acids Res*. 1995;23:4954-62.

178. Quigley GJ, Rich A. Structural domains of transfer RNA molecules. *Science*. 1976;194:796-806.

179. Robinson GS, Pierce EA, Rook SL, Foley E, Webb R, Smith LE. Oligodeoxynucleotides inhibit retinal neovascularization in a murine model of proliferative retinopathy. *Proc Natl Acad Sci U S A*. 1996;93:4851-6.

180. Leeds JM, Henry SP, Bistner S, Scherrill S, Williams K, Levin AA. Pharmacokinetics of an antisense oligonucleotide injected intravitreally in monkeys. *Drug Metab Dispos*. 1998;26:670-5.

181. Bennett MR, Schwartz SM. Antisense therapy for angioplasty restenosis. Some critical considerations. *Circulation*. 1995;92:1981-93.

182. Ferre-D'Amare AR, Zhou K, Doudna JA. Crystal structure of a hepatitis delta virus ribozyme. *Nature*. 1998;395:567-74.

183. Walter NG, Burke JM. The hairpin ribozyme: structure, assembly and catalysis. *Curr Opin Chem Biol*. 1998;2:24-30.

184. Dahm SC, Derrick WB, Uhlenbeck OC. Evidence for the role of solvated metal hydroxide in the hammerhead cleavage mechanism. *Biochemistry*. 1993;32:13040-5.

185. Narlikar GJ, Herschlag D. Mechanistic aspects of enzymatic catalysis: lessons from comparison of RNA and protein enzymes. *Annu Rev Biochem*. 1997;66:19-59.

186. Snyder RO, Flotte TR. Production of clinical-grade recombinant adeno-associated virus vectors. *Curr Opin Biotechnol*. 2002;13:418-23.

187. Liu XL, Clark KR, Johnson PR. Production of recombinant adeno-associated virus vectors using a packaging cell line and a hybrid recombinant adenovirus. *Gene Ther*. 1999;6:293-9.

188. Lai CM, Lai YK, Rakoczy PE. Adenovirus and adeno-associated virus vectors. *DNA Cell Biol*. 2002;21:895-913.

189. Lu QL, Bou-Gharios G, Partridge TA. Non-viral gene delivery in skeletal muscle: a protein factory. *Gene Ther*. 2003;10:131-42.

190. Walther W, Stein U, Fichtner I, Malcherek L, Lemm M, Schlag PM. Nonviral in vivo gene delivery into tumors using a novel low volume jet-injection technology. *Gene Ther*. 2001;8:173-80.

191. Harashima H, Shinohara Y, Kiwada H. Intracellular control of gene trafficking using liposomes as drug carriers. *Eur J Pharm Sci*. 2001;13:85-9.

192. Liu F, Huang L. Development of non-viral vectors for systemic gene delivery. *J Control Release*. 2002;78:259-66.

193. Templeton NS. Cationic liposome-mediated gene delivery in vivo. *Biosci Rep*. 2002;22:283-95.

194. Sorensen TU, Gram GJ, Nielsen SD, Hansen JE. Safe sorting of GFP-transduced live cells for subsequent culture using a modified FACS vantage. *Cytometry*. 1999;37:284-90.

195. Stoeber K, Tlsty TD, Happerfield L, Thomas GA, Romanov S, Bobrow L, Williams ED, Williams GH. DNA replication licensing and human cell proliferation. *J Cell Sci*. 2001;114:2027-41.

196. Ohta S, Koide M, Tokuyama T, Yokota N, Nishizawa S, Namba H. Cdc6 expression as a marker of proliferative activity in brain tumors. *Oncol Rep*. 2001;8:1063-6.

197. Sarman B, Toth M, Somogyi A. Role of endothelin-1 in diabetes mellitus. *Diabetes Metab Rev*. 1998;14:171-5.

198. Fadel BM, Boutet SC, Quertermous T. Endothelial cell-specific regulation of the murine endothelin-1 gene. *J Cardiovasc Pharmacol*. 2000;35:S7-11.

199. Bu X, Quertermous T. Identification of an endothelial cell-specific regulatory region in the murine endothelin-1 gene. *J Biol Chem*. 1997;272:32613-22.

200. Feoktistov I, Biaggioni I. Adenosine A2B receptors. *Pharmacol Rev*. 1997;49:381-402.

201. Yakel JL, Warren RA, Reppert SM, North RA. Functional expression of adenosine A2b receptor in Xenopus oocytes. *Mol Pharmacol*. 1993;43:277-80.

202. Minet E, Michel G, Mottet D, Raes M, Michiels C. Transduction pathways involved in Hypoxia-Inducible Factor-1 phosphorylation and activation. *Free Radic Biol Med*. 2001;31:847-55.

203. Maxwell PH, Ratcliffe PJ. Oxygen sensors and angiogenesis. *Semin Cell Dev Biol*. 2002;13:29-37.

204. D'Angio CT, Finkelstein JN. Oxygen regulation of gene expression: a study in opposites. *Mol Genet Metab*. 2000;71:371-80.

205. Michiels C, Arnould T, Remacle J. Endothelial cell responses to hypoxia: initiation of a cascade of cellular interactions. *Biochim Biophys Acta*. 2000;1497:1-10.

206. Dor Y, Porat R, Keshet E. Vascular endothelial growth factor and vascular adjustments to perturbations in oxygen homeostasis. *Am J Physiol Cell Physiol*. 2001;280:C1367-74.

207. Eldar-Finkelman H. Glycogen synthase kinase 3: an emerging therapeutic target. *Trends Mol Med*. 2002;8:126-32.

BIOGRAPHICAL SKETCH

Aqeela Afzal was born in Lahore, Pakistan in 1972. She was raised in England (UK), California (USA), and Kuwait. She received her Bachelors degree in 1995 in Medical Technology from Kuwait University. She then went to the State University of New York at Buffalo and received a Masters in Clinical Laboratory Sciences in 1997. In 1999, she came to Gainesville, Florida and joined the Ph.D. program in Veterinary Medical Sciences.

List of Publications.

Dandona, P., Mohanty, P., Ghanim, H., Aljada, A., Browne, R., Hammouda, W., Prabhala, A, Afzal, A, Garg, R. The Suppressive effect of dietary restriction and weight loss in the obese on the generation of reactive oxygen species by leucocytes, lipid peroxidation and protein carbonylation. *J. Clin. Metab*. 2001. Jan 86(1):355-62.

Lewis, P., Afzal, A. Human Ocular Histology. *Advance*. 2001; 53-56.

Afzal, M., Afzal, A., Jones, A., Armstrong, D. A rapid method for the quantification of GSH and GSSG in biological samples. Methods. Mol. Biol. 2002; 186:117-22

Afzal, A., Afzal, M., Jones, A., Armstrong, D. Rapid determination of glutamate using HPLC technology. *Methods. Mol. Biol*. 2002; 186:111-5.

Shaw, LC., Afzal, A., Lewin, AS., Timmers, A., Spoerri, PE., Grant, MB. Reduction of the expression of the IGF-1 receptor by ribozyme cleavage results in reduction of pre-retinal angiogenesis. *Invest. Ophthal. Vis. Res*. Accepted.

Afzal, A., Shaw, LC., Caballero, S., Spoerri, P., Lewin, AS., Zeng, D., Bellardinelli, L., Grant, MB. Reduction in pre-retinal neovascularization by ribozymes that cleave the A2B adenosine receptor mRNA. *Circ Res*. Submitted.

Abstracts

Afzal, A., Iwabuchi, S., Ellis, EA., Tamai, K., Samuelson, D., Armstrong, D. Localization of lipid peroxides at sites of oxidative stress in ocular tissues by the tetramethylbenzidine reaction. *Invest. Ophthalmol. Vis. Sci.* 41:S904, 2000

Armstrong, D., Aljada, A., Higa, H., Ghanim, H., Afzal, A., Iwai, S., Browne, R., Dandona, P. Activation of signal transduction in the retina by lipid hydroperoxide. *Invest. Ophthalmol. Vis. Sci*. 42:S243, 2001.

Iwai, S., Cahallers, S., Higa, A., Afzal, A., Ueda, T., Fukuda, S., Iwabuchi, S., Grant, M., Armstrong, D. Increased MMP activity in rabbit virtreous following exposure to lipid hydroperoxide (LHP). *Invest. Ophthalmol. Vis. Sci*. 42:S573, 2001.

Harding, R.J., Kallberg, M., Lewis, PA., Ellis, EA., Afzal, A., Samuelson, D. Immunocytochemistry of endothelin-1 receptors A and B in iridocorneal angles of the dog and monkey. *Invest. Ophthalmol. Vis. Sci*. 42:S328, 2001.

Afzal, A., Shaw, LC., Caballero, S., Ellis, EA., Grant, MB. The development of hammerhead ribozymes that specifically cleave the A2B receptor mRNA. *Invest. Ophthal. Vis. Sci*. 2002. 43:E-Abstract 3711

Samuleson, D., Kallberg, M., Lewis, P., Ellis, A., Afzal, A. Localization of endothelin-a receptor in iridocorneal angles of glaucomatous dogs. *Invest. Ophthal. Vis.Res.* 2002. 43. 43 E-abstract 1053.

Afzal, A., Shaw, LC., Caballero, S., Ellis, A., Zeng, D., Bellardinelli, L., Grant, MB. The development of hammerhead ribozymes that specifically cleave the A2B receptor mRNA. American Diabetes Association, San Francisco, CA, Jun 2002.

Spoerri, PE., Shaw, LC., Beadle, C., Afzal, A., Pan, H., Grant, MB. IGF-1R and VEGFR-1 hammerhead ribozymes affect glucose induced tight junction protein modifications in cultured human retinal endothelial cells. *Invest. Ophthal. Vis. S*ci. 2003. 44; E-Abstract 3911.